INTEGRATED ANALYSIS OF GPS, GIS, AND MACHINE DYNAMIC RESPONSE IN PRECISION LIQUID FERTILIZER APPLICATION

By

CHEE-WAN CHAN

A DISSERTATION PRESENTED TO THE GRADUATE SCHOOL
OF THE UNIVERSITY OF FLORIDA IN PARTIAL FULFILLMENT
OF THE REQUIREMENTS FOR THE DEGREE OF
DOCTOR OF PHILOSOPHY

UNIVERSITY OF FLORIDA

2000

To my beloved wife, Theresa Chan, my daughter, Clairine Chan, and my son, John Chan

ACKNOWLEDGMENTS

The author is greatly indebted to the scholarship support of the Malaysian Agricultural Research and Development Institute, Malaysia, without which this study would not have been possible.

The author is especially grateful to his advisor, Dr. William M. Miller, and co-chair, Dr. John K. Schueller, for suggesting the research topic and for their encouragement and patience throughout the research. Sincere gratitude and appreciation also go to the other members of his supervisory committee Dr. Jodie D. Whitney, Dr. J. David Martsolf, and Dr. J. Wayne Mishoe for their assistance, technical support, and guidance.

The author would like to express his special gratitude to the following people: Dr. John A. Cornell for statistical analysis, Stanley S. Latimer for his thoroughgoing support in the GPS/DGPS tests, H. Eugene Hannah in the navigation studies, Charles T. Hogan and his staff in providing the field maps for the navigation study, Greg Drouillard for his technical support, Mary Beth Freeman for gathering some of the GIS information and technical support, Tom Hart of Douglass Fertilizer for providing their sprayer for the field tests, Douglass Thompson of Chemical Containers for providing the sprayer information, and Arthur R. Taylor for scanning the slides and photographs.

TABLE OF CONTENTS

Abstract of Dissertation Presented to the Graduate School
of the University of Florida in Partial Fulfillment of the
Requirements for the Degree of Doctor of Philosophy

INTEGRATED ANALYSIS OF GPS, GIS, AND MACHINE DYNAMIC RESPONSE IN PRECISION LIQUID FERTILIZER APPLICATION

By

Chee Wan Chan

August 2000

Chairperson: William M. Miller
Major Department: Agricultural and Biological Engineering

The importance of accuracy in spatially variable rate application (SVRA) has been highlighted in many studies. The cost involved in achieving desired accuracy is high and may render SVRA inappropriate. A map-based spatially variable rate application (MBSVRA) system usually consists of a SVR sprayer navigated by a differential global positioning system (DGPS). The spraying unit, fitted with a DGPS receiver, is triggered automatically by the machine field location indicated in a desired map located in the operator console. The desired map is derived from geographical information system (GIS) analysis done using a yield map. Using a yield monitor fitted with a GPS receiver, yield maps can be developed with collected yield data, followed by data interpolation. It is important to analyze the integrated requirement of spatial parameters in a MBSVRA

system. The purpose of this study was to develop an integrated MBSVRA system error model for the assessment of accuracy requirements of a MBSVRA system in a tree-based orchard. A 3.6 ha Florida citrus (orange) planting in Manatee county was selected. Spatial parameters used in these studies were: two field boundaries (Y), five GPS static horizontal accuracy levels (G), two interpolation methods (P), two levels of navigation error (T) with two levels of DGPS sampling frequencies (F) and two levels of machine delay time (D). A theoretical model was developed to analyze errors among the spatial parameters. Static horizontal positioning accuracy of a citrus yield monitor (Goat) and another DGPS system (Omnistar) were evaluated. Dynamic horizontal positioning accuracy of the two DGPS systems were also measured for real-time machine navigation in MBSVRA. Yield maps were developed using Y, G and P. A desired map was subsequently derived using yield map based on recommended fertilizer rate of 4.45 kg nitrogen per ton (t) of harvested fruit. Spraying pattern, T and F were modeled to obtained the applied map based on appropriate desired map. Absolute error (AE) was used to quantify the difference between the desired and applied maps. An integrated model relating the influence of spatial accuracy requirements among G, T, F, and D using the best boundary and interpolation method was established.

CHAPTER 1
INTRODUCTION

Traditional agricultural practices consider the field or orchard as the minimum area of management. However variation in factors such as; soil, pests, and other farm production inputs can vary substantially within fields and affect crop yield. The development of geographic information system (GIS), global positioning system (GPS), differential GPS (DGPS), in-field and remote sensors, and spatial analysis tools have enabled management of farm operations on a site-specific basis. Site-specific farming (SSF) aims to improve production efficiency by adjusting crop treatments to conditions existing at specific areas within fields. The optimization of agricultural inputs resulting from SSF can improve economic returns and reduce the introduction of undesirable residues into the environment (Schueller, 1992).

Yield mapping is a logical starting point in SSF. Yield mapping for SSF has been done in recent years with an instrumented combine for grains which continuously records mass flow of crop as it is harvested and the position by reference to a satellite based global positioning system (GPS). A yield map may in itself provide valuable insight into possible problems in the field. It also provides the starting point to other farm management and field operation

activities such as; tillage, seeding and spraying (Stafford, 1996b; Blackmore and Marshall, 1996; Birrell et al., 1994; Schnug et al., 1993; Schueller, 1992; Whitney et al., 1998). A yield map also can be used to generate a spatially variable rate application (SVRA) plan, which is usually developed on the computer in the farm office, to be transferred to a mobile vehicle for field operation.

Spatially Variable Rate Application

SVRA has been extensively used in precision agriculture for many crops. One promising usage of spatially variable control is fertilizer application (Schueller, 1988). Generally, there are two broad classifications of SVRA; sensor-based and map-based (Schueller, 1992; Morgan, 1995). In a sensor-based system, field information is gathered by the sensors as the equipment moves through the field and data is processed in real-time to generate desired application rates to control a variable rate applicator. In the map-based system, field information is stored in a desired map developed from sampling of various relevant field parameters and establishing a relationship among the parameters. During field application, machine field position determined from a geo-position sensor system is used to read the desired application rate from a desired map to control a variable rate applicator. Each method can be used in a complementary manner. Map-based application is the most common.

Basically, there are three major components in map-based SVRA (MBSVRA) system; GIS/mapping, GPS/navigation and machine dynamics. GIS/mapping involves the development of a desired application map which could be transferred to an on-board computer in the tractor, mounted with a variable rate applicator equipped with a GPS. The setting on the desired map input level is made by the farmer based upon previous yield maps and supporting soil and crop data (Olieslagers et al., 1995; Blackmore et al., 1995). The desired map is usually converted to a usable map format for the variable rate applicator (Schueller, 1992). GPS/navigation are used in both the sampling of field data and machine navigation during field application. Typically, an operator will drive the tractor guided by a light bar device connected to a real-time DGPS positioning system, and the machine controller continuously reads the current machine position and then automatically applies the required inputs at the pre-determined levels in the field based on GPS tractor position indicated in the desired map (Figure 1-1). Machine dynamics deals with the response of the machine components of the applicator to changes in application rate during field application.

Accuracy Issues

The importance of accuracy in SVRA had been highlighted in numerous studies (Schueller and Wang, 1994; Cahn and Hummel, 1995; Schueller, 1996; Dobermann and Bell, 1997; Goense, 1997; Yang et al., 1998; Nowak, 1998).

Accuracy requirement in a MBSVRA system is costly and if an incompatible choice of equipment or other component is selected, it may render the MBSVRA system inappropriate due to its high cost.

Among the three major components in MBSVRA, many research works have addressed GIS/mapping accuracy especially those related to both spatial as well as attribute data in the development of a desired map. Generally, they are concerned with the map resolution and scale as well as the spatial analysis of the samples. Extensive research also has been carried out on GPS/navigation with respect to its error and accuracy related to static positioning and navigation. Limited studies have been done on the influence of GPS/navigation on a MBSVRA system. Studies on variable rate application machinery error and accuracy are limited when compared to work done on GIS/mapping and GPS/navigation.

Most of the MBSVRA research has involved system development rather than evaluation of the MBSVRA system accuracy. Schmitz and Moss (1998) developed a general economic model in estimating the economic benefits of variable rate application of nitrogen (N) for an arbitrary number of inputs and soil types in corn production. They analyzed the value of precision farming as a function of the coefficient of soil dispersion and degree of accuracy in classification. They concluded that the value of precision farming is a convex function of the accuracy of the technology. Schueller and Wang (1994) suggested further research work on understanding the effects of the various

error sources in spatially variable fertilizer and pesticide application. Meanwhile, Goense (1997) developed a calculation method to measure the accuracy of a map-based variable rate fertilizer spreader application. It is therefore important to assess the interaction of error and accuracy in GIS/mapping, GPS/navigation and machine dynamics for a MBSVRA.

A Case Study in Florida Citrus

Currently most of the spatially variable rate application research focus on cereal crops, where they are usually harvested with a combine, while limited research has been undertaken on tree-based horticultural crops. Production requirements and field environments are different for tree-based horticultural crops from combined crops. In tree-based crops, yield is derived from usually regularly spaced tree locations where only fruits from the trees are harvested. Harvested fruits are usually collected in a bin or pallet which are subsequently transferred to a nearby trailer.

In tree-based horticultural crop, Alcalā-Jiménez and Alamo-Romero (1998) reported trials on yield mapping of an olive orchard. Righetti (1997) reported the use of GPS receiver and bar-code reader to record field location and fruit quality of harvested pome fruits collected in a bin. He suggested the use of agrochemicals application, based on tree vigor, to increase orchard productivity. Whitney et al. (1998) reported yield mapping studies on Florida citrus production where manually harvested fruits are collected in a field

container (tub). The GPS position of fruits in a tub were recorded with an instrumented truck.

Current MBSVRA research on Florida citrus is focusing on yield mapping with no available MBSVRA data. The concept of a MBSVRA system for tree-based horticultural crop, such as Florida citrus, can be similar to cereal crops. For example, the derivation of a desired map for the application of agrochemicals can be based on tree vigor. Currently, there is no reported research work on the integrated analysis of GIS/mapping, GPS/navigation and machine dynamics of MBSVRA in Florida citrus.

The main emphasis of this study was to develop an integrated error analysis model for a MBSVRA system to assist agricultural operators in the selection and analysis of the spatial accuracy/resolution requirement of three major components; GIS/mapping, GPS/navigation and machine dynamics. The study was based on a hypothetical MBSVR fertilizer application system in a Florida citrus orchard. GIS/mapping data collected from a citrus orchard, simulated GPS/navigation data and machine dynamics data were used for a hypothetical MBSVRA fertilizer sprayer applicator to derive an integrated model.

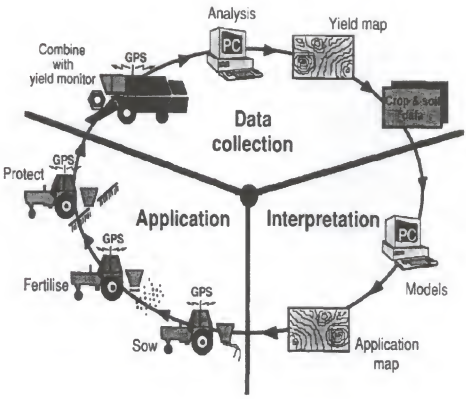

Figure 1-1. An example of a map-based spatially variable rate application system (from Stafford, 1996a).

CHAPTER 2
MBSVRA SYSTEM OVERVIEW

MBSVRA aims to apply farm inputs for maximum yield and/or maximized financial advantage while operating within environmental constraints. Farm production input in precision farming is highly complex. Figure 2-1 shows an example of the interaction between various elements in SVRA (Blackmore, 1994). MBSVRA has been used extensively in precision agriculture for grain and soybeans. Currently, there is very limited study on MBSVRA system on Florida citrus.

Horticulture Application

Citrus is Florida's most important agricultural crop, grown for both fresh fruit and processed fruit juice. The production unit ranges from small, individual 10- to 20-acre orchards to large corporations managing greater than 10,000 acres. Total citrus production of more than 300 million boxes was reported in 1997-98 with its on-tree value of about 1 billion US$ covering a total bearing acreage of 345,000 ha (Anon., 2000). There are three citrus growing areas in Florida; the well-drained soil (called the Ridge), poorly drained soils of the coastal areas, and the flatwoods and marsh soils of central and south Florida

(Jackson et al., 1995). The flatwoods is the real "growth" area and the Ridge area is declining in importance.

Citrus

The largest user of precision agriculture in Florida has been in citrus where several commercial operations are using a GeoFocus (GeoFocus Inc., Gainesville, FL) yield monitoring system to obtain a yield map of their farm. Whitney et al. (1998) developed a citrus yield mapping system using a conventional hydraulically operated fruit-loading truck equipped with an instrumented weighing system (Miller and Whitney, 1999), manual harvesters and a modified GeoFocus Crop Harvest Tracking System (CHTS) fitted with a Trimble GPS onboard receiver (Trimble, Sunnyvale, CA).

Similar Crops

Precision agriculture for many other crops has occurred later than for grains and soybeans which has been extensively tried and well documented. Other precision agriculture research includes use in potatoes (Schneider et al., 1996), sugar beets (Walter et al., 1996), peanuts (Perry et al., 1997), sugar cane (Cox, 1997), wine grapes (Lang, 1997), vegetables (Glancey et al., 1998), and horticultural crops (Righetti, 1997) yield mapping.

SVR Application System

Sensor-Based Application System

Field application in sensor-based methods utilize real-time sensors and feedback control to measure the desired field property on-the-go, and immediately use this signal to control the variable rate applicator. This technology does not require the use of a GPS or DGPS system. This method has not been extensively implemented due to the difficulty of accurate, reliable real-time sensing.

Map-Based Application System

In MBSVRA, the desired application map is converted to a usable form for the variable rate applicator (Anderson and Humburg, 1997; Schueller, 1992). The applicator may be navigated by an operator-assisted, map-based tracking software connected with a DGPS device. The DGPS system may be used to continuously correlate the location in the field with a coordinate on the map and the desired application rate for that coordinate. Based on the machine location as shown on the map, the variable rate applicator's controller then computes the desired amount of chemical to apply at each location. Command feed-forward control for the variable-rate controllers was suggested by Schueller and Wang (1994) to improve their performance. This control strategy takes into account the time required to change the rate coming out of the applicator.

Accuracy Issues

There exist significant variations in spatial accuracy requirements for the three components in a MBSVRA system; GIS/mapping, GPS/navigation and machine dynamic response. For example, the scale and resolution of base map used in GIS/mapping, the map resolution of desired application map needed by the machine controller, position accuracy of GPS receiver used in GPS/navigation, and machine response time of the applicator vary due to the availability of data and machine design. Dampney and Moore (1999) discussed an example of error sources limiting complete precision field application as being: navigation accuracy, measurement errors, errors within crop input decision model and crop input application errors. They reported that measurement and management costs may increase with a higher level of precision and that a cost-effective level is needed.

Required System Accuracies in MBSVRA

The concern about accuracy in SVRA has existed for some time (Anderson and Humburg, 1997; Schueller, 1992). Several research works had been done on GIS/mapping accuracy especially those related to both spatial as well as attribute data in the development of a desired application map. Generally, they are concerned with map resolution and scale as well as the spatial analysis of the samples. Some research has been carried out on GPS with respect to its method of positioning error and accuracy measurement

related to variable rate application (Clark, 1996; Lange, 1996; Monson, 1997; Saunders et al., 1996; Tyler et al., 1997). Studies on variable rate application machinery error and accuracy were limited when compared to the other two components mentioned earlier.

GIS/Mapping

Foote and Huebner (1995) defined accuracy as the degree of matching in information between that on a map with the true values. They highlighted differences in the accuracy requirement for particular applications. Four types of error were discussed: positional, attribute, conceptual and logical. Their analysis implied that the need for accuracy depends on the type of information coded and the level of measurement needed for a particular application in variable rate application. They discussed three main categories which cause: obvious sources, natural variations and processing. Obvious sources included: age of data, areal cover, map scale, density of observations, relevance, data format, data accessibility and cost. The second category included: positional accuracy, content accuracy and measurement error. The third category on processing error included: numerical processing, topological analysis, classification or generalization and digitizing and geocoding. The processing errors are believed to be the most difficult to be detected by GIS users. Foote and Huebner (1995) also identified the complication of error propagation and cascading which may affect horizontal, vertical, attribute, conceptual, and logical accuracy. They

emphasized the importance of checking data against ground truth and calibrating a GIS, such as by performing a sensitivity analysis to test the levels of accuracy required to meet system goals.

Pierce et al. (1997) reviewed principles and methods in yield mapping technology. They attempted to assess the accuracy of yield mapping technology and identify the sources of error which include: data collection and processing, sampling frequency and recording, and creating and interpreting yield maps.

GPS/Navigation

There are two major types of positioning systems; land-based and satellite-based positioning systems (Anon, 1997). Land-based systems consist of several radio towers that transmit signals in all directions with effective ranges of up to 48 km. Satellite-based positioning systems use U.S. Department of Defense (DoD) GPS which transmit L1 band (at 1575.42 MHz) standard positioning service (SPS) signal or coarse/acquisition (C/A) code. GPS/DGPS has been extensively used for mapping of crop yield, soil and environmental factors. In spatially variable rate application, field machine location detected by the machine GPS/DGPS receiver is used as input for controlling field application in a MBSVRA system.

The GPS can be used in two modes; single receiver mode and differential mode using two receivers. In the single mode, one receiver collects the timing information and processes it into position. This system is the least expensive

and easiest to use but its accuracy suffers due to the introduced positional errors. For improved accuracy the GPS can be corrected by using the differential mode. This system is known as a differential global positioning system (DGPS). The stationary receiver usually receives its real-time differential correction signals from the U.S. Coast Guard radio beacon system, geostationary satellite-based system or local FM differential correction sources. Tyler et al. (1997) reported various sources of real-time differential correction signals: local base as described earlier, FM sub-carrier provided by commercial firms, U.S. Coast Guard radio beacon at frequencies ranging from 287 kHz to 323 kHz, and wide area DGPS network.

Anderson and Humburg (1997) stated that DGPS is typically used with a positional accuracy of 5 m or less. They reported that DGPS gives ground speed accuracy to within 0.1 km/h, but temporal resolution is not adequate for metering control, especially when the applicator is starting or stopping. An accurate real-time kinematic GPS with a possible position accuracy of under 30 cm was suggested as suitable for vehicle navigation to minimize application skip and overlap.

Machine Dynamics

Machines do not respond instantly to changes in input rate when mapping or applying. These time-dynamic errors become spatial due to the motion of the agricultural machines. Harvesting machines introduced averaging and delays in

yield mapping (Searcy et al., 1989). Although the dynamic effects are known to be affected by machine adjustments, material flowrates, and crop conditions, the current commercial correction methodology assumes a fixed pure time delay when generating yield maps.

Anderson and Humburg (1997) discussed a site-specific applicator data flow model with reference to several commercial applicators. They highlighted the areas of possible error occurrence associated with machine components in the commercial applicator.

Schueller and Wang (1994) suggested further research work on understanding the effects of the various error sources in spatially variable fertilizer and pesticide application. They studied the dynamic response of an electric motor-driven diaphragm dual-pump, dual-tank sprayer system. Errors of three different application methods (constant rate, no pre-command and pre-command rate) were quantified using mean absolute error and root-mean-square error between desired average and applied average application rate. They demonstrated the desirability of command feed-forward control. Such control is implemented on some commercial applicators. The need for finding an integrated system errors to allow component accuracy versus cost and complexity design tradeoffs was stressed. Wang (1994) studied the transient error, transportation delay, and error due to non-uniform flow distribution on the above sprayer system. He also emphasized the need to quantify the overall error

in a MBSVRA such as; application errors of applicators, inaccuracies of machine locators, and the quantization of GIS data.

Yang et al. (1998) studied the effects of conventional uniform nitrogen, uniform nitrogen and phosphorus, and variable rate nitrogen and phosphorus on grain sorghum. A map-based commercial Ag-Chem FALCON® (Fertilizer Applicator Local Control Operating Network) controller (Ag-Chem Equipment Co. Inc., Minnetonka, MN) fitted with two hydraulic motor-driven centrifugal pumps was used on an 8-row (0.965m spacing) side dressing fertilizer applicator to apply two liquid fertilizers. They calibrated the desired and applied liquid as well as checked the machine dynamic response time at five different discharge levels ranging from 100 to 650 L/ha with a simulated ground speed of 8 km/h. The rise times for actual discharge spray rate were also checked. The percentage of error after rise time ranged from 2.15% to 4.70%. Mean error for discharge was expressed for chemical bins. Accuracy of application rate for the bin controller was compared based on selective samples collected by the FALCON® control system which sampled and recorded the desired and actual rate along with the GPS position. The effects of GIS map and GPS errors were not studied.

Al-Gaadi and Ayers (1999) reported a 6.1 m spatially variable rate herbicide application system and field tested the system in a 4.2 ha field. The system consist of variable rate boom sprayer with direct injection nozzles, Campbell Scientific 21X datalogger (Campbell Scientific, Inc., Logan, UT), a laptop computer equipped with MapInfo (MapInfo Corporation, Troy, NY)

mapping software, and DGPS system which received its real-time correction signals from a base station via a Pacific Crest RFM96 radio modem (Pacific Crest Corporation, Santa Clara, CA). They investigated the DGPS system accuracy, sprayer control system reaction time, and application system accuracy. The overall effect of GIS/mapping, GPS/navigation and machine dynamics in the MBSVRA was not investigated.

Map Resolution

Two categories of variable rate applicators have been described by Dobermann and Bell (1997): modular design with an open architecture for smaller farms and highly specific machinery exclusively designed for one or few tasks for large farms. For small farms, a Massey Ferguson tractor with a FIELDSTAR™ system (AGCO Corp., Duluth, GA) and a mounted variable fertilizer spreader was judged appropriate. A Terra-Gator 1903 (Ag-Chem Equipment Co. Inc., Minnetonka, MN) with Soilection Twin Bin™ (Soil Teq Inc., Waconia, MN) was selected for large farms. Variable-rates of up to five chemicals (3 granular, 2 liquid) may be applied by this Terra-Gator 1903 system based on the computerized map in one pass. Desired application map resolution is important for both small as well as big equipment. For small equipment, the effect of map resolution can be on the applicator width. As for big equipment, the map resolution effect is important on both its width and its nozzle controllability along the spray boom. If a spray boom is 20 meters wide and each nozzle

cannot be controlled independently, then the usefulness of variable-rate application may be limited. However, if each nozzle is independently controllable, then the resolution of the map being used to control the spray must be appropriate to the width and working speed of the applicator. Monson (1997) emphasized that the map resolution must correspond to the width and traveling speed of the application machinery where maps must contain a minimal resolution to properly control the desired inputs.

Integrated System Studies

Integrated studies on the requirement of a MBSVRA system requires considerations in the spatial requirements of GIS/mapping, GPS/navigation system and machine dynamics.

Several approaches have been attempted in the past to study the spatial relationship between various factors in a MBSVRA system. Most of these are in the evaluation of MBSVRA machine system while some involved theoretical studies to describe a relationship among the selected spatial parameters. However, none of these studies incorporated all three factors.

Machine System Evaluation

The previous section described Yang et al. (1998) studies on the machine dynamics of a liquid N and phosphorous MBSVRA system fitted with an Ag-Chem FALCON® controller. Besides machine dynamics, their studies also involved MBSVRA system evaluation. Laboratory tests on application accuracy

of the sprayer, based on the desired rate versus actual sprayer output, and dynamic response tests were also evaluated. Field experiments were also conducted on three 14 ha irrigated grain sorghum fields in 1997 growing season. Yield mapping data were collected by a yield monitor fitted with the NorthStar DGPS receiver. The interpolation method used in developing the yield map was not reported. Existing soil nutrient level was collected using grid soil sampling at a rate of about 2.5 samples/ha. Desired maps for N and phosphorus fertilizer were developed using Surfer (Golden Software Inc., Golden, CO) software based on soil analysis, suggestions from agronomists and farmers (as there is no standard fertilizer guide for grain sorghum in south Texas) based on a fixed yield target. Desired maps for the FALCON® controller were translated by SGIS software (Ag-Chem Equipment Co., Inc., Minnetonka, MN) with a cell size of 1.5 m x 1.5 m. The inability of sprayer controller in regulating a lower rate of less than 47 L/ha was reported. During field spraying, the FALCON® control system sampled and recorded desired rate and actual rate at selected field locations. A slightly lower applied rate than the desired rate was reported.

Al-Gaadi and Ayers (1999) studied the integrated effect of GIS and DGPS in the development of a MBSVR herbicide spraying system fitted with direct injection nozzles. The sprayer system consisted of a Raven® Industries, Inc. (Sioux Falls, S. Dak.) injection module, a piston injection pump, a 12-VDC gear motor driving the injection pump, a 57 L tank, a laptop computer connected to a Campbell Scientific 21X data logger, and a real time DGPS system which

consisted of two Ashtech SCA-12S 12 channel L1 code GPS receivers (Ashtech Inc. Sunnyvale, CA.) fitted with two Pacific Crest RFM96 radio modems. A georeferenced desired map for weed treatment of a 4.2 ha field was developed using an 18.3 m grid sampling soil data. The herbicide rate was based on sampled soil organic matter. The desired application rate varied from 3510 mL/ha to 5260 mL/ha. Georeferencing of map was done using DGPS and MapInfo mapping software. The desired rate was converted to a voltage command to the 21X datalogger from the laptop computer to the electric motor via a control program using MapBasic software (MapInfo Corporation, Troy, NY). The control program performed the following tasks every second: (1) receive sprayer location (latitude/longitude) from the DGPS; (2) identify those machine coordinates on the GIS map as received from the DGPS; (3) select the management zone on the GIS map for that coordinate; (4) read the corresponding command voltage from the selected management zone; and (5) output the command voltage to the electric motor. Additionally, they studied: the static accuracy of the DGPS system, control system response time and time delay at two step input rates of 585 ML/ha and 5260 mL/ha. The response time was for the control system output to reach from 10% to 90% of the step input and delay time was the time taken to reach 10% of the step input. The mean values and standard deviation of the calculated applied rates along with the desired rate were compared. The applied rate was converted into a georeferenced map

and compared using MapInfo mapping software with desired map obtained by scanning and creating raster images.

Theoretical Approach

Besides machine evaluation, theoretical studies in cell size selection using geostatistical analysis for SVRA was also attempted (Han et al., 1994). They proposed a mean correlation distance (MCD) as a determining criterion for upper cell size limit of a field management unit. The unit was described using square or rectangular cells. They suggest that the upper limit of cell size be the minimum MCD of all spatial variables.

Schueller (1992) describes various spatially-variable control strategies: homogeneous control, automatic control, temporary separate control, multivariate spatially-variable control, and historical spatially-variable control for an input-manage-output model. He also described some examples of input for each component in the input-manage-output model. An extensive review on various MBSVRA systems including GIS/mapping, GPS/DGPS and machine dynamic was presented. Further research into an integrated MBSVRA system (Figure 2-2) was suggested.

Schueller and Wang (1994) simulated an integrated MBSVR spraying system involving GIS/mapping and machine dynamics. The desired map for P_2O_5 fertilizer spraying was generated based on soil type, previous crop yield, and soil test P_2O_5 data. Field units of 40 m x 40 m cells was selected with a

hypothetical machine travel speed of 18 km/h. Machine spraying accuracy was based on a hydraulically-driven centrifugal pump model developed by Xu (1991). Transportation delay of the system also was studied while keeping the time constant of the model to be one second. The effect of pre-command on transportation delay in the MBSVRA system was investigated. Two measures of the system error were discussed; mean absolute error and root-mean-square error. The need to study locator errors, map errors and applicator transverse errors was highlighted. Finally, the need for studying the integrated system errors and an expression to be developed for errors and reasonably accurate typical numerical values was emphasized. This will allow a tradeoffs between accuracy versus complexity and cost. Wang (1994) defined the mean absolute application error using an integral equation in the same study.

Goense (1997) developed a calculation method to measure the accuracy of map-based variable rate fertilizer spreader application. Variance between desired and actual rate of application was calculated. His work involved five levels of map resolution, four range values of semivariogram, eleven different spreader effective working widths, four GPS navigation positional errors which ranges from 0.1 m to 2.0 m and five different types of fertilizer spread pattern. The method was based on variance calculation between desired rate and applied rate using geostatistics. Spatial variability of the application rate was described by a semivariogram, using an exponential model. The level of sill was set at 100 %, the nugget at 5 %. They found that the shape of the spreading

pattern had small influence on the accuracy of application. Also, the effect of GPS navigation accuracy depends on the desired map resolution and working width of independently controlled sections of the spreader. Goense did not study the effects of equipment dynamic response such as delay time, interpolation method used in GIS/mapping, GPS error in deriving desired map, sampling frequency of DGPS receiver.

Chan et al. (1999b) described a conceptual approach in studying the integrated effect of GIS/mapping, GPS/navigation and machine dynamics for a case study in a citrus orchard. The study involved identifying spatially variable parameters classified according to a desired map and applied map in the MBSVRA system. A theoretical approach in developing an integrated model considering GIS/mapping, GPS/navigation and machine dynamics could be attempted considering all those relevant factors described above for desired and applied maps. However, this would required identification/development of a map-based error analysis method.

Hypothetical MBSVRA System in Florida Citrus

The concept of a MBSVRA system for Florida citrus can be similar to cereal crops. The derivation of a yield map for tree-based horticultural crop, such as Florida citrus, involved yield data collection of trees using GPS/DGPS and other relevant field parameters like orchard aerial photograph and field

boundary. A yield map of a selected orchard boundary can be first generated using yield data as described in Whitney et al. (1998) and Chan et al. (1999a).

Subsequently, the yield map may be overlaid with other relevant maps such as soil properties maps to derived a desired map depending on the specific application decided by the farm operator.

Similarly, the desired map can then be transferred to a MBSVR applicator equipped with a DGPS to be converted to a map format which can be used as an input command map for the machine controller. The desired rate of agrochemical can then be automatically applied based on machine location shown in the application map located in the tractor console driven by an operator in between two tree rows in a regularly spaced tree orchard. A light bar system coupled with a real-time DGPS receiver could be used in machine guidance during field application.

The development of an integrated model incorporating GIS/mapping, GPS/navigation and machine dynamics in Florida citrus would require the evaluation/simulation of accuracy requirements of each relevant components/factors. Yield map interpolation parameters, accuracy of positioning system and machine dynamic response time are some of the essential components.

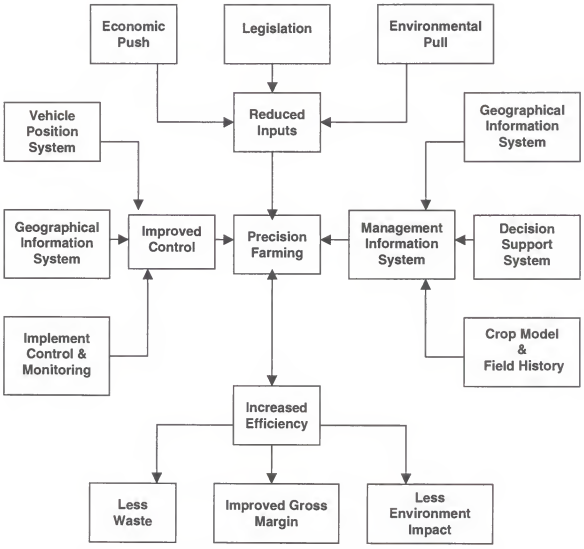

Figure 2-1. An example of interacting factors influencing a spatially variable rate application system (from Blackmore, 1994).

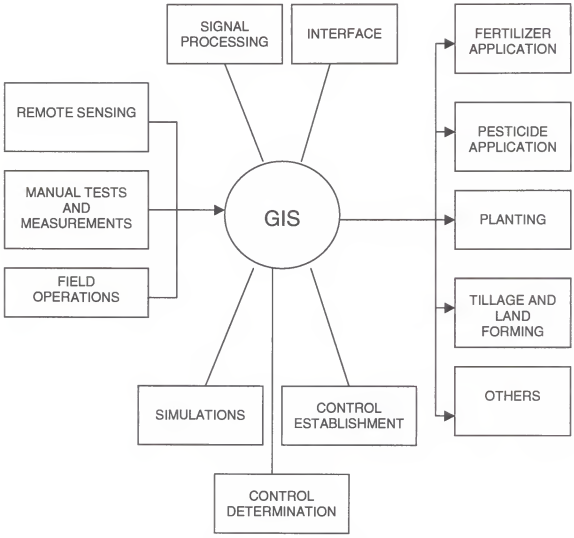

Figure 2-2. An example of integrated map-based spatially variable rate application system (from Schueller, 1992).

CHAPTER 3
A CONCEPTUALLY INTEGRATED ERROR ANALYSIS MODEL

Introduction

The needs for integrating GIS/mapping, GPS/navigation and machine dynamics in MBSVRA were detailed in Chapter 1 and 2. Based upon the concept of error modeling of Wang (1994), Schueller and Wang (1994), and paralleling some of the work of Goense (1997), a discrete modeling scheme describing the three components can be developed. Figure 2-2 shows an example of some essential components in an integrated MBSVRA system.

The purpose of the conceptual model was to establish a theoretical relationship between all the relevant spatial parameters affecting a MBSVRA system. The developed model will be used to assist users of variable rate applicators in their assessment of spatial accuracy requirements for components in the variable rate application.

The development process of a conceptual model involved; identification/selection of essential spatial parameters, defining a relationship for the accuracy of each parameter, developing an integrated analysis method, and establishment of a relationship among factors selected in the three components.

Identification of essential spatial parameters in each of the three major components in MBSVRA is important in the development of a conceptual model. The overall spatial error of each selected spatial parameter in GIS/mapping, GPS/navigation and machine dynamic are used in defining a relationship for the spatial accuracy of each selected parameter. Various accuracy factors described in the accuracy literature related to mapping, location and machine dynamics could be analyzed and integrated.

Subsequently, a map-based spatial analysis method can be used in studying the integrated effect of various selected agricultural inputs. A model for all selected essential parameters can be developed upon identifying the degree of influence of each factor.

A citrus crop production system was selected for this study. This example details the influence of three spatial factors described in the model (GIS/mapping, GPS/navigation and machine dynamics) in the development of a tree-based error model for a MBSVRA. Similar models could be derived for other crops using MBSVRA with similar procedure.

Factors in Desired Map

A desired map can be derived from farm layout, crop yield, soil nutrient, crop condition and water condition. Jackson et al. (1995) described several factors that must be considered in the development of a citrus nutrition program, including the importance of soils, site selection, soil pH, environment issues,

nutrient requirements, effect of nutrition on fruit quality, and the interactions of nutrition with other aspects of management. The process in developing a desired map depends on the purpose of its application, cost involved and the type of data needed. These objectives influence the type of map, hardware, method and degree of accuracy required. Generally, a desired map should reduce fertilizer costs, reduce chemical application costs, reduce pollution through proper use of chemicals, improve crop yields and provide better information for management decisions.

Geo-referenced base maps of topographic and physical features are essential before the developed application map can be implemented in the field. (Clark, 1996). He proposed that at least one base map, usually the topographic map, be constructed with high position and elevation precision to be used as standard which all other maps can be compared, tested and adjusted. He did not specify the accuracy level needed.

Besides the base map, development of a desired map requires analysis of various farm production inputs in the mapping of field variability. Field variability is highly complex, and includes many natural environment variables such as; weather, pest and diseases, etc. Mapping of all these variables is highly complicated (Larscheid and Blackmore, 1996). Yield mapping is a logical start in the development of a desired map.

Base Map

Clark (1996) suggested photogrammetry as the economical method for large areas topographic mapping as a base map, though less precise. He also mentioned recent techniques using robotic total stations, GPS, and laser systems combined with GPS for topographic mapping. Schueller (1992) mentioned that agricultural fields are usually undulating with small variation in elevation and the fields may be treated as a two-dimensional plane described by two coordinates. Besides considering the farmer's objective(s), the scope of mapping criteria needed for a base map generally include considerations for geographic referencing and data structure. The geographic referencing consists of coordinate/projection system, such as WGS84 or NAD27 coordinate systems or UTM/State plane projection system. The data structure consists of vector data structure, TIN (triangulation irregular network) or raster data structure (any grid-based data structure, such as column/row matrix and/or quadtree), and image data structure (any pixel-based structure, such as .PCX or .TIF).

Aerial photograph of a citrus orchard was used as the based map in citrus yield mapping (Whitney et al., 1998). Besides aerial photograph, other digital aerial photograph such as digital orthophoto quadrangle was attempted (Chan et al., 1999a).

Yield Mapping

Yield maps highly influence the decision making as well as machine control process. It is important that the maps actually represent the variation in the field and not other systemic errors. Two main errors were highlighted by Blackmore and Marshall (1996) for a yield map created by a combine lag time between detachment and sensing of the grain (which offsets the yield position along the route of the combine) and the unknown width of crop entering the header (which causes yield inaccuracies).

Many studies have been carried out to develop yield maps for cereal and horticultural crop using crop yield monitors. For cereal crops, yield maps are produced by fitting a yield monitor to a combine harvester to record the amount of grain harvested at any particular time. Pierce et al. (1997) described various yield monitor systems such as the Flowcontrol system (Dronningborg Industries, Denmark). There are also mechanical systems that monitor the volume of grain by using a paddle wheel or an impact sensor. On yield monitors, a differential global positioning system (DGPS) is used to record the actual position in Eastings and Northings. This data can then be filtered, converted and presented as a yield map.

The availability of mobile mounted GPS/DGPS systems allowed the collection of horticultural crop yield data based on accumulated mass-flow system. This approach allows yield maps to be produced for a variety of crops. There are two systems that use this approach, a trailer based weighing system,

and a conveyor based weighing system. Both systems provide a method of obtaining crop mass flow data that can be spatially referenced by using a DGPS and subsequently processed to produce yield maps (Walter et al., 1996). By adapting a trailer to incorporate a weighing system capable of working while moving, yield maps of a large range of crops can be produced. Whitney et al. (1998) described a modified truck-based weighing system equipped with a hydraulic arm which pick up tubs of manually harvested citrus fruits in the field. A commercial yield monitor fitted with a GPS/DGPS locates the positions of those tubs. A citrus yield map can be developed using interpolation method (Figure 3-1).

Relevant spatial factors influencing citrus yield mapping can be classified as data collection and data analysis.

Data collection

Data requirements for the implementation of a citrus yield map depends on the application of a MBSVRA. The collection of spatial data involves identifying appropriate data needed for the objectives desired by the farmer and sampling of field data. An intensive ground based system and/or remote sensing methods are used. Besides obtaining the attribute values of citrus field data, the field location of the data collected is recorded.

Intensive ground based system. For high precision machine control operation, intensive ground based sampling is usually used. Other features of data involved interpolation of spatial and temporal data for generation of desired

maps. In citrus yield mapping, essential spatial parameters in data collection include the selection of a base map, intensive ground base collection of tub locations filled with harvested fruits, orchard boundary selection and interpolation of the tub positions. Whitney et al. (1998) described a citrus yield mapping system using an adapted commercial yield monitor equipped with a GPS receiver. A similar system using a DGPS receiver also was reported (Whitney et al., 1999b).

Remote sensing. Intensive ground based grid sampling is considered time-consuming and expensive. Besides intensive ground-based data collection methods, several studies on remote sensing over a large area have been conducted. Anderson and Yang (1996) studied the mapping of grain sorghum management zones using aerial videography. In this study, color infrared digital video images of two grain sorghum fields in south Texas were acquired and then classified into several management zones using unsupervised classification. Sampling points were selected within each zone at which plant, leaf and soil samples were taken. Results from this study indicate that airborne videography is an effective tool for establishing within-field management zones.

The advantage of aerial videography is due to its immediate availability for both visual interpretation and digital processing. Image processing software can be used to statistically cluster image data into regions of homogeneous spectral response. These regions can then be used as management zones for

the field with reduced samples required to characterize the spatial variability of the field.

Glazer et al. (1998) studied the semi-automated analysis of aerial citrus orchard images in locating individual trees using a set of computer vision algorithms. Their intent was to identify, count, measure size, and rate of health of citrus trees in digital images.

Positioning system. The GPS was developed by the U.S. DoD for accurate positioning of military personnel and targets. The earth is banded by twenty-four GPS satellites that transmit very accurate timing information. The GPS receiver picks up the signals from available satellites as they pass within its field of view. A greater number of satellites corresponds to a more reliable positioning system. So as to restrict access to this position information, the signals were encrypted with a randomized positional error that could be turned on and off. With this error turned on (normal situation) the inherent horizontal accuracy of the GPS is approximately $\pm$100m 95 % of the time (Zhao, 1997). Position dilution of precision (PDOP) is a GPS unitless figure, expressing the relationship between the error in user position and the error in satellite position. PDOP varies throughout the day. A low PDOP indicates a higher probability of GPS positioning accuracy. If the inherent accuracy of a GPS is about 20m it is based on a 95% probability that the position given will be within 20m of the true position (Saunders et al., 1996). It is reported that obstruction such as trees and tall buildings close to the receiver will interfere with the accuracy due to the

satellite constellation occlusion and multipath errors due to satellite signal reflection (Monson, 1997; Lachapelle and Henriksen, 1995). Zhao (1997) summarizes an example of typical receiver errors on the position output of the GPS receiver (Table 3-1).

It is important that the position of citrus tub collected in the field, indicated by the GPS/DGPS of a yield monitor, represent the true centroid of that harvested area. The static accuracy of the GPS/DGPS device of the yield monitor constitutes a very essential spatial parameter influencing the overall spatial resolution requirement of a MBSVRA. A higher accuracy level of GPS/DGPS device usually costs more than that of a lower grade GPS/DGPS receiver.

Data analysis

Subsequent data analysis for the development of a yield map upon completion of spatial data collection required consideration for the intended application of the yield map. Usually a boundary defining the crop growing area is needed in the development of a desired map used for field application of a MBSVRA. Upon identifying the boundary, the spatial data points are further processed using surface interpolation methods to describe the yield surface for the identified field boundary.

Boundary selection. Boundary selection constituted another essential spatial parameter in yield mapping of a citrus orchard. Selecting too large a boundary may have a dilution effect around the edges of the orchard boundary

and likely to cause a larger area of yield map proceeds fertilizer application map resulting in unnecessary wastage of fertilizer. The need for accurate boundary determination was pointed out by the response of some veteran citrus growers to GeoFocus's advertising literature (Chan et al., 1999b). Their confidence in the reliability of a yield map was degraded by illogical and excessive interpolated yield decline around the edge of the field block due to boundary enclosing too large of an area.

Interpolation methods. Many studies have reported different techniques used in interpolating yield surface. Kriging method was most commonly used though it is complicated when compared to other simpler methods like local averaging. Several computer software programs are available for creating yield map surfaces. Moore (1997) discussed four methods used in interpolating a combined yield data using Surfer software; nearest neighbor, local averaging, inverse distance and kriging. Grid size and search radius were varied within each method while search rules were standardized for each method. A smaller grid size yielded a higher correlation between original and interpolated data but the computational time increases with a smaller grid size.

Map Presentation

Map presentation of desired map level is the step where certain data treatments are applied for better visualization. Detection and removal of

systematic errors as well as interpolation, especially for spatial data, makes visual analysis much easier.

Other Factors

A treatment map shows the precise location and quantity of the treatment or application within the field. This could be in terms of seed, fertilizer or spray application or other field treatments such as cultivation. Upon developing the yield map, a subsequent step entails development of a desired application map to be used by the MBSVR applicator. Factors limiting the yield potential of areas within a field are considered. These limiting factors can be further classified which of these are controllable, then assessed and prioritized for management actions.

There are many interacting factors, some of which are included in Table 3-2, which influence crop growth and ultimately yield. Some of these cannot be controlled directly, e.g. soil texture (proportions of sand, silt and clay), climate (temperature, sunshine hours and precipitation) and topography. These factors have a direct effect that may be influenced by varying management inputs.

Jackson et al. (1995), described various nutrition requirements for Florida citrus production. N application was described as the cornerstone of citrus production that is believed to have the greatest effect on production. They emphasized that N has to be applied on a regular basis as it is readily leached from the soil. Typical application N rate range from 112 to 336 kg/ha/yr (100 to

300 lb-N/acre/yr) depending on age and condition of trees, intended market, soil conditions and whether the orchard is irrigated.

Desired Map Resolution

Different desired map resolution level classifications will affect the number of discharge settings required by the applicator controller in adjusting to different desired rate. By classifying too low a level may result in machine not able to discharge the desired low rate. Additional sophisticated machine components may be required to dispense the desired rate. Assuming that an applicator controller is able to discharge the whole range of desired rates, the desired map resolution must correspond to the width and traveling speed of the applicator as discussed earlier.

Applied Map in MBSVRA

Upon development of a desired map, the implementation of an automated machine controlled MBSVR field applications involve in-field positioning and precision application mechanisms with automatic control. In machine navigation with high precision DGPS also allows the tractor mounted implement to navigate without any visual input (O'Connor et. al., 1996). Field operation of a MBSVRA involves sensing of machine field location, usually by a DGPS device.

Field Navigation

The accuracy of sensing machine field location during field operation of a MBSVRA system can contribute significantly to the overall error in an integrated system model. Several machine navigation methods have been described for a MBSVRA system, with many using real-time DGPS to guide the operator in field application operation.

Zhao (1997) described autonomous location and navigation systems designed to various levels of complexity. The complexity of the system is believed to be determined by the trade-offs involving various architectural constraints in system level requirements in accuracy of location, cost of the system, the complexity of the supported navigation functions and other field specific application requirements. He mentioned that a complicated navigation system requires greater positional accuracy, sophisticated human-machine interfaces, powerful guidance abilities, or integrated radio location receivers.

Tyler et al. (1997) mentioned that a guidance system could assist the machine operator in maintaining a steady course during field operation. They described the use of a real-time DGPS device incorporating an on-board computer, and additional guidance aids like a direction light bar and graphic screen for highly accurate positioning. An automatic parallel track-line system for field navigation is discussed where the user selects a line in a field and the navigation system automatically determine a set of parallel lines offset from this initial line. A light bar indicator is frequently used a visual guidance device. A

one second update rate by the DGPS device is considered typical. Recently, a new Trimble AgGPS 170 (Trimble Navigation Ltd., Sunnyvale, CA) computer system for MBSVRA, uses similar concept in field navigation.

Stoll and Kutzbach (1999) described the necessity and benefits of automated land vehicles guidance systems incorporating position measurement, path planner, vehicle controller and safety systems. They reported the new development of GPS receivers using real-time kinematics offering position update rates up to 10 Hz and accuracies of a few centimeters which is said to be suitable for automatic steering. They summarized possible positioning sensors for vehicle guidance (Table 3-3) from various references. They suggested that GPS-dead reckoning systems are useful for operations in vineyards, orchards or forest though using this system for controlled steering in these farms are still considered too inaccurate.

Various degree of navigation error or DGPS dynamic horizontal error may be identified and analyzed if the navigation path of the MBSVRA system can be modeled based on an ideal machine path for field operation similar to that as described in the Trimble AgGPS170 computer system for a MBSVRA system. Besides navigation error, the update frequency of a DGPS receiver coupled with machine traveling speed also affects the spatial resolution of field application.

Currently, there is no available MBSVR applicator for citrus tree application. Field application in a citrus orchard is usually guided between two tree-rows. A light bar system could help in minimizing navigation error caused by

the operator not following closely to the actual path shown on the desired map. It is hypothesized that a light bar system coupled with a real-time DGPS receiver is used for the integrated error modeling in this study.

Machine Dynamics

Schueller and Wang (1994) identified transportation delay and time constant in a simple first order system using Xu's (1991) result in the modeling of a hydraulically-driven centrifugal pump of the type used on larger commercial MBSVRA systems.

Yang et al. (1998) studied the dynamic response of a MBSVRA using FALCON® controller. They observed laboratory test results on rise time and steady state mean error between desired and actual discharge spray rate. They did not model the SVRA system transfer function.

Machines do not respond instantly to changes in application rate when applying. These time-dynamic errors caused by a delay in machine dynamic response become spatial due to the motion of the agricultural machines. The overall machine dynamic response may be quantified by its delay time in applying the desired rate once a desired input rate is acquired by the machine controller.

Developing a Theoretical Model

Figure 3-2 described a flowchart showing the development process of a theoretical model relating the integrated effect of selected spatial parameters in a MBSVRA system.

Identification/Selection of Factors

A MBSVRA system should be defined prior to the model development process where all relevant production inputs/factors influencing the MBSVRA system are identified. Identification and selection of relevant factors in an integrated analysis of a hypothetical MBSVRA system is important before any modeling is attempted. Six major spatial parameters were selected considering all those relevant factors described earlier in both the desired and applied maps and the data available for Florida citrus. For the present study, boundary offset (Y), GPS/DGPS static horizontal positional error (G) and interpolation method (P) in desired map were selected. These factors represent the GIS/mapping and GPS components of a MBSVRA system. Meanwhile, DGPS dynamic horizontal positional error (T), DGPS sampling frequency (F) and machine delay time (D) were considered essential in the development of applied map for a Florida citrus MBSVRA system.

Boundary Condition

Different input ranges for the six identified spatial parameters: Y, G, P, T, F and D can be identified/evaluated either through laboratory tests, field tests, or

literature reviews. The best desired map could also be identified by defining the boundary conditions of its spatial factors and selecting that which correlate closest to the ground truth. This best desired map could later be used as the control in quantifying mapping/application errors.

Definition of Mapping Error

Mapping error in the development of a desired map for a MBSVRA system can be simply defined as the difference between the best desired map and the other desired map. A simple relationship described below can be used to define an error function in term of Y, G and P. For the present study involving MBSVRA of liquid N fertilizer:

Desired mapping error, $E_{DM} = [DM_{BEST} - DM_{REJECT}]$

where the best desired map,

DM_{BEST} = f (k, Y, G, P) and correlate closest to the ground truth

in which,

k = conversion factor for nutrient requirement based on crop yield and soil map recommendation

Y = Boundary offset based on map scale and resolution of a digital aerial photograph used as a base map

G = GPS static horizontal positional error of yield monitor, m

P = Yield map interpolation method error

and the other desired map,

DM_{REJECT} = f (k, Y, G, P) and any other maps which does not correlate closest to the ground truth

This equation of $E_{DM} = [DM_{BEST} - DM_{REJECT}]$ will compute the desired N errors in both positive and negative values. An absolute error value can be used to quantify the effect due to Y, G and P. For the whole map, a weighted mean absolute error value can also be computed to representing the effect of the treatments.

The absolute error equation would be, $E_{DM} = | [DM_{BEST} - DM_{REJECT}] |$

Definition of Application Error

Application error in a MBSVRA can be simply defined as the difference between desired and applied rate or quantity. A simple relationship described below can be used to define an error function in term of desired map and applied map. For the present study involving MBSVRA of liquid N fertilizer:

Error, $E = [DM_{BEST} - N_{applied}]$

where desired map factors includes:

DM_{BEST} = f (k, Y, G, P)

and, applied map factors involved:

$N_{applied}$ = f (T, F, D)

in which,

T = DGPS Dynamic horizontal error or navigation error, m

F = DGPS sampling frequency error, Hz

D = Machine control time delay error, s

This equation of $E = [DM_{BEST} - N_{applied}]$ will compute the N application errors in both positive and negative values. An absolute error value can be used to quantify the effect due to GIS/mapping, GPS/navigation and machine dynamics. For the whole map, a weighted mean absolute error value can also be computed to representing the effect of the treatments.

The error equation would be, $E = | [DM_{BEST} - N_{applied}] |$

Integrated Analysis and Modeling

Current theoretical error analysis such as the calculation method described in Goense (1997) and the integration method described in Schueller and Wang (1994) were limited in their ability to perform an integrated approach incorporating GIS/mapping, GPS/navigation and machine dynamics. Furthermore, the distribution and characteristics of GPS/DGPS in static positioning of yield data and machine navigation were not studied. Yield map interpolation and field boundary were also neglected in their studies.

Machine evaluation approach described by Yang et al. (1998) and Al-Gaadi and Ayers (1999) earlier did not consider GIS/mapping, GPS/navigation and machine dynamics components all together. Besides, they did not describe an integrated analysis method in their studies.

A map-based error analysis can be developed using a GIS software, raster-based grid-cell geoprocessing system. This geoprocessing system is available in the ArcView Spatial Analyst 1.1 program (Environmental Systems Research Institute (ESRI), Redlands, CA). The spatial values of both the desired and applied maps can be analyzed statistically and compared. Using the best available spatial resolution for each selected spatial parameter as the base, the effect of different spatial resolution for each parameter can be studied and quantified by computing their absolute error maps. A weighted mean absolute value can be generated from each absolute error map and an example integrated error model can be developed using statistical analysis.

Table 3-1. GPS receiver errors

Error	Typical GPS (m)	Worst case GPS (m)	Typical DGPS (m)
Satellite clock	2 - 3	25	< 0.5
Satellite orbit	1 - 2	5	< 0.5
Selective availability	30 - 50	100	< 0.5
Emphemeris prediction	3 - 5	15	< 0.5
Ionospheric delay	10 - 15	100	< 0.5
Tropospheric delay	3 - 5	30	<.5
Multipath	10	300	10
Receiver noise	5	15	5
Total effect	100 (95 %)	300 (99.99 %)	15 (95 %)

From Zhao, 1997.

Table 3-2: Factors influencing yield variation

Little control	Possible control
Soil texture	Soil structure
Climate	Available water
Topography	Water-logging
Hidden features	Nutrient levels

Table 3-3. Possible positioning sensors for vehicle guidance

	Accuracy (cm)	Velocity (m/s)	Range (m)
Physical paths	10-30	$\leq$ 3	-
Mechanical feeler	2	0.9	-
Ultra-sonic	2 - 5	1.3-3.6	-
Computer vision	5	0.8	-
Virtual paths			
Laser scanner	5	0.5	$\leq$ 400
Microwaves	< 100	2.7	$\leq$ 500
Radio frequency	20	6.7	$\leq$ 5000
RTK DGPS	200	3.0	$\propto$
RTK DGPS with Gyro	< 10	0.8	$\propto$
RTK DGPS (4 Antennas)	5	2.0	$\propto$
	< 2.5	0.33	$\propto$
	< 11	3.0	$\propto$

From Stoll and Kutzbach, 1999.

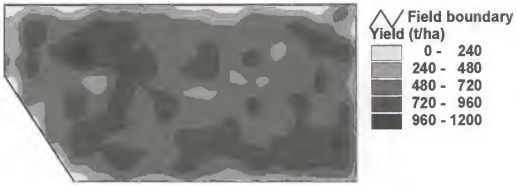

Figure 3-1. An example of a citrus yield map.

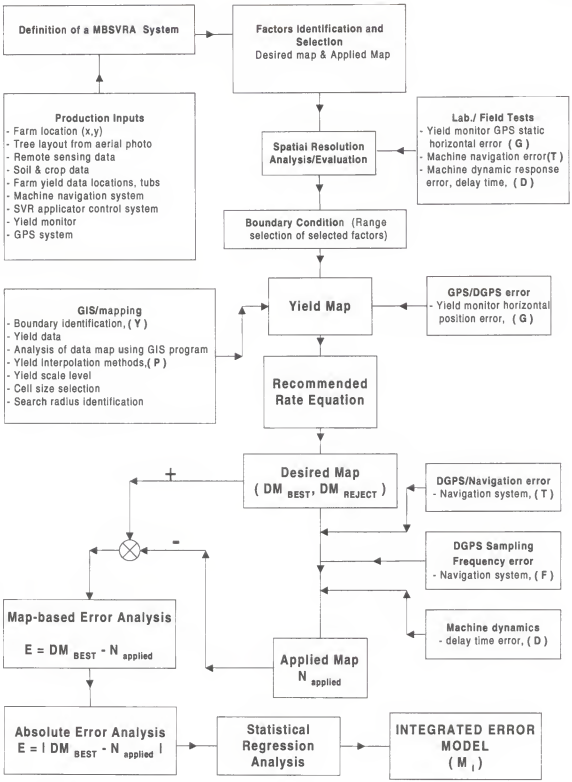

Figure 3-2. A flowchart of MBSVRA model development using an integrated analysis in a MBSVRA system.

CHAPTER 4
OBJECTIVES

Main Objective

The main purpose of this study was to develop a conceptual model considering the overall effects of GIS/mapping, GPS/navigation and machine dynamic response on a map-based variable rate application of liquid chemical application for a citrus orchard. The conceptual model was to establish a theoretical relationship between all the relevant parameters affecting a map-based variable rate applicator. The developed model will be used to assist users of variable rate applicators in their assessment of the accuracy requirements of the variable rate application systems and their components.

Sub-objectives

1. To develop a map-based error analysis method integrating GIS/mapping, GPS/navigation and machine dynamic response.

2. To investigate static horizontal predictable accuracy of GPS/DGPS receiver systems in a MBSVRA system.

3. To investigate dynamic accuracy of DGPS receivers for use in machine navigation for field application in a MBSVRA system.

4. To investigate the influence of G, Y and P in the development of a desired map for MBSVRA in a citrus orchard.

5. To model machine navigation system horizontal error and spraying pattern in a MBSVRA system.

6. To investigate the integrated effect of machine response time of a fertilizer applicator in a MBSVRA system.

7 To investigate the influence of multiple field applications (such as split N applications) of a MBSVR fertilizer applicator on the integrated model.

CHAPTER 5
IN-FIELD POSITIONING AND NAVIGATION SYSTEMS

Introduction

The implementation of MBSVRA requires an in-field positioning and navigation system for mapping/sensing of field attributes and for the application of production inputs. Positioning system requirements for mapping/sensing and application of farm inputs are different in terms of position resolution, reliability and dynamic performance (Stafford, 1999).

In-field positioning systems, based primarily on GPS, have been used extensively in yield sampling of cereal crops for the development of yield maps. Citrus yield mapping requires the collection of stationary in-field position of manually harvested fruits tub locations as described by Whitney et al. (1998).

A MBSVRA using real-time DGPS system for machine navigation alone may not be sufficient due to the loss of real-time differential correction signals in poor environmental conditions such as tree obstructions or weak DGPS signal coverage areas. Field application of liquid fertilizer in a MBSVRA for a tree-based crop may require an integrated field machine navigation system using real-time DGPS and dead reckoning system. Balsari et al. (1997) tested a dead-reckoning system for directional control of tractors in dry fields and paddy fields.

They concluded the needs in using GPS for correcting compounded eventual errors of position due to lateral deviation of tractor in successive runs. Stoll and Kutzbach (1999) described a farm vehicles guidance system using a digitized field map guided by an integrated system using GPS coupled with other positioning devices based on a dead reckoning system. They suggested that the combination of GPS-dead reckoning is useful for operations in vineyards, orchards or forests. Monson (1997) emphasized the importance of maintaining vehicle position with respect to the application map as it is one of the most significant error sources in MBSVRA. He then described a combination of GPS with a inertia navigation system which is capable of accurate differential equivalent machine positioning in areas of poor DGPS signal reception such as under tree cover.

Other ground-based navigation systems studies have been reported: parallel swath in banana plantation using a combination of satellite based real time DGPS and light bar system Molin and Ruiz (1999), integrated radar-gyroscope-DGPS (real time) system (Hellebrand and Beuche, 1997), real time DGPS with a light bar (Vetter, 1995) and real-time DGPS with speed sensors and fluxgate compass sensor dead reckoning system (LeBars and Boffety, 1997).

Two DGPS systems were tested in this study; the Goat system (GeoFocus Inc., Gainesville, FL) (Figure 5-1) and the Omnistar system (Figure 5-2). The Goat system has been used in citrus yield data collection while the

Omnistar system is a stand alone DGPS unit. Besides yield data collection, the potential of the two systems for machine navigation in field application was also evaluated.

The objective of this study was to measure the static predictable accuracy (for in-field data collection) and dynamic repeatability accuracy (field navigation) of both the Goat and the Omnistar DGPS systems.

Review

There are several studies on error and accuracy of GPS used in yield mapping and spatially variable rate application. It is important to understand the GPS signals characteristics and sources of GPS errors in the evaluation of static in-field GPS positioning system and navigation system.

GPS Signals Characteristics and Sources of Error

Barnes and Cross (1998) described a range of factors affecting the quality of GPS positioning: whether positioning is absolute or relative, length of the baseline for relative positioning, atmospheric conditions, GPS signal (phase or code), number of frequencies capable of being received by the receiver, processing model of the receiver, local environmental condition, GPS antenna type, static or kinematic data collection methods used, differential signal correction in real time or post processing. Accuracy in positioning system is dynamic and affected by both spatial and temporal factors. Sources of errors in both in-field positioning and navigation systems include selective availability,

atmospheric (ionosphere and troposphere), satellite clock and emphemeris, multi-path and receiver noise. Sampson (1985) reported that the positioning error due mainly to satellite geometry is not within manufacturer's control but the ranging error (error due to range measurement process of a receiver) is within the manufacturer's control.

Differential correction has been used to improve position resolution either through post or real-time processing of uncorrected signals. Post processing of differential signals can be done using downloaded base station files from various web sites. There are many methods in transmitting real time differential correction signals such as US Coast Guard beacon RTCM SC-104, local base AM, FM subcarrier, and wide area based satellite.

The Navstar specifications defines expected accuracy as in Table 5-1 (Monson, 1997). Navstar (Anon, 1995) described four performance specifications of GPS standard positioning service (SPS) signal: coverage, service availability, service reliability and the positioning and timing accuracy. Coverage is where at least 4 satellites are in view with a precision dilution of position (PDOP) value of not more than 6. Service availability is the next performance parameter denoting the percentage of time when satellites are transmitting a ranging signal near the earth. The third parameter described service reliability where the percentage time interval of instantaneous predictable horizontal error is within a specified reliability threshold. Finally, the positioning and timing accuracy performance standard of GPS positioning given

the coverage, service availability and service reliability of GPS. Four areas of accuracy were described by Navstar; predictable, repeatable, relative and time transfer accuracy. They characterized the behavior of GPS position solution error as changing considerably over time at any given location. A 24 hours sampling interval is used in their accuracy performance standard. They reported the measured average daily variations of GPS 24-hour 95% error statistics over 30 days of steady-state measurement as 15% along east-west, 14% along north-south, 10% vertical and 10% horizontal. A larger variation is expected when the ranging error behavior changes for one or more satellite. The geographic variations in positioning errors is reported to be higher in the north errors than the east errors after latitude 18 degree where the north error is reported to be 22% larger than the east error. A nominal SPS horizontal error distribution representing the expected error distribution performance irrespective of latitude was also presented. A similar graph was described by Diggelen (1998). Anon (1995) reported that the characteristics of GPS position error are not necessarily Gaussian. Similar observations were reported in Anderson (1997) and in Mertikas et al. (1985).

In-Field Positioning System in Data Collection

Rupert and Clark (1994) studied the accuracy of a L1 band, C/A code GPS receiver using post processing of differential correction signals for point data collection. They described the importance of PDOP as a major contributing

factor in positioning error. The mean horizontal position error decreased from 3 to 2 m for 100 km baseline distance between rover and base GPS receiver as sampling time of the rover GPS receiver at a static position increased from 2 to 10 minutes.

Mack (1997) reported the static positioning performance of a high quality and a standard GPS receivers over a 24-hour period at a precisely known point. He described a high quality receiver as having more channels, using advanced signal observation techniques, and makes better use of carrier and doppler observations. He suggested the use of a wide area satellite-based differential correction signal system for coverage over a large area farm.

Borgelt et al. (1996) measured grid points of soil sample in the field using carrier phase hand held GPS receivers and GPS card receivers and post processing of differential signal. Sampling time at each location was collected over a 60-second period. They concluded that carrier phase receivers provided better position accuracy resolution than a C/A code receiver but a C/A code differential GPS system is not suitable for instantaneous distance or velocity measurements.

Stafford and Ambler (1994) studied the static accuracy of a GPS receiver sampled at 1 Hz. A 1.9 m 2dRMS(2 standard deviation root mean square) position resolution was reported with the S/A off. However, this position resolution degraded to 5-15 m after the S/A was turned on.

Murphy et al. (1994) reported that the position resolution of GPS receiver is price dependent - the more expensive the GPS receiver, the more precise the position fixes.

Machine Navigation in Field Application

Larsen et al. (1988) investigated requirements of a real-time DGPS field navigation system for field application. They described an operator-assisted navigation using pre-determined machine path shown on the operator control graphic screen.

Spruce et al. (1993) used GPS to track a site preparation skidder and a small farm tractor under both forest canopy and open sky conditions using a 6-channel hand-held GPS and using post processing method for differential correction. They concluded that machine navigation was satisfactory in open sky conditions while forest canopy significantly degraded GPS signal quality. They suggested further investigation into combination GPS-dead-reckoning navigation systems.

Clark and Worley (1994) studied the accuracy of a C/A code GPS receiver, with 1 Hz sampling rate, using post processing differential corrections for a moving vehicle traveling at speeds of 16.1, 32.2, 48.3, 64.4, and 80.5 km/h. They found that the maximum average trajectory error was 2 m and with a maximum point trajectory error of about 11 m. The base station was located 12 km away.

Vetter (1995) studied an operator assisted Airstar (SATLOC, Inc., Casa Grande, AZ) swath guidance system. The system consists of a computer, narrow correlation-type GPS receiver, 900 MHz radio receiver/data modem, cockpit display screen and keypad, dash-mounted light bar display, and power supply. The system was fitted to a car and tested on a 1000-m long test section in an airport. Traveling speed during test runs ranged from 15.0 to 20.3 m/s. Actual machine path was video taped during test runs and the cross-track error for each run was analyzed. With position sampling set at 1 Hz, variation in distance between position recorded by video camera and real-time DGPS receiver was compared. They reported a 50/50 percentile distance error of 0.38 m, a 10/90 percentile error distance of 0.89 m, and a maximum error distance of 1.88 m for this guidance system.

Hellebrand and Beuche (1997) field tested a machine guidance system using a real-time DGPS integrated with a piezoelectric vibrating gyroscope dead-reckoning system. Differential correction was via a FM receiver. They concluded that the accuracy of positioning systems for agricultural applications should be better than three meters using real-time DGPS. However, they reported that real-time DGPS is not always reliable due to satellite availability and electromagnetic wave transmission disturbances. Dead reckoning by an independent location system is said to improve the machine guidance performance.

Buick (1998) tested two operator-assisted light bar parallel swath machine guidance systems in New Zealand in comparison with a foam marker system mounted on a 24-m sprayer boom. In the light bar system, he used two types of GPS receiver; sub-meter DGPS and a centimeter accuracy real-time kinematic (RTK) GPS receiver. The test track was 500 m long located in a bean field. A GPS sampling rate of 1 Hz with machine speed ranges from 10 km/h to 14 km/h was tested. Average cross-track error of 1.61 m, 0.57 m and 0.23 m were reported for the foam marker, sub-meter DGPS and centimeter-accuracy RTK DGPS system respectively. Application overlap (double applications) and skip (missed application) were computed for each pair of adjacent swaths and expressed as a percentage of swath area. Application overlap percentages of 2.04 %, 1.00 % and 0.59% were reported for foam-marker, sub-meter DGPS and centimeter-accuracy RTK DGPS respectively. While application skips of 0.35 %, 1.46 % and 0.77 % were obtained for foam-marker, sub-meter DGSP and RTK DGPS respectively.

Molin and Ruiz (1999) tested a SATLOC SwathStar light bar parallel swathing system in a banana plantation using a real-time DGPS system with an Omnistar receiver fitted to a tractor. The sampling frequency of Omnistar DGPS receiver was not mentioned. Tests were conducted at 7.92 and 13.50 km/h over a 200-m long test path. Three groups of 40 points along the 200-m test path were sampled for each pass and analyzed for cross-track error. Average error of 1.65 m (50 percentile) and 2.5 m (90 percentile) were reported at a tractor speed

of 7.92 km/h and 1.75 m (50 percentile) and 2.10 m (90 percentile) for a speed of 13.50 km/h.

Materials

Two systems were tested in this study; Goat and Omnistar system. Goat (GeoFocus Inc., Gainesville, FL) is a commercial yield monitor, model number 1002-103, fitted with an OEM Trimble (Trimble, Sunnyvale, CA) Lassen-SK8 (8-channel, L1-band, C/A code) GPS board connected to a compact active micropatch GPS antenna via a 5 m cable (Appendix A). It was also fitted with a CSI (CSI Inc., Calgary, AB) SBX-2 DGPS board and a CSI MBA-3 beacon whip antenna capable of receiving real-time RTCM SC-104 differential correction signals from the U.S. Coast Guard. The available signals were 312 kHz from Egmont Key, FL and 289 kHz from Cape Canaveral, FL. Recorded positional data from the Goat in the Trimble TSIP format were downloaded via a key card and read by a key card reader, connected to a personal computer. Sampling interval of the Goat unit was set at 0.1 s. An ATC (ATC, Lancaster, PA) 422 flip-flop timer was used in continuous data collection over a 24-hour period.

The Omnistar system used an 8-channel, L1-band, C/A code Omnistar (Omnistar Inc., Houston, TX) model OS7000 DGPS receiver capable of receiving real-time Omnistar satellite-based differential correction signals from its SPACENET 3 satellite transmitting at C-band (3750/4250 MHz). Data output from the Omnistar unit was connected with a RS-232 serial cable to a notebook

computer at 4800 baud rate. The data output is in NMEA 0183 format showing data in position, DOP and time at 1 Hz. (Appendix B).

Methods

Saunders et al. (1996) reported a methodology for evaluating DGPS systems, which included static accuracy, static stability, dynamic stability, dynamic repeatability and precision tests. Anon (1995) described a means for measuring GPS static accuracy performance that included predictable static accuracy of a fixed location. The predictable static accuracy and dynamic repeatability of the Goat system and the Omnistar system were tested using methods similar to those described in Saunders et al. (1996). The effect of non-differential GPS signal for the Goat system was evaluated over a 24-hour period by physically disconnecting the DGPS cable connection to the Goat yield monitor during data collection.

Predictable Static Accuracy Tests

For the Goat system, GPS and DGPS antennae were placed at a fixed position on the roof of the Geoplan Center at the University of Florida in Gainesville, FL, at latitude 29^0 38.854914' N and longitude 82^0 20.498121' W, 2.02 m away from the Geoplan Center base station. The location of the base station is at latitude 29^0 38.854779' N and longitude 82^0 20.499361' W. Position data recording was set at a 1 minute interval using the ATC 422 timer and

collected over a 24-hour period. The weather conditions during test were calm and fair with minimal cloud cover.

In the Omnistar system, the DGPS receiver was placed in another nearby location on the roof but with a fixed location at latitude 29^0 38.854779' N and longitude 82^0 20.498121' W, 2.00 m away from the Geoplan Center base station. Positional data was recorded using the default setting at 1 Hz and collected over a 24-hour period on another day. Similar weather conditions were experienced as in the day of the Goat system test.

Circular error probable (CEP), root means square (RMS), twice the distance RMS (2dRMS), horizontal 95-percentile (R95), mean, etc. have been used to define GPS spatial accuracy (Diggelen, 1998). Anon, (1995) described a direct method using 95 percentile Euclidean horizontal error of GPS static position collected over a 24-hour period to quantify the static position resolution of a GPS receiver. They also described the data distribution, coverage, availability and reliability of GPS data. Saunders et al. (1996) also quoted the 95-percentile horizontal error and Euclidean horizontal error about the mean of all data point. Meanwhile, Huff (1997), compared the performance of nine GPS systems using their 24-hour data on horizontal dilution of precision (HDOP), easting error, northing error and number of satellite. Mean position and standard deviation were used to quantify their performance. An integrated method of analysis based on Saunders et al. (1996), Anon (1995) and Huff (1997) was used in this study which consider data distribution and satellite signals (HDOP,

satellite number). The 95 percentile Euclidean horizontal error was used to quantify the static predictable horizontal error of each system.

Dynamic Repeatability Tests

Monson (1997) developed a methodology for quantifying the capabilities of various GPS and DGPS based systems for dry fertilizer application. He described a measurement method for GPS system latency in quantifying the dynamic error of a GPS receiver used in field navigation. Three types of accuracy of location data were discussed: static position accuracy, static multiple position accuracy and dynamic accuracy. Dynamic accuracy of GPS/DGPS equipment was considered important for navigation during variable rate application. Mertikas et al. (1985) reviewed various ways in analyzing GPS navigation accuracy data. Saunders et al. (1996) described a dynamic repeatability test in quantifying the capability of a GPS navigation system. Clark and Worley (1994) studied the deviation of machine path, indicated by a post-processed differential GPS signal, from a surveyed field path.

Similar methods for dynamic repeatability tests described in Saunders et al. (1996) were used in the evaluation of the Goat and Omnistar systems. A relatively flat field plot planted with about 4 m height citrus trees, with 4.57 m within row and 6.10 m between row spacing, located at the University of Florida, Gainesville, FL, was selected for these tests. A rectangular surveyed path of 173.98 m (side A) x 61.57 m (side B) x 173.56 m (side C) x 61.58 m (side D) was

marked out using wooden stakes and displayed in the field by connected strings tied to those wooden stakes (Figure 5-3). Total length of the surveyed path was 470.69 m. The Goat DGPS systems was tested on March 10, 1999 while the Omnistar DGPS system was tested on March 16, 1999. During this field test, the antenna (Goat unit) or DGPS receiver (Omnistar unit) was mounted on the top of the vehicle at the middle section of a small Kawasaki 4-wheel farm transporter. A 1.5 m pole was fitted in front of the vehicle, at the middle section of the driver cab and aligned with the DGPS receiver/antenna, to serve as a visual guidance marker for the operator to follow the surveyed machine path displayed by the nylon string. The small transporter was driven at an average speed of 3 km/h by an experienced operator between two rows of citrus tree. Data recording of the Goat unit was performed manually by pressing the push button for each DGPS signal indicated on the Goat display screen while the Omnistar unit output was continuously stored into a laptop computer via a RS-232 serial cable.

Mean deviation of machine path from the surveyed path or cross-track error distribution of the navigation system from the surveyed/pre-determined path was used to quantify the accuracy of the navigation system.

Results and Discussions

Static Predictability Accuracy Tests

A total of 1378 static non-differential GPS positional records were collected for the Goat GPS receiver over a 24-hour period. Due to unexplained

reasons in the electronic circuit of the Goat GPS receiver and the ATC 422 timer set up which worked well initially and intermittently missed 62 samples. This problem might be due to the problem in debouncing time interval for the push button in the Goat unit. Overall, 44.78 %, 51.96 % and 3.27 % of the 1378 data were collected at 60 s, 61 s and about 120 s time intervals respectively.

The latitude and longitude error distribution for the Goat GPS non-differential signals shows a somewhat Gaussian distribution for 24 hours sampling duration (Figure 5-4a, 5-4b). However, there is a long-tailed distribution in the latitude error. An error distribution for 12 hours (6 a.m. to 6 p.m. where field data collection is usually carried out) exhibited a similar distribution pattern (Figure 5-4c, 4d). Scattered horizontal position data for the same set of data shows some outliers in the southwest direction from the mean (Figure 5-5). A scatter plot of latitude and longitude error shows an oval shape error distribution pattern centered at the mean with some outliers in the southwest direction (Figure 5-6). A similar error distribution also was observed in the scattered latitude and longitude error for the base station (using Trimble Pro-XL GPS receiver) collected over the same time period (Figure 5-7). Further analysis of the PDOP, HDOP, number of satellite in sight, and the distribution of latitude, longitude and horizontal error over the 24-hour sampling period was undertaken to explain the long-tailed error distribution. The GPS signal coverage, availability and reliability stated by Anon (1995) were met. However a significant deviation in both the latitude and longitude error occurred during the

time interval from 3 p.m. to 4 p.m. on March 4, 1999 (Figure 5-8). This coincided with the lowest number of 4 satellites sighted by the Goat GPS receiver. A comparison with the base station GPS horizontal error (Figure 5-9) revealed that the Goat GPS receiver has a less scattered horizontal error than the base station GPS receiver though the error distribution of the Goat non-differential signals showed a long-tailed distribution. A frequency plot of the Goat unit non-differential horizontal error distribution over 12 hours and 24 hours period (Figure 5-10a, 5-10b) resemble similar graph pattern as described in Anon (1995) and Diggelen (1998).

Similar analysis was performed on the real-time Goat differential GPS signals data collected from March 5, 1999 to March 6, 1999 over a 24-hour period. A total of 574 static position data were collected from March 5, 1999 to March 6, 1999 where 96 % of the data are real-time DGPS and 4% are non-differential. Again, these missed 866 positional records could be due to the unexplained problem in the internal electronic circuit of the automatic data collection set up using the ATC 422 timer with the Goat unit. There were two major intervals of missing data; 1 hour and 12 hours and 20 minutes (between March 5, 1999 11:50 p.m. to March 6, 1999 12:10 p.m.) as the automatic triggering of data collection was believed to be not functioning. However, data recording was automatically working again for the last three minutes of data collection before recording was finally stopped. It was observed that these missing data occurred immediately after non-real-time DGPS data was recorded.

The 13 hours of 574 continuous data collected from March 5, 1999 to March 6, 1999 was selected for analysis among which 549 records were DGPS (95.64 %) and 25 records were GPS (4.36 %). In the 549 DGPS data 78 %, 17 % and 5 % were sampled at 60 s, 61 s and about 120 s (120 s - 121 s) respectively. Latitude and longitude error distribution of the selected 549 DGPS data showed a Gaussian pattern with a narrow spread indicating a high position resolution in both the latitude and longitudinal direction (Figure 5-11a, 5-11b). Figure 5-12 and 5-13 shows the scatter distribution of 574 position records for latitude/longitude position and latitude/longitude error of both real-time DGPS and GPS data. Obviously, DGPS position data had a better position resolution than the GPS data. There were two outlier DGPS points measured by the Goat real time DGPS unit with latitude/longitude error at -18.38 m/ -16.24 m and 44.22 m/ 13.93 m from the Goat surveyed position. These two points were recorded at 2:56 a.m. and 4:36 a.m. March 6, 1999 where only four satellites were detected by the receiver (Figure 5-14). Further analysis on the influence of PDOP and HDOP suggested good positional satellite geometry recorded by the receiver. The reason for many non-differential readings on March 6, 1999 is believed to be caused by poor reception of the US Coast Guard RTCM SC-104 signal as the Gainesville location is on the outer fringe area of this RTCM SC-104 signal coverage, being 230 km from the transmission site.

A total number of 86399 position records, sampled at 1 s interval, for the Omnistar real-time DGPS were collected over a 24-hour period from March 25,

1999 to March 26, 1999 where 30,350 (35.13 %) records were DGPS data. A final set of 567 DGPS records were selected from these 30,350 records using the beginning second of every minute for further analysis on its position resolution. Latitude and longitude error distribution showed a Gaussian pattern with a similar small spread of position resolution (Figure 5-15). Scatter distribution of the latitude and longitude DGPS position indicated an oval data distribution (Figure 5-16). The scatter distribution of latitude and longitude error in Figure 5-17 shows the error is slightly bias towards the west along the longitudinal direction. HDOP values recorded by the receiver were low coupled with a high number of satellite at around eight most of the time. There was no significant outlier recorded in the Omnistar DGPS as compared to the Goat DGPS unit (Figure 5-18).

Table 5-2 summarizes the static position resolution for the two systems. A more intensive and longer duration of evaluation, such as 3 months period of 24-hour recording may be necessary to obtain a representative distribution of position resolution of the three systems (Anon. 1995). Nevertheless, this study gave an indication of the static position resolution of the Goat and the Omnistar system where Omnistar had the best position resolution followed by the Goat DGPS system and Goat GPS system. These results are noted in the 95 percentile, mean difference, standard deviation and dRMS error where the Omnistar system has the lowest deviation (0.756 m) and best position resolution (2.493 m at 95 percentile). These results suggested the importance of DGPS

signal in position resolution where the absence of differential correction can degrade the position resolution to 60.463 m (95 percentile) for the Goat unit. Furthermore, static position resolution results obtained from these tests can also be used to compare with those as specified in the manufacturer's catalog since DGPS position resolution is dynamic and dependent on user's location. This evaluation will also enable a potential user of a positioning system in selecting an appropriate static position resolution level to be used as input in evaluating the integrated spatial accuracy requirement of a MBSVRA involving GPS, GIS and machine dynamics.

Dynamic Repeatability Tests

Visual observations of all the actual machine paths traveled using ArcView version 3.1 (Environmental Systems Research Institute (ESRI), Redlands, CA.) computer program indicated large deviations from surveyed path in some test runs for both the Goat DGPS (Figure 5-19) and Omnistar DGPS system (Figure 5-20). Only those machine paths indicated by the real-time DGPS signal was analyzed. Measurement of maximum cross-track error and percentage of real-time DGPS position data for each round of test was visually measured using the ArcView computer program using its measuring tools.

Table 5-3 summarizes the dynamic repeatability performance of the Goat unit when driving 5 rounds in clockwise and 3 rounds in counter-clockwise direction following closely to the surveyed rectangular path. The highest

percentage of about 44 % estimated real-time DGPS data point was observed in test run number 2 in the clockwise direction. However, a high maximum cross-track error of 82 m was observed in test run 2 along machine path A. It is believed that the presence of a 69 kV high-tension cable above machine path B could caused the loss of real-time signal as no real-time DGPS signal was detected by the Goat unit throughout all the test runs. Overall test run number 1 yielded the best results with maximum cross-track error ranges from 3.85 m to 8.85 m and an overall 39 % of estimated real-time DGPS data point. For MBSVR field application using this navigation system was inadequate as indicated by its low overall percentage of real-time DGPS signal couples with high maximum cross-track errors. The possibility of integrating Goat real-time DGPS with a dead-reckoning system while making use of fixed between-tree-row distance should be explored.

Table 5-4 summarizes the dynamic repeatability performance of the Omnistar unit when driving 5 rounds in both clockwise and counter-clockwise directions following closely to the surveyed field path. Generally, the percentage of real-time DGPS signal detected by the Omnistar receiver was low, where only 6 test runs out of 10 were successful. Furthermore, the overall percentage of real-time DGPS signal position data was low compared with the Goat unit. The presence of 69 kV high-tension cable also caused the lost of real-time DGPS signal for all test runs except a small section in test run 2. Generally, the magnitude of maximum cross-track error of the Omnistar receiver was lower than

the Goat unit with the highest of 12.98 m being observed in machine path A during test run 4. These results suggested the inadequacy of the Omnistar real-time DGPS receiver to be used for machine navigation in a MBSVRA. A reliable real-time DGPS machine guidance system should provide a consistently low cross-track error. The possibility of integrating Omnistar real-time DGPS with a dead-reckoning system while making use of fixed between-tree-row distance should be explored.

Conclusions

Static Predictability Accuracy Tests

Real time DGPS signals is important for static positioning as indicated by the higher position resolution for both the Goat and Omnistar receiver than the Goat non-differential signal. However, there are lower number of DGPS position data collected for both the Goat and Omnistar DGPS receiver when compared with the Goat non-differential receiver. This could be attributed to the location of test site in the fringe area of receiving the US Coast Guard beacon signal. The reason for similarly low real-time DGPS signal for Omnistar unit, which used satellite-based differential correction signal, may require a more extensive test. Also, these results suggested that there was a need for post processing of field position data, collected with these real-time DGPS units in areas where the real-time signal is weak.

The Goat and Omnistar unit had a horizontal 95-percentile error of 4.017 m and 2.493 m (R95) respectively. The standard deviation of position resolution for the Omnistar unit (0.756 m) was lower than the Goat unit (2.317m). These horizontal 95-percentile error levels of the Goat unit (4.02 m) and the Omnistar unit (2.49 m) could be used for the selection of range values of GPS static horizontal positional error (G) in the model development.

Dynamic Repeatability Tests

Using only the Goat DGPS or Omnistar DGPS receiver for real-time machine guidance in a tree-based MBSVR field application was not good enough. This was reflected in a very high percentage of DGPS positional data recorded in path A, B, C and D coupled with a high cross-track error. The presence of factors such as high-tension electricity may degrade the DGPS signal. The possibility of integrating the real-time DGPS receiver with a dead-reckoning system, as reported in other studies, should be explored.

Table 5-1. Navstar system performance specification

Position	50-Percentile	dRMS
Horizontal (m)	40	50
Vertical (m)	47	70
Spherical (m)	76	86
Velocity		
any axis (m/s)	0.07	0.1
Time		
GPS (ns)	95	140
UTC (ns)	115	170

From Monson, 1997.

Table 5-2. Comparison of GPS predictable static position resolution

Test No.	Receiver / sample size	Differential/ method	Dimension	R95 (m) ##	Mean difference (m) *	Standard deviation or dRMS error (m) @	Standard deviation (m) #
1	Goat / 1378	No	Northing	-	-0.395	27.391	27.391
			Easting	-	-2.079	21.445	21.445
			Horizontal**	60.463	29.322	34.788	18.846
2	Goat / 549	Yes/ US Coard Guard beacon	Northing	-	-0.242	1.721	1.721
			Easting	-	1.488	2.322	2.322
			Horizontal **	4.017	2.238	2.891	2.317
3	Omnistar / 567	Yes/ Omnistar satellite	Northing	-	-0.204	1.023	1.023
			Easting	-	0.000	0.948	0.948
			Horizontal **	2.493	1.183	1.023	0.756

Computed from rank and percentile of sample population for error of each computed position from a known base reference point.

* Difference between GPS/DGPS mean position and position computed from a known base reference point

@ Standard deviation with reference to a known base position

\# Standard deviation reference to the mean of measured GPS/DGPS

** Euclidean distance computed from northing and easting

Table 5-3. An example of dynamic repeatability performance for Goat DGPS

Test No. / Direction	Machine path	Max. cross-track error (m)	Percentage of real-time DGPS point (%)*
1	A	8.85	38
/clockwise	B	-na-	0
	C	3.85	52
	D	6.06	45
	Overall	-	39
2	A	82.00	21
/clockwise	B	-na-	0
	C	7.07	68
	D	10.42	85
	Overall	-	44
3	A	4.97	61
/clockwise	B	-na-	0
	C	1.96	28
	D	6.01	73
	Overall	-	42
4	A	4.89	11
/clockwise	B	-na-	0
	C	19.07	29
	D	7.25	58
	Overall	-	22
5	A	3.90	25
/clockwise	B	-na-	0
	C	26.93	34
	D	4.61	34
	Overall	-	26
6	A	3.86	12
/counter-clockwise	B	-na-	0
	C	27.91	32
	D	5.77	54
	Overall	-	24
7	A	2.63	15
/counter-clockwise	B	-na-	0
	C	4.50	24
	D	2.44	18
	Overall	-	17
8	A	-na-	0
/counter-clockwise	B	-na-	0
	C	7.91	26
	D	4.11	50
	Overall	-	16

g. Estimated total number of data point for path A (173.98 m), B (61.57 m), C (173.56 m), and D (61.58 m) are 209, 74, 208 and 74 respectively.

-na- No data

Table 5-4. An example of dynamic repeatability performance for Omnistar DGPS

Test No. / Direction	Machine path	Max. cross-track error (m)	Percentage of real-time DGPS point (%)
1/clockwise	A, B, C, D	- na -	- na -
2	A	- na -	0
/clockwise	B	4.21	23
	C	6.45	31
	D	10.09	78
	Overall	-	25
3	A	4.48	23
/clockwise	B	- na -	0
	C	4.64	17
	D	- na -	0
	Overall	-	15
4	A	12.98	12
/clockwise	B	- na -	0
	C	3.96	25
	D	- na -	0
	Overall	-	13
5	A	5.05	18
/clockwise	B	- na -	0
	C	- na -	0
	D	- na -	0
	Overall	-	7
6	A	- na -	0
/counter-clockwise	B	- na -	0
	C	3.09	19
	D	- na -	0
	Overall	-	7
7/counter-clockwise	A, B, C, D	- na -	- na -
8/counter-clockwise	A, B, C, D	- na -	- na -
9/counter-clockwise	A	- na -	0
	B	- na -	0
	C	1.88	37
	D	- na -	0
	Overall	-	13
10/counter-clockwise	A, B, C, D	- na -	- na -

h. Estimated total number of second for path A (173.98 m), B (61.57 m), C (173.56 m), and D (61.58 m) are 209, 74, 208 and 74 respectively.

-na- No data

(a)

(b)

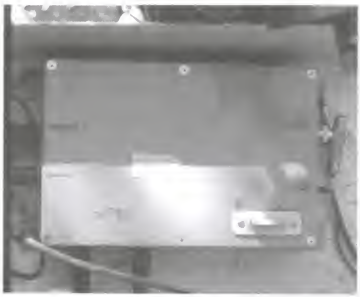

(c)

Figure 5-1. Goat system showing (a) display box, (b) antennas and (c) GPS and DGPS receiver box.

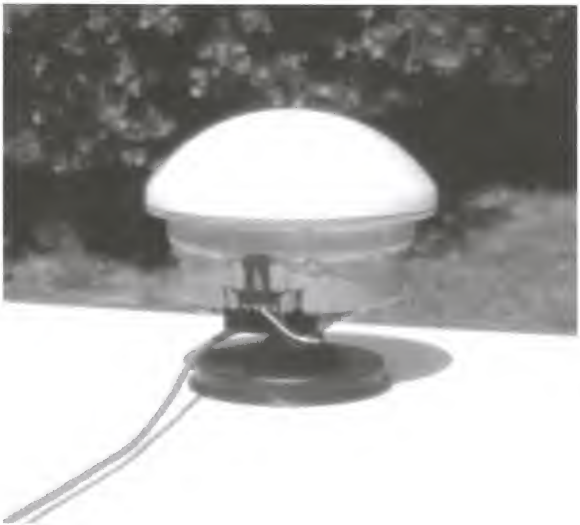

Figure 5-2. Omnistar DGPS system

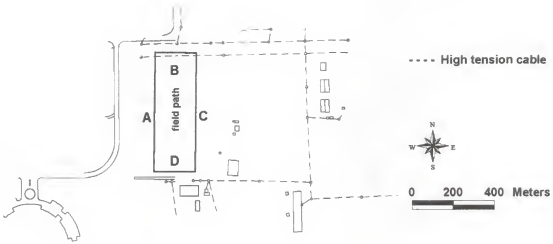

Figure 5-3. Layout of a surveyed rectangular path in a citrus field located in the University of Florida campus, Gainesville, Florida showing path section A, B, C and D for machine navigation studies.

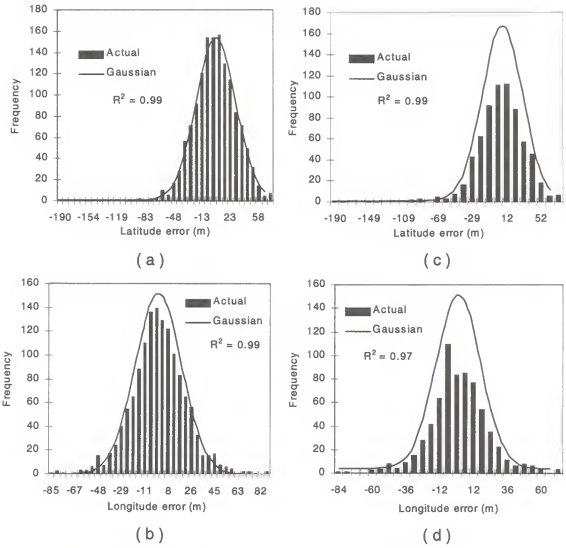

Figure 5-4. Distribution of latitude and longitude error over 24-hour (a, c) and 12-hour (b, d) periods of non-differential static positional data of the Goat unit GPS receiver.

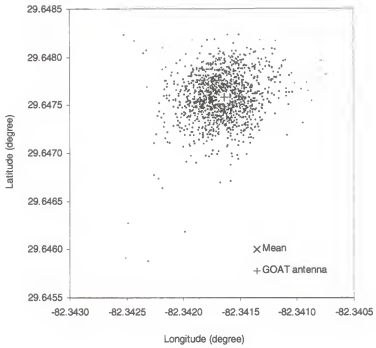

Figure 5-5. Scatter distribution of latitude and longitude non-differential static positional data of the Goat unit GPS receiver over a 24-hour period.

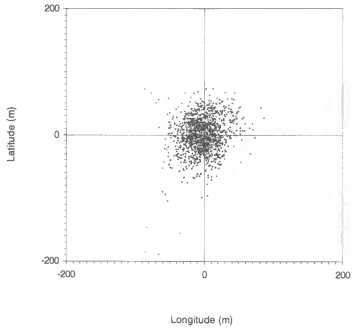

Figure 5-6. Scatter distribution of latitude and longitude error of non-differential static positional data of the Goat unit GPS receiver over a 24-hour period.

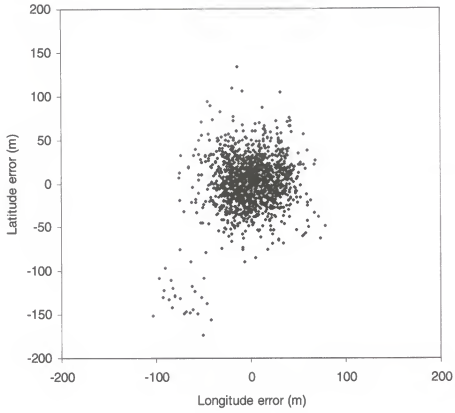

Figure 5-7. Scatter distribution of latitude and longitude error of non-differential static positional data for a base station GPS receiver over a 24-h period.

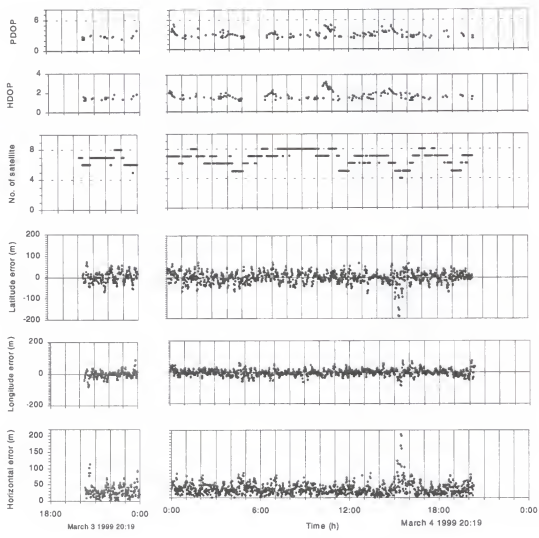

Figure 5-8. Distribution of PDOP, HDOP, number of satellite, latitude error, longitude error and horizontal error of the Goat unit GPS receiver's non-differential static positional data over a 24-hour period.

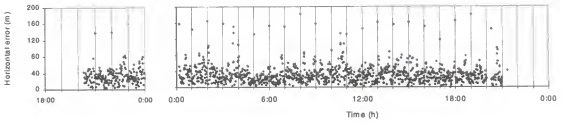

Figure 5-9. Distribution of horizontal error for the base station GPS receiver, non-differential static positional data over a 24-hour period.

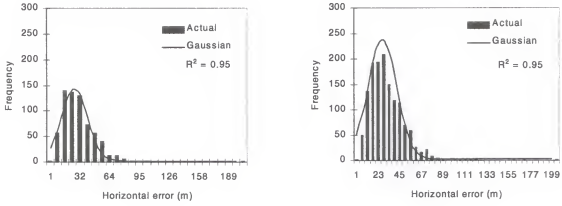

Figure 5-10. Distribution of horizontal error over (a) 12-hour and (b) 24-hour periods of the Goat unit GPS receiver's non-differential static positional data.

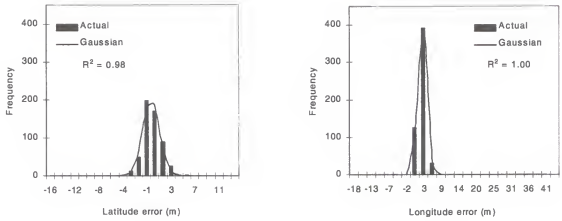

Figure 5-11. Distribution of static position latitude and longitude error over a 13-hour period for the Goat unit real-time DGPS receiver.

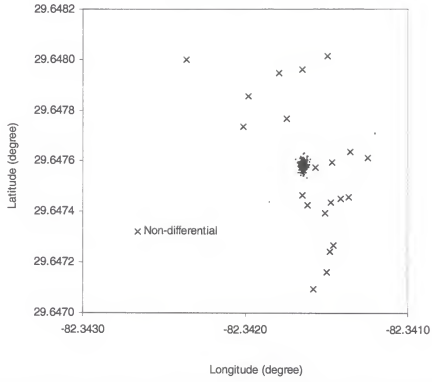

Figure 5-12. Scatter distribution of latitude and longitude static positional data of a Goat unit real-time DGPS receiver over a 13-hour period (black dots).

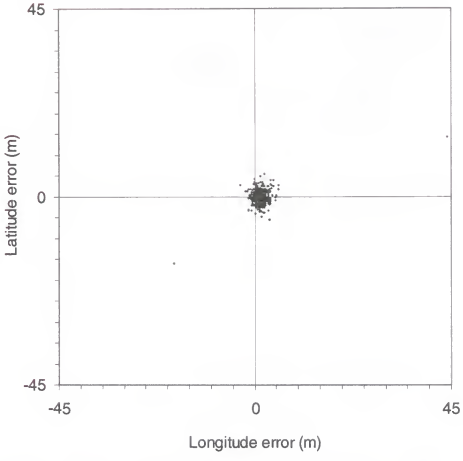

Figure 5-13. Scatter distribution of latitude and longitude error of static positional data for a Goat unit real-time DGPS receiver over a 13-hour period.

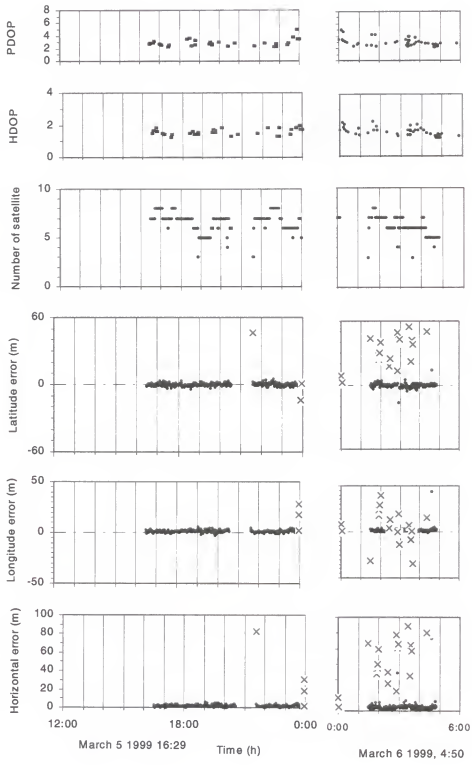

Figure 5-14. Distribution of PDOP, HDOP, number of satellite, latitude error, longitude error and horizontal error of the Goat unit real-time DGPS receiver's static positional data over a 14-hour period. (X = non-differential)

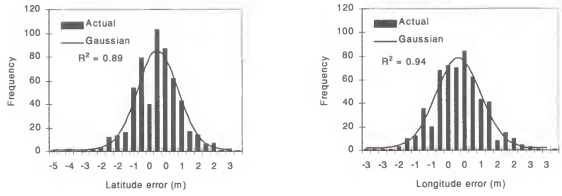

Figure 5-15. Distribution of latitude and longitude error of static positional data over a 24-hour period for the Omnistar real-time DGPS receiver.

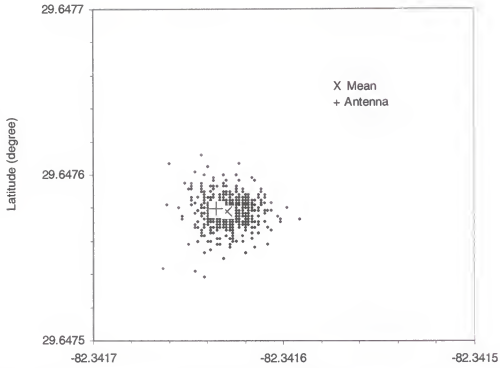

Figure 5-16. Scatter distribution of latitude and longitude static position data of an Omnistar unit real-time DGPS receiver over a 24-hour period.

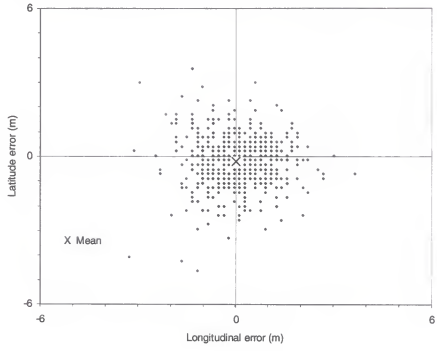

Figure 5-17. Scatter distribution of latitude and longitude error of static position data for an Omnistar unit real-time DGPS receiver over a 24-hour period.

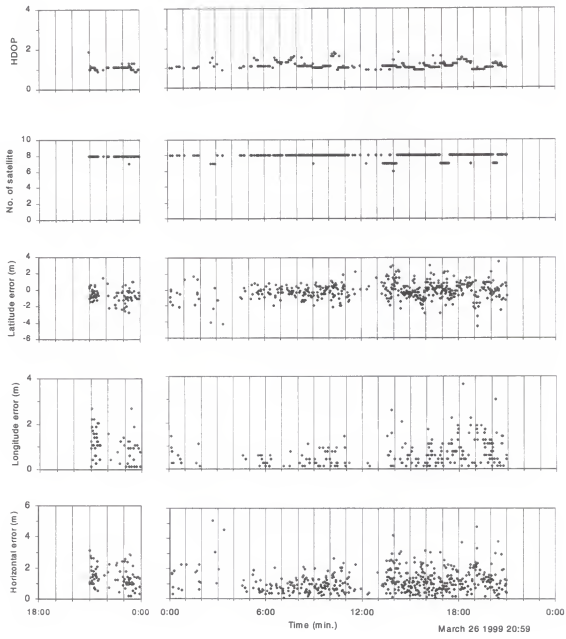

Figure 5-18. Distribution of HDOP, number of satellite, latitude error, longitude error and horizontal error of the Omnistar unit real-time DGPS receiver's static positional data over a 24-hour period

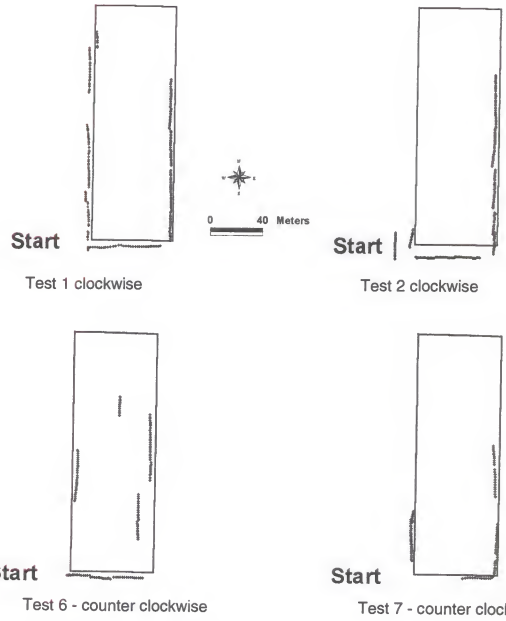

Figure 5-19. Four examples showing actual machine path over the surveyed rectangular path in a citrus field (from Figure 5-3) using the Goat real-time DGPS navigation system.

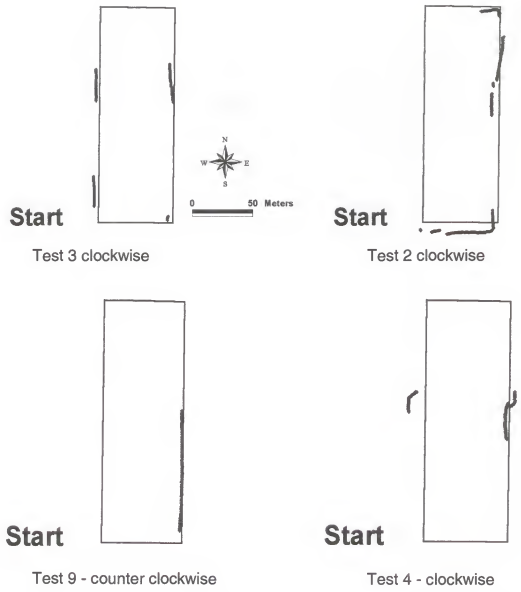

Figure 5-20. Examples of four test runs showing actual machine path over the surveyed rectangular path in a citrus field (from Figure 5-3) using the Omnistar real-time DGPS navigation system.

CHAPTER 6
DEVELOPMENT OF CITRUS YIELD MAP

Introduction

The user application, cost and time involved in acquisition and type of data needed will dictate the type of yield mapping. These objectives will dictate the hardware and software selection as they influence degree of accuracy required in the development of a yield map. Yield maps should represent actual variation in the field and not other systemic errors.

Citrus yield mapping involved the collection of manually harvested fruit in tub GPS locations in a citrus orchard. These data points were then overlaid in a base map, using a GIS computer program, for data processing to generate a yield map. Examples of citrus yield mapping were described in Whitney et al. (1998, 1999a), Schueller et al. (1999) and Chan et al. (1999a, b).

Accuracy in citrus yield mapping is very important as the starting point in the development of an application map for a MBSVRA system. An application map will highly influence the machine control process through the set point input commands to the machine controller.

Three major spatial factors influence the development of a citrus yield map: base map, GPS static predictability resolution (in recording manually

harvested fruit tub location) and yield map interpolation method. Scale of the base map will influence the shape and size of the boundary used in yield mapping. Chan et al. (1999a) studied the errors in yield mapping due to four different orchard boundaries with area increments of 7.98 %, 9.26 %, and 15.11 % over the smallest boundary defining the outer edges of the tree canopy visible from a 3 m resolution digital orthophoto. A dilution effect showing a lower yield at some edges of selected boundary of up to 350%, was reported. Besides boundary selection, Chan et al. (1999b) compared errors in yield mapping using two interpolation methods; kriging and inverse weighted distance (IWD). Both of these interpolation methods underestimated the overall yield by less than 7% when compared to the actual yield. Whitney et al. (1999a) used a higher resolution geo-referenced aerial photograph than that used in Chan et al. (1999a) in citrus yield mapping. He compared the interpolated yield variation due to density and IWD interpolation methods versus the ground truth by analyzing the whole field area by dividing them into square cells of two-row tree wide (18.2 m). The two interpolation methods overestimated the mean ground truth yield by 8 %. Hence, optimal selection of a yield mapping method to represent ground truth yield requires investigation. The effect of GPS static predictability resolution in citrus yield mapping has not been studied. Integrated effects of base map, GPS static predictability resolution and yield map interpolation method in yield mapping need to be further investigated. They influence the choice of GPS hardware, interpolation method and degree of

accuracy of aerial photograph needed for the base map required in the citrus yield mapping development.

Using similar citrus yield mapping examples as described in Whitney et al. (1999a) and Chan et al. (1999b), the choice of yield mapping parameters were investigated to obtained the best map representing the ground truth yield. Also, yield maps for subsequent processing into application maps to study the integrated effects of base map accuracy, GPS static predictability resolution and interpolation method on citrus yield mapping for a citrus MBSVRA system were developed. The objectives of this study were to identify the best parameters and methods in citrus yield mapping to obtained the best yield map. Citrus yield maps for subsequent processing into N application maps using three major spatial parameters: different field boundaries (2) selected from two base maps, static predictable GPS/DGPS position resolutions (5) and interpolation methods (2) were developed.

Review

Yield Data

Current practice in the harvesting of Florida citrus is manual picking by workers using ladders, and picking bags and placing the fruits in a field containers (tubs or pallet bins) which normally have a capacity of 10 field boxes (approximately 0.7 m^3 by volume). Whitney et al. (1999a) described the operation of collecting tub location in a citrus orchard using a specialized truck

equipped with a commercial yield monitor, Goat, fitted with a GPS unit (Figure 6-1a). Figure 6-1b shows the field data collection. A description of the same unit is in Chapter 5. The Goat unit was controlled by an operator, recording fruit tub position in latitude, longitude, date and time, manually pushing a button located on the Goat unit display box. The yield data collected from the field was then downloaded via a RS232-connection using a software interface program developed by GeoFocus. Further data post processing was needed in non-differential GPS positional data for differential correction. Whitney et al. (1999b) reported an upgraded version of the Goat unit using real-time DGPS signals. No further data post processing was needed for those DGPS positional data. To facilitate weight measurement of harvested fruits, Miller and Whitney (1999) incorporated a weighing system in the Goat unit. Ideally, the fruit tub location should represent the true yield point representing those fruit trees where they were harvested. They reported that the fruit tub locations in the field were chosen by the harvester and it was assumed that the container was near the centroid of the harvested area as the harvester wants to minimize the average distance he carries the fruit. Meanwhile, Schueller et al. (1999) reported that the volumetric consistency in filling a fruit tub by the worker may be achieved as the worker will not overfill the fruit tub to maximize their income (which is dependent on how many tubs they have harvested) and the management will not let them underfill.

However, problems in recording wrong yield data due to field operation by Goat truck operator have been reported (Whitney et al., 1999a; Schueller et al., 1999). This human error can be minimized when an automated yield data recording system using the Goat is available. Schueller (1999) suggested that implementation of mechanized citrus harvesting operation may be able to alleviate this problem by measuring the weight of the recovered fruit from each tree after the machine had completed removing the fruit from that tree.

Yield Mapping

Base map

Whitney et al. (1999a) described a geo-referenced aerial photograph used as a base map in citrus yield mapping where the field boundary was identified. Meanwhile Chan et al. (1999b) used the same set of data but used a 3-m resolution digital orthophoto quadrangles downloaded from the web site http://www.labins.org/doqq/county.htm to study the effects of four boundary selections on citrus yield mapping error. The selection of different scale of base map will offset the boundary used in yield mapping.

Interpolation methods

Kriging is an advanced interpolation procedure that generates an estimated surface from a scattered set of points with attribute values. Before kriging interpolation, the spatial variation of attribute values is analyzed to produce a semivariogram. The semivariogram is estimated using the input point

data set. The value of the sample semivariogram for a separation distance of h (referred to as lag) is the average squared difference in attribute value between pairs of input sample points separated by h. Subsequently, the semivariogram is modeled by fitting a theoretical function to the sample semivariogram. The best estimation method for generating the output surface is obtained based on the best fitted semivariogram.

Kriging is based on the regionalized variable theory which assumes spatial variation represented by the attribute values is statistically homogeneous throughout the surface. This hypothesis of spatial homogeneity is fundamental to the regionalized variable theory.

Kriging interpolation then uses a weighted moving average technique to assign an estimated value to a particular location. Kriging estimates the value of a spatially distributed variable from adjacent values while considering the interdependence expressed in the semivariogram. A weighted moving average equation is developed to estimate the true value of a regionalized variable at specific locations. This equation is designed to minimize the effect of the relatively high variance of the sample values by including knowledge of covariance between the estimated point and other sample points within the range.

Other linear unbiased estimators exist, such as polygonal, triangulation, IWD, but Kriging is believed to be the best linear unbiased estimator. It is the

minimum variance estimator, that is, it minimizes the variance of the estimation errors.

McCauley and Engel (1997) described kriging interpolation as attractive and complex to an untrained person. Isaaks and Srivastava (1989) mentioned that ordinary kriging (one of the kriging methods) is one of the most computational intensive and mathematically tedious point estimation methods. This method accounts for nearby clustering data as well as for their distance to the point being estimated. The choice of selecting an appropriate semivariogram is important. They described IWD as suitable for regularly gridded data but with an inability to account for data clustering.

Ordinary kriging includes: spherical, circular, exponential, Gaussian, and linear methods. It assumes that the variation in attribute values is free of any structural component (drift).

The IWD interpolation assumes that each input point has a local influence that diminishes with distance. Points closer to an estimated point carry weights greater than those farther away. A specified number of points, or all points within a specified radius, can be used to determine the output value for each location.

Materials and Methods

Similar steps described in Whitney et al. (1999a) and Chan et al. (1999a, b) were used in the development of citrus yield maps. A summary of the variables used in the yield mapping is described in Table 6-1. A GIS software,

ArcView version 3.1 with Spatial Analyst extension version 1.1 (Environmental Systems Research Institute (ESRI), Redlands, CA) was used in the data analysis and yield mapping.

Site

The study area was a 3.6 ha orchard of citrus trees, located in Manatee County, FL, centered at longitude 82.2775^{0}W and latitude 27.6423^{0}N which had been planted in 1986 with 'Hamlin' orange on 'Carrizo' rootstock. The site was typical of flatwoods areas in Florida with poorly drained soils, and a relatively high water table. The between rows tree spacing was 9.14 m and an in-row spacing of 4.3 m. The trees had formed a continuous hedgerow in this study as reported in Whitney et al. (1999a) and were 4 to 5 m high.

Yield Mapping

Yield data

The same set of 620 data points from Whitney et al. (1999a) were used in this study. It was assumed that each data point represented the best position for yield location within the 3.6 ha orchard.

Base map and boundary

The same 1:30,000 scale, 0.32 m pixel resolution, geo-referenced black and white aerial photograph described in Whitney et al. (1999a) and 1:40,000 scale, 3 m pixel resolution, color digital orthophoto quadrangles (DOQ) described in Chan et al. (1999b) were selected.

A rectangular field boundary was selected to exclude the effect of irregularly shape field boundary in yield mapping. A boundary B of 3.1 ha was selected using the 1:30,000 scale geo-referenced black and white aerial photo by visually viewing the aerial photo on a computer screen overlaid with yield data points marking out the outer edges of the tree canopy in the 3.6 ha orchard (Figure 6-2). The outer edges of the tree canopy were selected and the purpose of the yield map was for subsequent development of desired fertilizer application map to be used by a MBSVR applicator. It was hypothesized that the applicator operation is initiated when a tree canopy is detected by the applicator sensor. Marking of the boundary was started from the top right corner of the last row of harvested trees and adjusted by the number of between tree rows spacing of 9.14 m along the east-west direction and 4.3 m in-row tree spacing along the north-south direction. This boundary was considered the best boundary for this study. A total of 506 tub data points were enclosed by boundary B.

Similar steps were used in defining boundary L using the 1:40,000 scale 3-m resolution DOQ (Figure 6-3). Boundaries B and L were overlaid together and Boundary L appeared to be shifted along the south-west direction due to the effect of a lower resolution in the 3 m DOQ than the black and white aerial photo (Figure 6-4). A total of 503 tub data points were enclosed by boundary L.

Modeling of tub GPS static location

Five levels of GPS static horizontal positional error (circular) (G) of 0 m, 0.5 m, 1 m, 3 m and 5 m were selected in this study. The original tub location

data set was assumed to represent the true yield points influencing the crop yield having a 0 m G. Goense (1997) described GPS horizontal error as represented by a standard deviation of 0, 0.5, 1, and 2 m in his developed calculation model. Similar definition was used in this study to describe the G. Modeling of the other four levels of G were based on the worst case GPS 2dRMS circular error scenario and was assumed that the GPS data are randomly distributed along the 2dRMS circle. For example, in a G of 1 m, all the 506 data points were modeled using a spreadsheet computer program by randomizing the angular distribution of each yield points at 1 m from the original yield point. Figure 6-5 shows a sampled view of some of the points at five different levels of G. Only one set of the 506 data points was modeled for each error level of G as the 506 data points used in the randomized modeling of G was considered sufficiently large.

Map interpolation

The number of selected tub locations used in map interpolation was based on all those data points contained completely within either Boundary B or L. The citrus yield mapping involved interpolation of a yield density map to produce point estimation of yield density values at each tub location followed by surface interpolation of tub locations, using either IWD or ordinary kriging method. Detailed descriptions of the steps for interpolation method using density method and IWD surface interpolation method were described by Whitney et al. (1999a) except that the search radius which will be identified. Details of similar

methods used for ordinary kriging interpolation method were described in Chan et al. (1999a). Appendix C provides a summary of both the IWD and kriging interpolation methods.

Isaaks and Srivastava (1989) described various criteria (for example, lowest standard deviation, smallest mean absolute error, smoothness of output) and methods in the selection of point estimation method. They used univariate and bivariate descriptive tools to compare the distribution of estimated data points using different interpolation methods. The univariate distribution of estimated data was said to indicate close matching to the true data distribution. The bivariate distribution of estimated data will indicate the point estimation performance. The goal was to produce an unbiased estimation. They mentioned the reality of always having some error in estimation and that the best method depends on the preferred criteria in the selection of estimation method.

Yield map analysis was performed by a raster-based grid-cell geoprocessing system called *Grid* available in the ArcView Spatial Analyst 1.1 program. A grid was first divided into uniform square cells each represents an actual portion of geographic space. The cell size selected was small enough to capture the required details but large enough so that computer storage and analysis was performed efficiently. The yield map square cell size selected for this study was 0.457 m, less than the smallest resolution of G at 0.5 m and 1/20 the between tree rows spacing (9.14 m).

Density interpolation was the first step in point estimation of tub locations for subsequent yield surface interpolation. Accurate density interpolation required a selection of the best parameters used. Besides cell size, kernel density calculation method was chosen to calculate the yield data found in the search neighborhood, which was distributed out around each point, and divide by the area of the search circle thus giving a smoother output. The next important parameter selected was the best search radius in density mapping. This was the distance used to search from each cell in the output grid for points to be used in the density calculation. Isaaks and Srivastava (1989) suggested at least the closest four samples to be included in the search radius for pseudo regular grid data. They reported a simple formula for calculating average spacing between data equal to the square root of total area covered by samples divided by the number of samples. In this study, for 506 data points used in boundary B or L, the computed search distance would be 7.82 m. Obviously this distance was inappropriate as it is shorter than the between tree-row spacing of 9.14 m. Whitney et al. (1999a) used a search radius of 18.2 m considering the influence of fruit yield harvested from the width of two rows of tree spacing or 18.2 m. Considering the distribution of tub locations in Figure 6-2, three search radii of 9.14 m, 18.28 m and 22.85 m were selected to investigate the best search radius using 506 data point in boundary B for density map interpolation. A search radius of 9.14 m was chosen as it represented the between tree-row spacing while 18.28 m was for the same reason mentioned in Whitney et al.

(1999a). Finally, the choice of 22.85 m covers the distance from the middle of two tree rows until the outer row of tree in adjacent two rows of trees (as some tubs points appears to be located at a distance further than 18.28 m). Evaluation of the best search radius was carried out by comparing the density map yield versus the ground truth yield on a sub-block basis (Figure 6-6).

Similar comparisons in the selection of the best yield interpolation method between IWD and ordinary kriging were conducted using the best search radius identified above. In ordinary kriging, the selection of the best lag distance and ordinary kriging model was chosen by using the semivariogram evaluation at three different lag distances of 4.3 m, 9.14 m and 18.28 m and four fitted models (spherical, circular, exponential and Gaussian). The choice of the best interpolation method was evaluated for its point estimation when compared to the density map estimated values and by sub-block analysis of the interpolated yield versus ground truth.

Yield maps were developed using 20 combinations of variables described in Table 6-1 using Y (2), G (5) and P(2). The best search radius, cell size and lag distance were used in both interpolation methods.

Results And Discussions

Boundary Selection

Yield map interpolation was based on the analysis of yield data points located within a region. Identification of a correct boundary containing yield data

points was therefore important to accurately represent yield distribution of the region. The location of the boundary was dependent on the scale of the base map used when selected by visual observation from the digitized aerial photograph. Boundary L was shifted by about 4.6 m towards the south-west direction from Boundary B and thus introduced some mapping errors. Obviously, a higher scaled base map such as the 1:30,000 geo-referenced aerial photograph could provide a more accurate field boundary selection than the 1:40,000 DOQ.

Yield Data

Yield data were the bases of yield mapping. Ideally, the yield sampling should be based on individual tree yields. Nevertheless, the present method of yield data collection offered a good alternative in obtaining "true" ground yield for a citrus orchard.

Modeling of Tub GPS Static Location

The present simple method of modeling tub locations using the original tub points provides a means to compare the effects of DGPS error on yield mapping. It is based on the worst case scenario where all the data points are randomly located at a fixed horizontal error distance away from a known point. In reality, the GPS/DGPS horizontal error distribution may not be at the same error level throughout the whole field as shown in the study on static GPS/DGPS static predictable accuracy evaluation for Goat and Omnistar GPS/DGPS

receivers. Future study may include modeling of GPS/DGPS data using a fitted model describing the error distribution of a GPS/DGPS receiver with field data collected over a 24-hour period. Several repeated simulations to model G at different error levels could also be done based on a representative static horizontal positional data distribution of a GPS/DGPS receiver collected (over an appropriate period) in a specific citrus orchard.

Map Interpolation

Figure 6-7a, b and c show three different yield density maps using three different search radii at 9.14 m, 18.28 m and 22.85 m. The distribution of yield surface for search radius of 9.14 m was discontinuous along the east-west direction resulted in strips of 0 to 20 t/ha yield areas. Table 6-2 summarizes the sub-block analysis of interpolated yield density maps using 506 tub data points in boundary B. Search radius of 9.14 m shows a high coefficient of yield variation (C.V.) of 78.6 % despite having the closest overall yield estimation to the ground truth yield coupled with the highest coefficient of correlation (0.51). Observations of trees distribution in the orchard from aerial photograph and harvested fruit tubs locations suggested that the discontinuous yield density surfaces using 9.14 m search radius is unacceptable. Search radii of 18.28 m and 22.85 m resulted in a continuous density yield surface along the east-west direction with a lower C.V. of 25.5% and 24.2% estimated yield surface variation than search radius of 9.14 m. These yield surfaces were more representative of

the fruit yield considering the tree distribution in the orchard. A search radius of 18.28 m was selected as its estimated mean yield of 63.56 t/ha relates closest to the ground truth yield of 66.33 t/ha coupled with a C.V. of 7.1 %. Figure 6-8 shows the distribution of estimated yield versus ground truth along the 12 sub-blocks from A to L where search radius of 18.28 m obviously provide the best estimated yield among the three search radii.

The density interpolation method available in the GIS software was limited in its ability to analyze the spatial continuity of the present set of yield data as it uses a circular search neighborhood method. This limitation was reflected in the choice of a search radius of 9.14 m which relate closest to the ground truth yield with the highest correlation coefficient but was rejected due to its high C.V. in the estimated yield and a discontinuous interpolated yield surface along the east-west direction. The present set of yield data shows a distinct orientation along the north-south distribution. Other search methods such as the anisotropic search neighborhood (Isaaks and Srivastava, 1989) could be explored with a different GIS software.

Figure 6-9 a, b and c are semivariograms using kriging method with lag distances of 4.3 m, 9.14 m and 18.28 m respectively. The distance for semivariograms was limited to a maximum distance equal to half the sampled dsitance, 110 m (Ingram, 1998). A lag distance of 18.28 m for exponential and Gaussian model was rejected as the fitted model was poor. A lag distance of

9.14 m using exponential and Gaussian models were selected for final analysis as most of their modeled points fitted closely to the actual points.

An analysis of estimated yield data points among the three surface interpolation methods; IWD, kriging-exponential (kriging method using exponential model) and kriging-Gaussian (kriging method using Gaussian model) was performed with the density method (Table 6-3). The IWD method appeared to provide the best point estimation of the density yield data points. Table 6-4 provides a summary of error distribution among IWD, kriging-exponential and kriging-Gaussian methods where IWD has the best estimation of the density estimated yield data points. Scatterplots of density yield data point versus IWD, kriging-exponential and kriging-Gaussian were developed on Figure 6-10 where IWD provided the closest estimation of density yield data points.

Apparently IWD method seems to provide the best point estimation to the density yield data points. However, Isaaks and Srivastava (1989) reported the inadequacy of IWD interpolation method in accounting for clustered data. Clustered data was reported to cause a larger spread of error distribution than non-clustered data in IWD method. Figure 6-2 shows the citrus yield tub data point distribution that is clustered along the north-south directions. They mentioned that ordinary kriging method does account for these spreads of error distribution for cluster data as it minimizes the variance of the estimation errors.

This was also reflected in a smoother yield map surface in kriging-Gaussian method than density and IWD methods (Figure 6-11).

Figure 6-11 shows three yield maps developed by density interpolation, kriging-Gaussian and IWD methods. They appeared to be similar except variations in some field locations in the selected field block. With the absence of individual tree yield data, a sub-block analysis was needed to compare how closely these three yield maps estimated the ground truth. The yield map which provide closest estimation to the ground truth with the lowest standard deviation was considered as the best estimation method. Table 6-5 summarizes the analysis for all the 12 sub-blocks from A to L where kriging-Gaussian method provided the best estimation of the ground truth yield with an overall mean yield of 66.33 t/ha. Figure 6-12 shows the sub-block mean yield distribution, standard deviation and sub-block yield estimation error for the three estimation methods for sub-block A to L. Kriging-Gaussian method resulted in the best overall estimation (66.33 t/ha) closest to the ground truth with the lowest standard deviation (3.96) coupled with the best coefficient of correlation (0.48) to the ground truth yield and was therefore selected as the best yield map to be used as comparison for all the other yield maps.

Yield Maps for Desired Maps

Figures 6-13 to 6-16 were subsequently generated using the variables listed in Table 6-1 for further data processing and development of desired maps

for a map-based fertilizer application using a MBSVR applicator. For ease of visual comparisons, yield levels were classified to 5 equal intervals of 20 t/ha ranging from 17 t/ha to 117 t/ha. Generally, yield zones in maps for kriging-Gaussian interpolation methods appeared smoother than the IWD method.

Conclusions

Several choices of citrus yield mapping parameters were investigated to obtain the best map representing the ground truth yield using a GIS software, ArcView version 3.1 with Spatial Analyst extension version 1.1. Comparisons of three different search radii (9.14 m, 18.28 m and 22.85 m) in density point estimation method, with sub-block analysis in the present set of data, found that 18.28 m was the best distance which relate closest to the ground truth yield. The density interpolation method available in the GIS software was limited in its ability to analyze the spatial continuity of the present set of yield data in the choice of a search radius of 9.14 m which relate closest to the ground truth yield with the highest correlation coefficient but was rejected due to its high C.V. in estimated yield and a discontinuous interpolated yield surface along the east-west direction. A square cell size of 0.457 m was selected for all the map interpolation. Two interpolation methods, IWD and kriging-Gaussian, were evaluated. Kriging-Gaussian interpolation method using a search radius of 18.28 m with a lag distance of 9.14 m in boundary B having yield data point of 0 m GPS horizontal error was selected as the best yield map estimation to the

ground truth yield. Twenty yield maps for subsequent processing into application maps for a MBSVR fertilizer applicator to study the integrated effects of two different field boundaries selected base on two base maps scale, five static predictable GPS/DGPS position resolution and two interpolation methods were developed.

Table 6-1. Summary of variables used in the development of citrus yield maps

Boundary	GPS static horizontal error (m)	Interpolation method
Boundary B - obtained using a Geo-referenced black and white aerial photo at a scale of 1:30,000 with a pixel resolution of 0.32 m	0	Inverse weighted distance
	0.5	Kriging
	1	
	3	
Boundary L - obtained using a color digital orthophoto at a scale of 1:40,000 with a pixel resolution of 3m	5	

Table 6-2. Comparisons of ground truth yield per field sub-block basis versus estimated yield using three different search radius selections in density map interpolation.

Field sub-block	Ground truth (t/ha)	Estimated yield in density map (t/ha)					
		Search radius (m)					
		9.14		18.28		22.85	
		Mean*	Range	Mean*	Range	Mean*	Range
A	69.10	68.57	0 - 213.80	60.00	10.57 - 98.00	55.63	17.47 - 97.59
B	78.82	72.57	0 - 202.24	67.39	4.08 - 97.47	66.90	10.12 - 97.43
C	65.96	73.71	0 - 242.08	68.82	4.29 - 95.88	67.10	11.43 - 92.98
D	63.02	62.90	0 - 191.59	58.90	7.39 - 89.22	58.98	17.14 - 88.73
E	62.82	66.33	0 - 228.69	63.06	18.57 - 91.22	61.39	21.06 - 84.33
F	66.20	61.76	0 - 216.37	57.96	4.98 - 86.90	58.04	9.47 - 88.49
G	56.53	66.33	0 - 210.41	63.02	5.84 - 90.20	62.12	11.67 - 89.84
H	66.20	68.29	0 - 250.65	63.31	13.43 - 90.57	62.29	16.98 - 89.96
I	58.12	63.02	0 - 208.04	61.96	18.08 - 91.59	61.59	20.69 - 79.80
J	70.90	68.69	0 - 253.22	65.63	25.76 - 94.73	65.31	29.27 - 90.37
K	67.51	77.47	0 - 245.76	73.92	29.02 - 89.76	72.04	30.20 - 89.96
L	70.90	69.35	0 - 213.96	62.37	18.45 - 86.86	57.47	16.98 - 87.55
Overall mean	66.33	65.42	67.76	63.56	63.51	62.40	62.29
Standard deviation	5.98	4.68	53.22	4.50	16.20	4.73	15.06
C.V. (%)	9.0	7.2	78.6	7.1	25.5	7.6	24.2
Coefficient of correlation	-	0.51	-	0.30	-	0.20	-

* = Weighted mean

Range = yield values of grid cell

Table 6-3. Summary statistics for the distribution of point estimated "Truth" and estimated yield values for the tub locations.

Parameters	Estimated yield (t/ha)			
	Density "Truth"	IWD	Kriging Exponential	Kriging Gaussian
Sample size	506	506	506	506
Mean	69.84	69.84	69.84	69.84
Standard deviation	14.61	14.61	12.90	13.22
Coefficient of variation C.V. (%)	21	21	18	19
Minimum	26.16	26.20	33.43	32.78
25 percentile	58.82	58.78	60.29	60.12
Median	71.96	71.92	71.71	71.76
75 percentile	81.88	81.80	80.65	80.86
Maximum	94.78	94.69	93.22	94.53
Correlation coefficient	-	1.000	0.993	0.987

Table 6-4. Summary statistics for the error distribution of point estimated "truth" obtained from interpolated density map and three estimated yield methods values for the tub locations.

Parameters	Estimated yield (t/ha)		
	IWD	Kriging Exponential	Kriging Gaussian
Sample size	506	506	506
Mean	0.00	-0.04	0.00
Standard deviation	0.04	2.41	2.65
Minimum	-0.33	-12.33	-10.16
25 percentile	0.00	-1.10	-1.43
Median	0.04	0.41	0.41
75 percentile	0.04	1.55	1.71
Maximum	0.37	4.49	5.96
Mean absolute error	0.04	1.76	2.03
Mean square error	0.09	140.33	169.76

Table 6-5. Comparison of ground truth yield per field sub-block basis versus estimated yield of field block yield using three different interpolation methods for the tub locations.

Field sub-block	Truth (t/ha)	Estimated mean yield (t/ha)					
		Density *		IWD		Kriging Gaussian	
		Mean	Range	Mean	Range	Mean	Range
A	69.10	60.00	10.57 - 98.00	70.12	40.29 - 94.08	69.10	42.20 - 93.55
B	78.82	67.39	4.08 - 97.47	70.82	38.61 - 91.06	69.18	36.78 - 93.39
C	65.96	68.82	4.29 - 95.88	73.39	39.14 - 94.69	71.39	40.78 - 95.10
D	63.02	58.90	7.39 - 89.22	63.02	40.37 - 84.61	62.41	40.24 -88.45
E	62.82	63.06	18.57 - 91.22	66.90	40.65 - 89.31	65.22	39.71 - 87.96
F	66.20	57.96	4.98 - 86.90	61.92	34.16 - 86.24	60.78	32.73 - 86.24
G	56.53	63.02	5.84 - 90.20	65.80	26.65 - 89.59	64.29	28.49 - 87.76
H	66.20	63.31	13.43 - 90.57	65.96	28.20 - 88.16	64.45	28.53 - 88.04
I	58.12	61.96	18.08 - 91.59	63.88	31.47 - 91.10	62.98	32.41 - 89.02
J	70.90	65.63	25.76 - 94.73	66.98	35.88 - 94.45	65.88	38.45 - 92.73
K	67.51	73.92	29.02 - 89.76	75.76	43.39 - 89.31	74.08	38.61 - 88.24
L	70.90	62.37	18.45 - 86.86	69.47	26.20 - 86.78	68.53	32.53 - 88.04
Mean	66.33	63.56	63.51	67.71	67.59	66.33	66.12
Standard deviation	5.98	4.50	16.20	4.19	11.88	3.96	12.78
C.V. (%)	9.0	7.1	25.5	6.1	17.6	6.0	19.30
Coefficient of correlation	-	0.30	-	0.46	-	0.48	-

Note:

a. * = Search radius of 18.28 m
b. Truth = Ground truth yield
c. Mean = Weighted mean
d. Range = Estimated yield of grid cell value
e. Coefficient of correlation is based on the 12 samples (A to L) of ground truth yield

(a)

(b)

Figure 6-1. (a) An instrumented truck equipped with a GeoFocus Goat GPS (yield monitor) (b) used in collecting manually harvested citrus field tubs.

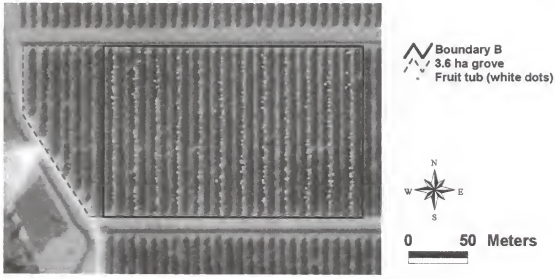

Figure 6-2. Original location of tubs of harvested fruit (dots) overlaid on a geo-referenced aerial photograph of the 3.6 ha orchard.

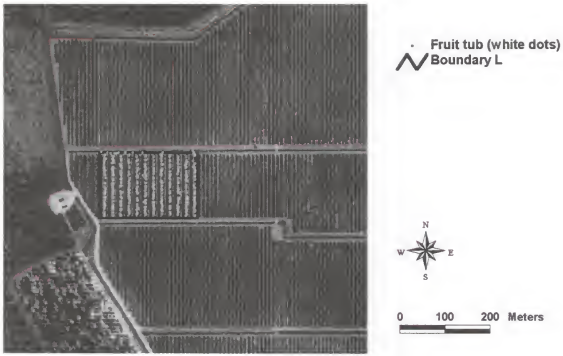

Figure 6-3. Original location of tubs of harvested fruit (white dots) overlaid on a 3 m resolution digital orthophoto quad map of the 3.6 ha orchard.

Figure 6-4. Two selected rectangular boundaries B and L (3.1 ha) of the 3.6 ha orchard.

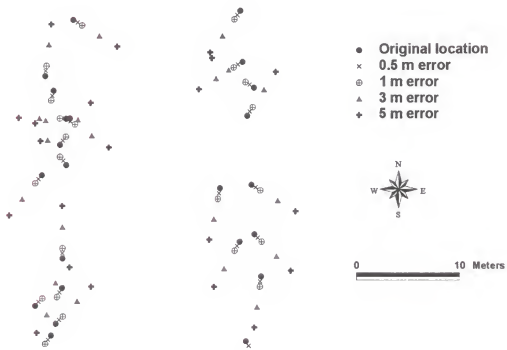

Figure 6-5. A sample distribution of two adjacent rows of tubs representing harvested fruits locations with four modeled GPS static horizontal positional errors at 0.5, 1, 3 and 5 m.

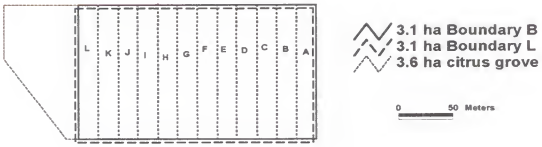

Figure 6-6. Field sub-blocks A, B, C, D, E, F, G, H, I, J, K and L of a selected rectangular boundary B (3.1 ha) of the 3.6 ha orchard overlaid with boundary L.

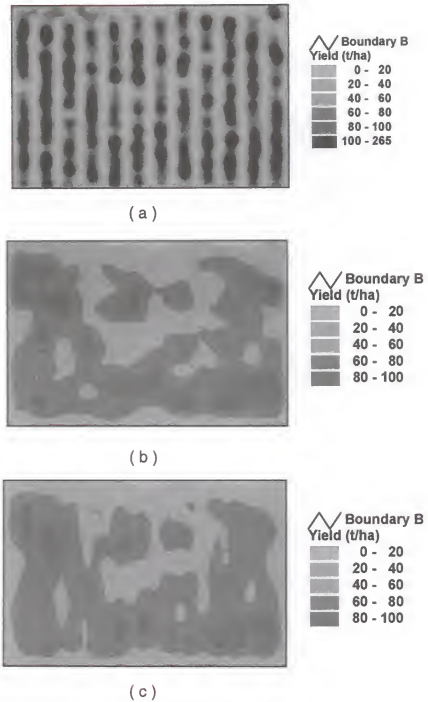

Figure 6-7. Interpolated yield density maps using 3 search radii at (a) 9.14 m, (b) 18.28 m and (c) 22.85 m.

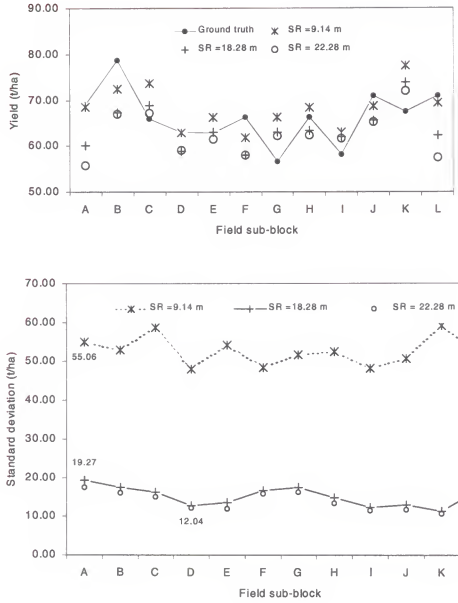

Figure 6-8. Field sub-block comparisons of weighted mean yield and standard deviation of interpolated density yield maps using three different search radii (SR) at 9.14, 18.28 and 22.85 m.

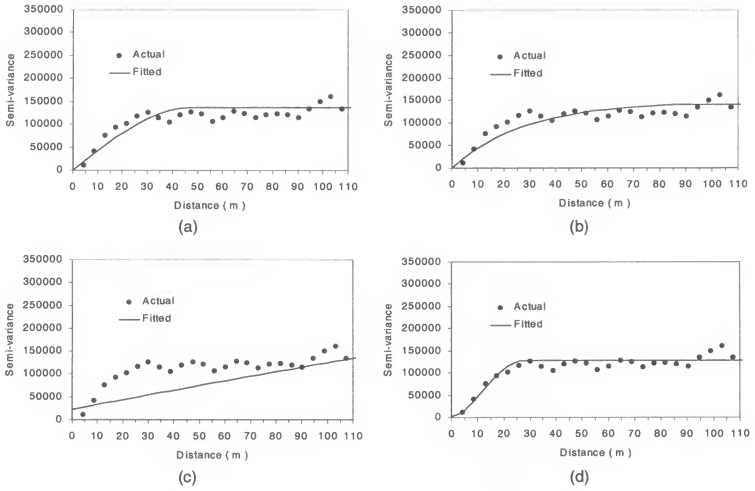

Figure 6-9 a. Semi-variograms of harvested fruit tub yield data using four models; (a) spherical, (b) exponential, (c) circular and (d) Gaussian at a lag distance of 4.3 m and a search radius of 18.28 m

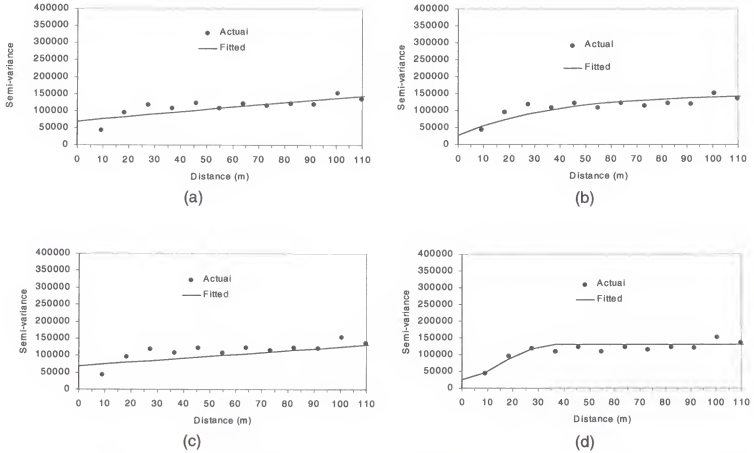

Figure 6-9 b. Semi-variograms of harvested fruit tub yield data using four models; (a) spherical, (b) exponential, (c) circular and (d) Gaussian at a lag distance of 9.14 m and a search radius of 18.28m.

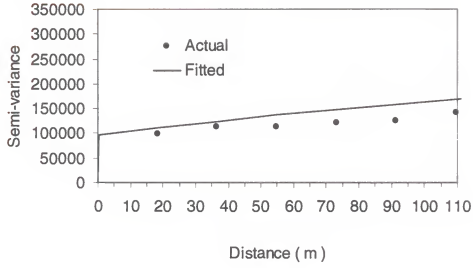

(a)

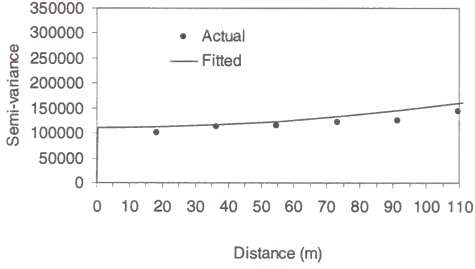

(b)

Figure 6-9 c. Semi-variograms of harvested fruit tub yield data using two models; (a) exponential and (b) Gaussian) at a lag distance of 18.28 m and a search radius of 18.28 m

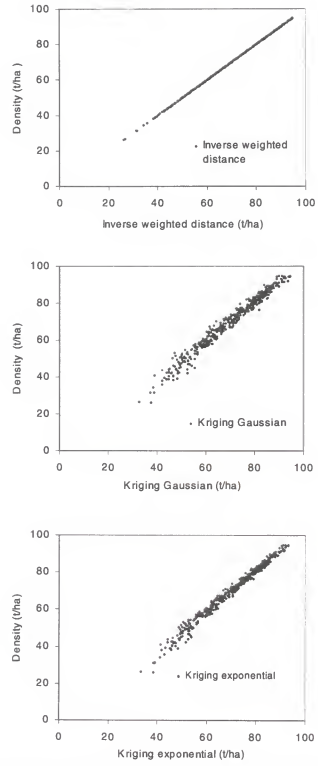

Figure 6-10. Scatterplots of density yield point values of each tub versus interpolated yield point values obtained using inverse weighted distance, kriging-Gaussian and kriging-exponential methods.

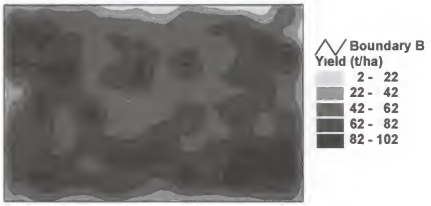

(a)

(b)

(c)

Figure 6-11. Yield maps of (a) density, (b) kriging-Gaussian and (c) inverse weighted distance (IWD) interpolation methods in Boundary B

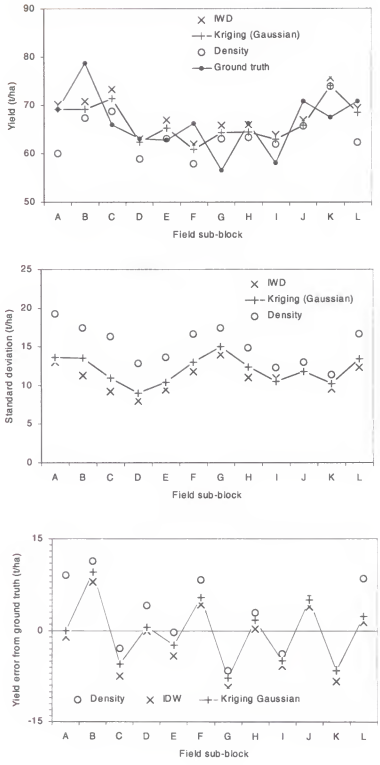

Figure 6-12. Field sub-block comparisons of ground truth yield versus inverse weighted distance (IWD), kriging-Gaussian and density yield estimation methods.

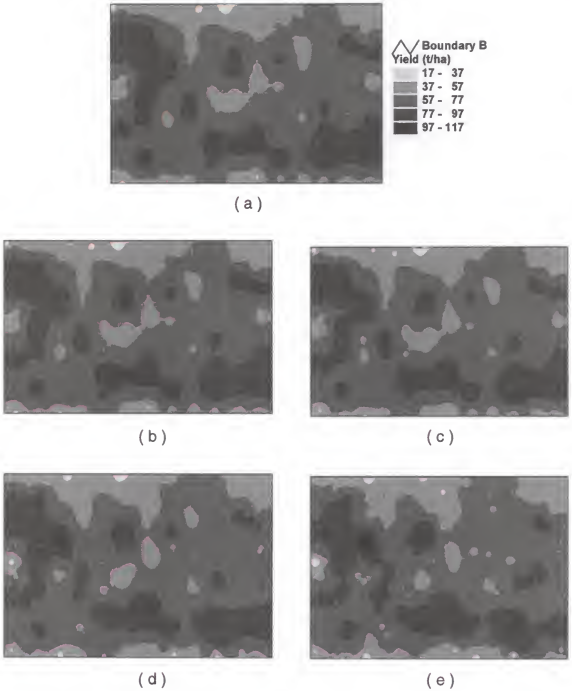

Figure 6-13. Interpolated yield maps using inverse weighted distance method in boundary B for GPS static horizontal error of (a) 0 m, (b) 0.5 m, (c) 1 m, (d) 3 m and (e) 5 m.

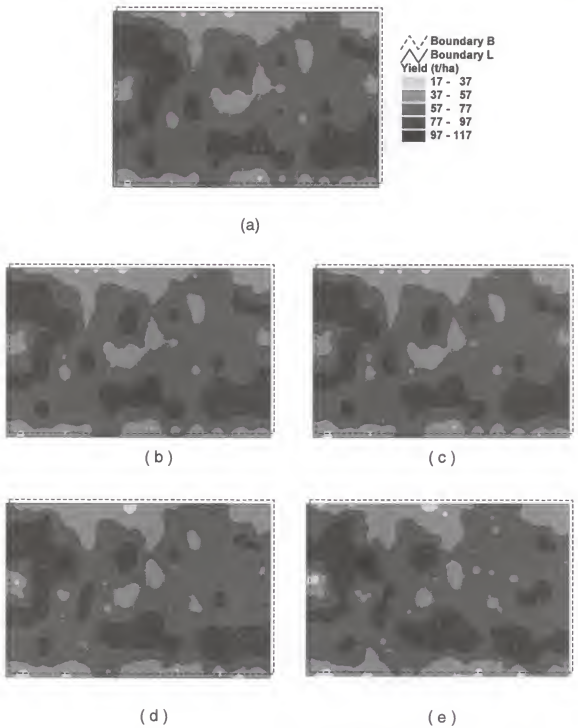

Figure 6-14. Interpolated yield maps using inverse weighted distance method in boundary L for GPS static horizontal error of (a) 0 m, (b) 0.5 m, (c) 1 m, (d) 3 m and (e) 5 m.

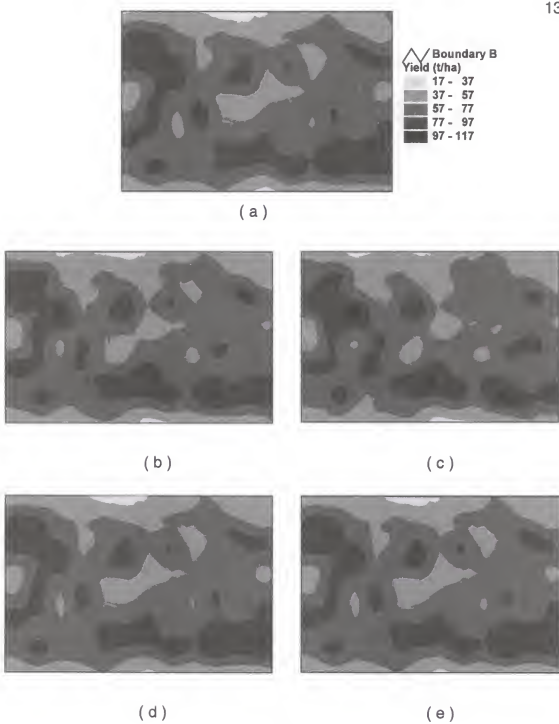

Figure 6-15. Interpolated yield maps using kriging-Gaussian method in boundary B for GPS static horizontal error of (a) 0 m, (b) 0.5 m, (c) 1 m, (d) 3 m and (e) 5 m.

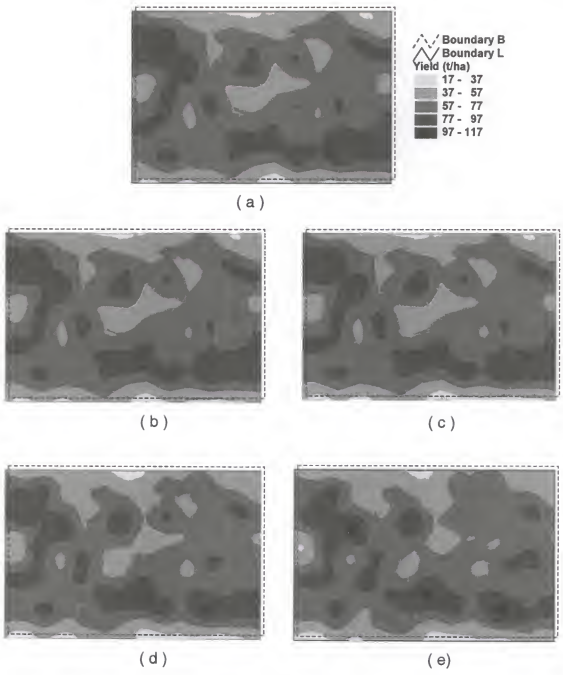

Figure 6-16. Interpolated yield maps using Kriging-Gaussian method in boundary L for GPS static horizontal error of (a) 0 m, (b) 0.5 m, (c) 1 m, (d) 3 m and (e) 5 m.

CHAPTER 7
DESIRED MAPS FOR MBSVRA OF FERTILIZER

Introduction

A desired map or treatment map shows the precise location and quantity of the treatment or application within the field. After developing the yield maps of Chapter 6, subsequent steps involved development of desired application maps to be used by the MBSVR applicator. Usually, factors limiting the yield potential of areas within a field should be considered. Controllable factors are assessed to prioritize possible management actions in terms of economic advantage. There are many interacting factors influencing crop growth and ultimately yield. These factors have a direct effect influencing management inputs. The controllable variables can be mapped either using intensive ground-based grid sampling or remote sensing.

N application was described as the cornerstone of citrus production and is believed to have the greatest effect on production (Jackson et al., 1995). They emphasized that N has to be applied on a regular basis as it is readily leached from poor soils on the Ridge growing areas or causing surface contamination in the flatwoods areas. The citrus orchard selected in this study is located in a flatwoods area with two type

of soil series; pomello and waveland (Figure 7-1). They are moderately well and poorly drained soil.

Jackson et al. (1995) reported that N is required for tree growth and fruit production and replacement of the N removed by fruit harvest is the main N requirement in a mature orchard. They highlighted that management practices needed in improving fertilizer efficiency include leaf analysis, selection of fertilizer formulation to match existing conditions, careful placement of fertilizer over the root zone, timing to avoid leaching in the rainy season, split applications, irrigation management to maximize production and minimize leaching, and meter N rate to the expected yield level needed. They suggested N application rate of 0.18 kg (0.4 lb) N per box (40.8 kg) for oranges and 0.14 kg (0.3 lb) N per box of grapefruit harvested from the field. So far there is no widely-accepted relationship defining various farm production inputs in maximizing yield potential of a citrus crop other than that described by Jackson et al. (1995).

Determining a citrus nutrition program requires considerations in many factors such as those described in Jackson et al. (1995) and Scholberg et al. (2000). Scholberg et al. (2000) reported that current recommended nitrogen fertilizer rate ranges from 107 kg/ha to 178 kg/ha. Higher N fertilizer rates (178 kg/ha to 214 kg/ha) might be required for certain citrus variety and/or when leaf tissue nitrogen concentrations fall below 2.2 %. N fertilizer applications exceeding 178 kg/ha to 214 kg/ha were reported to be typically not recommended unless appreciable N is lost due to excessive rainfall. They

mentioned that yield response to increased or reduced N fertilizer applications may only becomes obvious after one to two years. Yearly leaf analysis combined with using three to five years of yield averages was suggested as a "fine-tuning" for fertilizer practices. It is beyond the scope of this study to consider various factors described in Jackson et al. (1995) and Scholberg et al. (2000) in deriving a N desired map.

The focus of this study was to develop simple desired N fertilizer application maps based on available recommendation for a MBSVR applicator so that the integrated effects of selected spatial parameters in GIS, GPS and machine dynamics can be evaluated. The objective of this chapter was to develop desired maps based on two boundaries, five GPS horizontal errors and two interpolation methods listed in Table 6-1. The integrated effects of these variables on the desired map were also investigated.

Review

Fergusson et al. (1996) studied the effect of grid soil sampling in developing desired maps for spatially rate application of N based on a recommended equation relying on three variables; expected yield, residual soil nitrate-N , and organic matter content in corn production.

Materials and Methods

A GIS computer program, ArcView 3.1 and Spatial Analyst 1.1, was used in the analysis and development of desired maps for N application in a selected

boundary B of the citrus orchard. A simple relationship of recommended rate based on 4.45 kg N for each t of harvested fruit was used in all the computation in the development of N application desired maps. For the purpose of evaluating a MBSVR field application error, it was assumed that the rate of N used in the desired map is based on one single application.

The attribute tables of 20 yield maps derived in Chapter 6 (Figures 6-13 to 6-16) were selected and the recommended rate of N was computed by multiplying the yield in t/ha by a factor of 4.45 to derive a new field in the attribute tables showing kg of N per ha for each location in the attribute tables. Each legend of the twenty yield maps was then edited by selecting the new field, kg/ha, to be displayed in the map. This will be the desired map to be used for a MBSVRA system.

For visual comparison of a desired map, the scale was classified into five equal intervals of 85 kg/ha based on the highest and lowest values among all the 20 desired maps. In this study, it was assumed that the machine controller used for the MBSVR applicator was able to read the desired map input, at a map square cell size resolution of 0.457 m, and varies its spraying output in a continuous manner as the machine is traveling forward.

Subsequent analysis on the integrated effects of Y, G and P on desired map was done by comparing the recommended N rate (kg/ha) in each spatial location of the desired map with the best desired map. The desired mapping error equation, $E_{DM} = [\, DM_{BEST} - DM_{REJECT} \,]$ was used. The best desired map

was developed using the best yield map identified earlier in Chapter 6, that is using boundary B with zero GPS horizontal error (G = 0 m) and using kriging-Gaussian method. Spatial differences in N rate between two maps were computed using a raster-based grid-cell geoprocessing system, *Grid*, available in the ArcView Spatial Analyst 1.1 program. The square cell size for all the analyses was maintained at 0.457 m. Nineteen absolute error maps were derived using the equation, $E_{DM} = | [DM_{BEST} - DM_{REJECT}] |$, in *Grid* analysis. These nineteen maps were then converted to integer grid maps. The attribute table of each integer grid absolute error maps was then exported to a file to be analyzed using a computer spreadsheet program to derive a weighted mean absolute error in N rate for the whole map. Each weighted mean absolute error value was computed from a total of 149,280 square cells size of 0.457 m in each integer grid absolute error map. Statistical analysis using multiple regression was used to analyze the weighted mean absolute error in N rate for the 20 desired maps.

Results and Discussions

Desired Map

Figure 7-2 shows 5 desired N application maps using boundary B with IWD interpolation method with GPS horizontal error at 0, 0.5, 1, 3 and 5 m. These maps appeared to be different especially for those at a higher GPS horizontal errors at the 3 m and 5 m level. Similar desired N maps were derived

using boundary B, kriging-Gaussian method at GSP horizontal error at 0, 0.5, 1, 3 and 5 m (Figure 7-3) and appear to be smoother than those in Figure 7-2. With boundary L, desired maps using IWD at 5 different GPS horizontal error levels (Figure 7-4) and kriging-Gaussian method at 5 different GPS horizontal error levels (Figure 7-5) were also developed.

It is important to maintain all the maps square cell size used in the computation at 0.457 m for the same reasons as explained in Chapter 6 even though this may increase the computation time as well as the computer storage space.

Absolute Error Map

Figures 7-6 to 7-9 show nineteen absolute error maps of desired map derived from the 20 desired maps using the best desired map as the control. Figure 7-6 and 7-7 shows that 3 m and 5 m GPS horizontal errors appear to cause higher absolute errors than 0 m, 0.5 m and 1 m. Meanwhile, Figure 7-8 and 7-9 show a high concentration of absolute error at the 4 % areas at the top and right side within boundary B due to the shift in boundary L which wrongly defined the true field boundary. Similar trends showing a higher absolute error at the 3 m and 5 m GPS horizontal error than the 0 m, 0.5 m and 1 m were observed (Figure 7-8 and 7-9).

Integrated Effect of Boundary, GPS, and Interpolation Method

Table 7-1 summarizes the weighted mean absolute error of N rate for the 20 desired maps. The biggest difference of 34.31 kg/ha in the weighted mean absolute error occurred between best desired map and that on boundary L using IWD interpolation method and 5 m GPS horizontal error. Figure 7-10 shows the relationships of weighted mean absolute errors computed from 19 absolute error maps using three spatial parameters; boundary (B and L), GPS horizontal error (0, 0.5, 1, 3 and 5 m) and interpolation method (IWD and kriging -Gaussian).

The four prediction equations, M1, M2, M3 and M4, for weighted mean absolute error versus GPS horizontal error showed a good correlation with R^2 exceeding 0.99 (Figure 7-10). Comparing lines M1 and M3 indicate a linear relationship in the weighted mean absolute error versus GPS horizontal error for kriging-Gaussian interpolation method as the boundary changes from B to L. There is a quadratic relationship in the weighted mean absolute error versus GPS horizontal error for IWD interpolation method as the boundary changes from B to L (lines M2 and M4). Between lines M2 and M3, their differences in weighted mean absolute errors increase for G ranges from 0 m to 5 m.

From statistical analysis using multiple regression method, the integrated effects of G, Y and P on the weighted mean absolute error for the present set of data can be given by the relationship as:

$$M_s = 9.56 + 3.94\ G + 4.43\ Y + 2.58\ P \qquad R^2 = 0.967$$

where Y and P are coded dummy variables and,

G = 0, 0.5, 1, 3 and 5 m

Y = -1 if boundary B is used, and 1 if boundary L

P = -1 if kriging-Gaussian method, and 1 if IWD method

It was assumed that the factor for G, Y and P were additive since the predicted lines are parallel (Figure 7-11). With this assumption, a simple first order model using data from Table 7-1 was developed. The integrated model equation provide a good representation of the data with $R^2 = 0.967$. The coefficient for Y or P represents the expected change in M_s for a unit change in Y or P when all other variables are held constant. The estimated coefficients for parameter G, Y and D are significant at the 0.025 level using t-test. The intercept coefficient of 9.56 cannot be interpreted by itself alone as the parameters Y and P are coded variable (equal to -1 and 1) and are not equal to zero. As G ranges from 0 m to 1 m, a shift in boundary location from B to L by 4.6 m towards the south-west direction appeared having the greatest influence on M_s where Y is 1.72 times P. However, the effects of P reduces as G increases beyond 2 m to 5 m. The effect of boundary L appear to be significant when G increases from 2 m to 5 m. The first order model provides a good representation of the data (96.7 %) even though all the lines are not parallel indicating some interacting effects among G, Y and P. However, this interacting effect is small and will only account for 3.3 % of the variation in these data. Hence, a first order model assumption was believed to be good model.

Conclusions

Twenty desired maps for a hypothetical MBSVR N fertilizer application in a citrus orchard using three spatial parameters: Y, G and P were developed. An integrated relationship based on the weighted mean absolute error of the present set of desired maps generated from Y, G and P is given by $M_s = 9.56 + 3.94G + 4.43Y + 2.58D$ with a correlation coefficient of 0.967. The parameters Y and P are coded dummy variables where Y = -1 (if boundary B is used), and 1 (if boundary L), P = -1 (if kriging-Gaussian method), and 1 (if IWD method) and, G = 0, 0.5, 1, 3 and 5 m. For G ranges from 0 m to 1 m, boundary offset (Y) have the highest influence follow by GPS horizontal error (G) and interpolation method (P).

Table 7-1. Summary of weighted mean absolute error for desired maps

GPS horizontal error (m)	Weighted mean absolute error of N rate (kg/ha)			
	BG#K	BG#I	LG#K	LG#I
0	0	10.63	11.46	19.05
0.5	3.36	10.91	12.46	19.30
1	5.25	11.70	14.82	20.02
3	14.91	17.78	24.48	25.72
5	24.87	26.81	33.31	34.31

Note:
B = Boundary B
L = Boundary L
G# = GPS horizontal error with # represent the number (m)
K = kriging-Gaussian interpolation method
I = IWD interpolation method

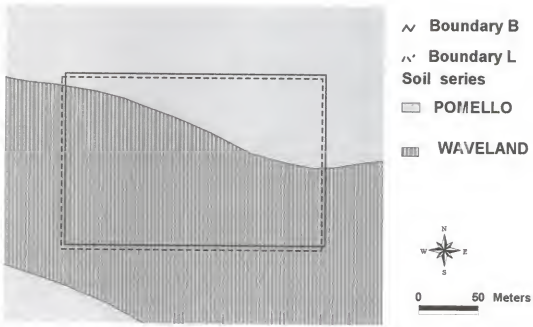

Figure 7-1. Soil map for the study area overlaid in boundary B and L

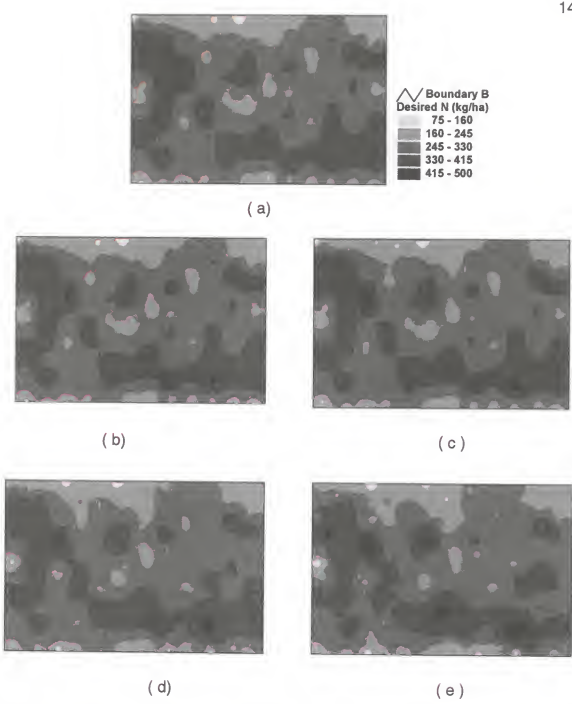

Figure 7-2. Desired N application maps derived from yield maps using boundary B, inverse weighted distance interpolation method at GPS static horizontal error of (a) 0 m, (b) 0.5 m, (c) 1 m, (d) 3 m, (e) 5 m and a rate of 4.45 kg N per t of oranges harvested.

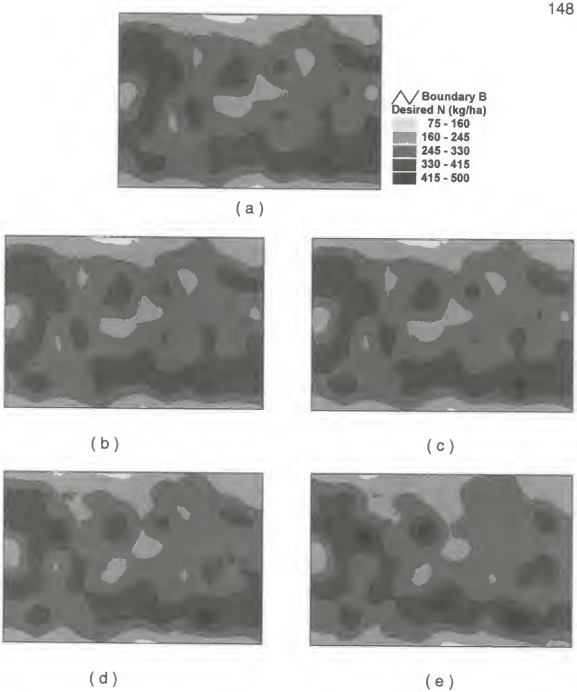

Figure 7-3. Desired N application maps derived from yield maps using boundary B, kriging-Gaussian interpolation method at GPS static horizontal error of (a) 0 m, (b) 0.5 m, (c) 1 m, (d) 3 m, (e) 5 m and a rate of 4.45 kg N per t of oranges harvested.

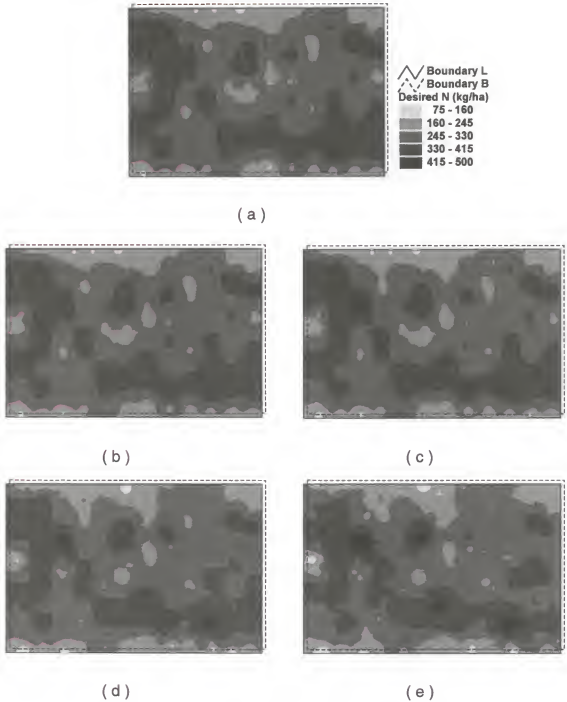

Figure 7-4. Desired N application maps derived from yield maps using boundary L, inverse weighted distance interpolation method at GPS static horizontal error of (a) 0 m, (b) 0.5 m, (c) 1 m, (d) 3 m, (e) 5 m and a rate of 4.45 kg N per t of oranges harvested.

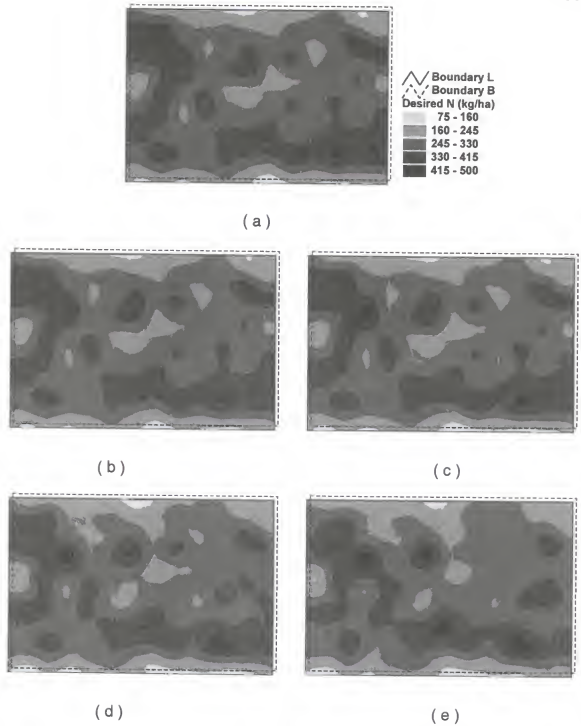

Figure 7-5. Desired N application maps derived from yield maps using boundary L, kriging-Gaussian interpolation method at GPS static horizontal error of (a) 0 m, (b) 0.5 m, (c) 1 m, (d) 3 m, (e) 5 m and a rate of 4.45 kg N per t of oranges harvested.

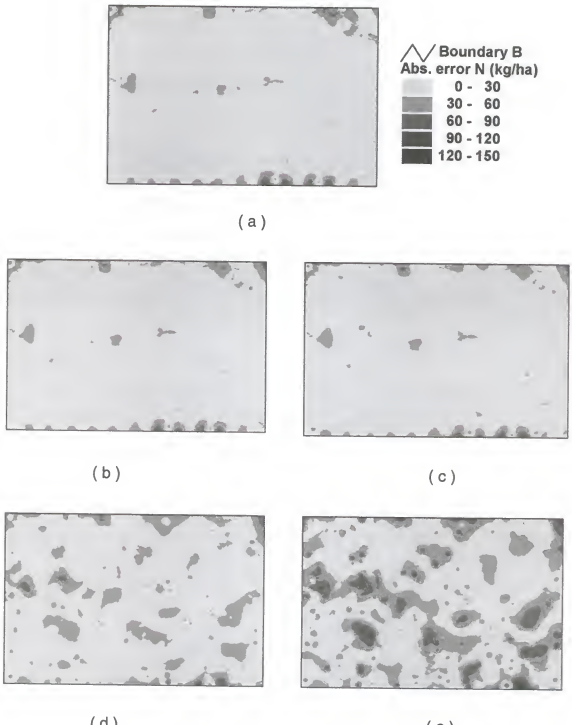

Figure 7-6. Absolute (Abs.) error between desired N application map derived from boundary B, kriging-Gaussian interpolation method, GPS static horizontal error at 0 m and desired maps obtained at GPS static horizontal error of (a) 0 m, (b) 0.5 m, (c) 1 m, (d) 3 m, (e) 5 m with boundary B and inverse weighted distance method.

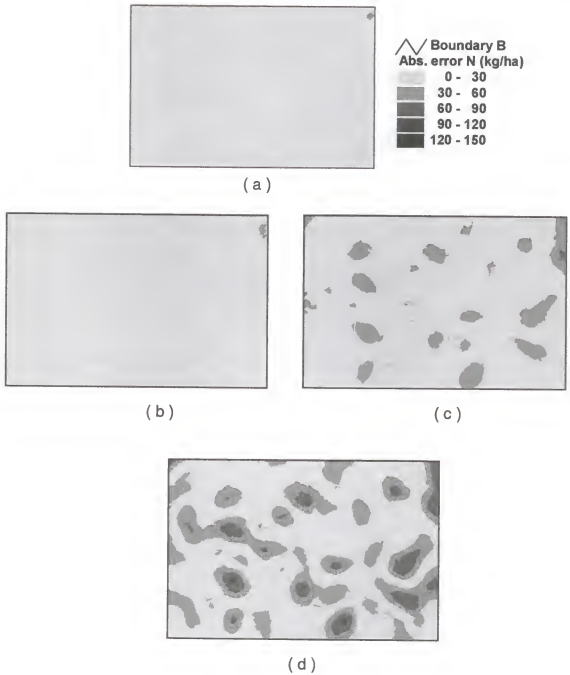

Figure 7-7. Absolute (Abs.) error between desired N application map derived from boundary B, kriging-Gaussian interpolation method, GPS static horizontal error at 0 m and desired maps obtained at GPS static horizontal error of (a) 0.5 m, (b) 1 m, (c) 3 m, (d) 5 m with boundary B and kriging-Gaussian method.

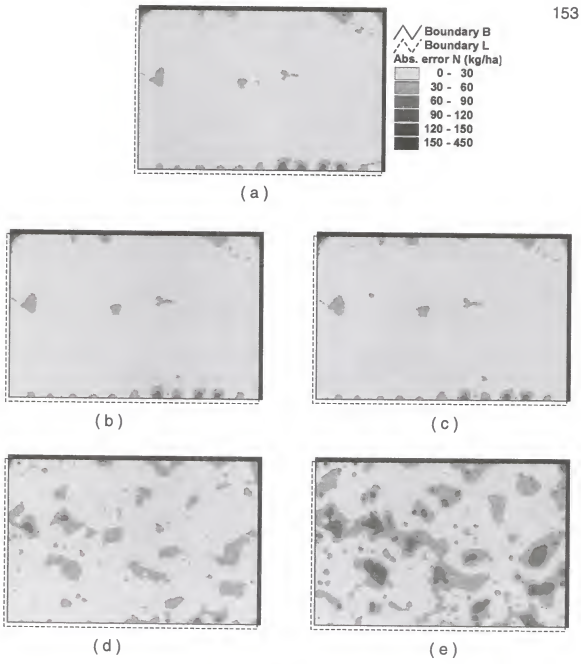

Figure 7-8. Absolute (Abs.) error between desired N application map derived from boundary B, kriging-Gaussian interpolation method, GPS static horizontal error at 0 m and desired maps obtained at GPS static horizontal error of (a) 0 m, (b) 0.5 m, (c) 1 m, (d) 3 m, (e) 5 m with boundary L and inverse weighted distance method.

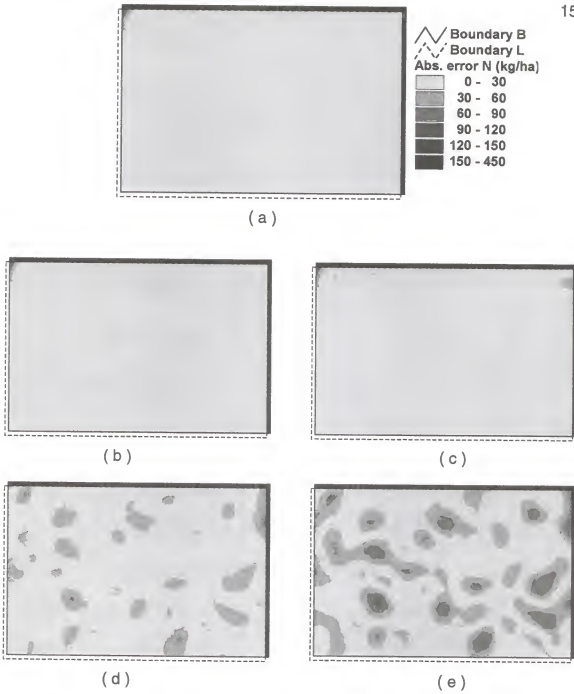

Figure 7-9. Absolute (Abs.) error between desired N application map derived from boundary B, kriging-Gaussian interpolation method, GPS static horizontal error at 0 m and desired maps obtained at GPS static horizontal error of (a) 0 m, (b) 0.5 m, (c) 1 m, (d) 3 m, (e) 5 m with boundary L and kriging-Gaussian method.

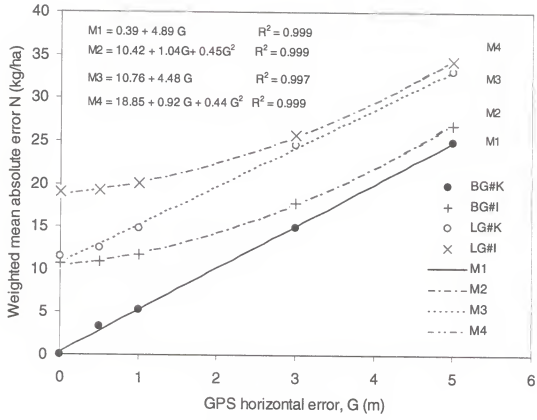

Figure 7-10. Summary of weighted mean absolute errors of desired maps using BG0K as the best desired map where G# = GPS horizontal error level, B and L represent the boundary, K and I represent interpolation method and M1, M2, M3, M4 (weighted mean absolute error) are the fitted lines for BG#K, BG#I, LG#K and LG#I respectively (all estimated G's are significant at the 0.025 level using t-test).

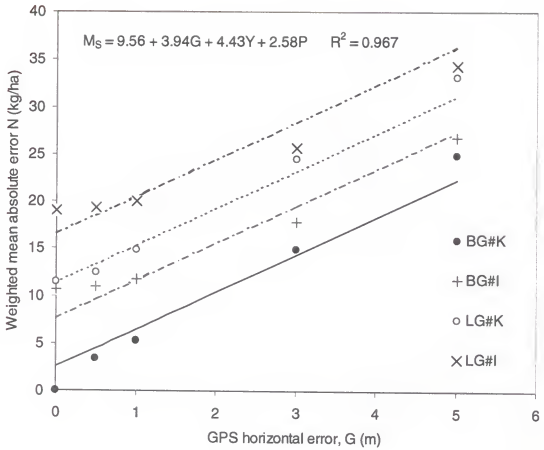

Figure 7-11. Summary of weighted mean absolute errors of desired maps using BG0K as the best desired map where G# = GPS horizontal error level, B and L represent the boundary, K and I represent interpolation method. (where Y = -1 if boundary B, and 1 if boundary L, P = -1 if kriging-Gaussian method, and 1 if IWD method). M_S = sub-model equation for weighted mean absolute error.

CHAPTER 8
MACHINE DYNAMICS AND INTEGRATED ERROR ANALYSIS

Introduction

Currently there are no reported MBSVR applicator for citrus fertilizer application in use. A modular design MBSVR applicator may be used for fertilizer application in a citrus orchard as the application width is limited by the between tree-row spacing. A hypothetical MBSVR applicator fitted with a real-time DGPS receiver integrated with a dead-reckoning machine navigation system and assisted by a light bar system is assumed in this study (as discussed in Chapter 3). Major applicator system components used in this hypothetical MBSVR fertilizer sprayer applicator for citrus include a control system capable of reading desired rate from a desired map located in the operator console. The real-time DGPS receiver would provide real-time position of the applicator in a citrus orchard for the machine controller to read the desired spraying rate from a desired map. It was assumed that the operator-assisted applicator is capable of maintaining the spraying path in the middle between two rows of trees. An example of a liquid applicator used in a citrus orchard is shown in Figure 8-1a and 8-1b.

There are many factors affecting the accuracy of a MBSVR sprayer application such as: map resolution of desired map, DGPS dynamic horizontal position resolution (or navigation error), DGPS receiver sampling frequency, field terrain, tree obstruction, soil surface conditions, human error, applicator working speed, applicator controller algorithm, design and configurations of the applicator system controller and actuators, spraying width and physical characteristics of chemical used. Generally, such factor can be classified into three categories of error sources: desired map, navigation and sprayer application errors.

Accuracy of a desired map was shown to be affected by Y, G and P. Map resolution was an important factor affecting the accuracy of field application in a MBSVRA system. The importance of map resolution of desired map have been highlighted by many researchers (Dobermann and Bell, 1997; Monson, 1997). Usually raster map format was superior to vector format in a desired map for a MBSVRA as reported in Anderson and Humburg (1997) and Tyler et al. (1997) who cited quicker data access from the desired map to the machine controller. G is considered the most important variable among the three factors : Y, G and P affecting accuracy of a desired map that affect the choice of a desired map.

Machinery components do not respond instantly to changes in application rate when applying fertilizer in a MBSVR applicator, thus creating applicator machine errors. Many machine factors contribute to the overall dynamic behavior of a variable rate applicator. The importance of delay time in accuracy

of machine application have been highlighted in many studies (Schueller and Wang, 1994; Anderson and Humburg, 1997; Tyler et al., 1997; Cahn and Hummel, 1996; Qiu et al., 1998; Zhu, et al., 1998; Sudduth et al., 1995; Rockwell and Ayers, 1996). The overall applicator machine delay time in its response to a desired map set-point input reflects the composite effect of applicator controller algorithm, design and configurations of the applicator system controller and actuators and the physical characteristics of chemical used. It is important to considered the overall delay time of a MBSVR applicator in studying its effect on the accuracy of a MBSVRA system field application.

An integrated model relating the effect of boundary offset, GPS static horizontal error and interpolation method have been identified earlier using a map-based GIS software and relating their weighted mean absolute error. A similar approach can be used in analyzing the integrated effect of selected spatial parameters for desired and applied maps derived from navigation and machine errors.

The objectives of this study were to developed applied maps for a MBSVR fertilizer applicator using three selected parameters: DGPS dynamic horizontal error, DGPS receiver sampling frequency and overall machine delay time, and to develop an integrated model based on four major spatial parameters in a MBSVRA system: GPS static horizontal error, DGPS dynamic horizontal error, DGPS sampling frequency and machine delay time.

Review

Tyler et al. (1997) discussed an automatic parallel track line system in machine navigation and guidance for a MBSVRA with the machine position update rate usually at 1 Hz (as in Chapter 3). Similar system is also used in commercial units, for example Trimble AgGps 170. DGPS receivers can provide ground speed accuracy to within 0.1 km/h at an update rate of 1 Hz (Anderson and Humburg, 1997) . They mentioned that DGPS receiver typically has a position accuracy of 5 m or less whereas positional accuracies of below 30 cm were possible for a real-time kinematic GPS. Machine forward working speed and DGPS sampling frequency affect the spatial resolution of the spraying operation. Paice et al. (1996) described two type of spatial resolution important for spraying application: lateral and longitudinal. The lateral resolution is determined by the spraying width while the longitudinal resolution is proportional to both the spraying system response time and machine forward speed. Currently, there is no reported study on the effect of machine navigation error and DGPS sampling frequency on the accuracy of field application.

There are several studies on the effects of spraying machine delay time on a variable rate sprayer most of them are focus on injection sprayer. Xu (1991) studied a hydraulically-driven centrifugal pump spraying system and developed a transfer function for the model with a transportation delay of 0.2 s. The transportation delay was defined by the volume of liquid from the point of interest

to the nozzles divided by the flow rate. Transportation delay is affected by the location of interest or chemical mixing in the fluid circuit, the flow rate of liquid, and the length and area of the hoses. Besides transportation delay, the time constant of the system represents the delay in the system response to an input command change. Schueller and Wang (1994) used a transportation delay of 5 s with a 1 s time constant to study a model a MBSVR liquid fertilizer application system operating at 18 km/h using a map resolution of 40 m x 40 m and an application width of 20m. They introduced a 5.7 s feed forward command time to reduce the effect of overall machine delay on application error but did not incorporate the machine navigation error and desired map error.

Direct injection nozzles were reported to be used to overcome transportation delay by placing the chemical injection point as close as possible to the boom and nozzles (Anderson and Humburg, 1997). Sudduth et al. (1995) studied the dynamic and steady state performance of a commercial chemical injection system for herbicide application to a step change. The delay time of the injection pump, injection controller and transportation delay was found to be 4 s, 1 s and 14 to 21 s respectively. Meanwhile Paice et al. (1996) described injection metering as capable of accurate steady-state application but its dynamic dose accuracy and resolution in the direction of application limited by the overall machine response time caused by transportation delay and dynamic flow response characteristics of the metering system. Qiu et al. (1998) studied the simulated performance of a direct injection sprayer for herbicide application

considering three type of nozzles, hose diameters and flow rates. They reported transportation time delay ranged from 10.1 s to 22.2 s and 1.5 s to 2.9 s without and with feed forward command respectively. Zhu et al. (1998) also studied the effect of transportation delay time for an injection sprayer. They found that hose diameter greatly influence the transportation delay where a hose diameter increase from 1.07 cm to 2.09 cm almost doubled the delay time, while the viscosity of water-soluble and non-water soluble liquids had little influence on delay time after sudden changes in travel speed. The delay time without feed forward command ranged from 11.8 s to 18.9 s for a 1.07 cm hose diameter.

In integrating the various factors affecting a MBSVRA system, Goense (1997) derived a calculation method for a spatially variable rate fertilizer spreader (as discussed in Chapter 2).

Materials and Methods

Development of an integrated error analysis model first involved the generation of applied maps using selected desired maps to be used with three selected field operating factors: machine delay time (D), navigation error (T) and DGPS sampling frequency (F). Applied maps were subsequently analyzed and compared with the best desired map using an overall mean absolute error to quantify their differences so as to develop an integrated model.

Desired Maps

From Chapter 7, desired maps derived from analysis using boundary B, kriging-Gaussian method and at five levels of GPS static horizontal error were selected. The rationale for this selection is that the best base map, such as a farm survey map, can be identified when they are available. Furthermore, current farm practices with some commercial equipment allow the boundary to be marked using accurate DGPS receiver. Besides boundary, comparing the interpolated yield map with the ground truth yield especially when individual tree yield data are available can identify the best interpolation method.

Throughout this study, a map resolution of raster format with a square cell size of 0.457 m was selected based on the same reasons as explained in Chapter 6. The selection of this cell size is to account for both the choice of a 0.5 m GPS static horizontal error as well as that used in yield map interpolation mentioned in Chapter 6. It was assumed that the MBSVR applicator was capable of reading continuously the application rate table for each corresponding raster cell in the desired map.

Machine Transportation Delay Time

A commercial citrus fertilizer applicator was field tested to study the typical range of sprayer response time. This sprayer (Figure 8-1a and 8-1b) was mounted to a John Deere model 7210 four-wheel tractor (Deere and Co., Moline, IL) equipped with a MidTech® TASC 6300 (Midwest Technologies, Inc.,

Springfield, IL) sprayer controller, boom control switch box (Figure 8-2a) and three 2.23-m spray boom sections with 11 nozzles at each boom section spaced at 20 cm (Figure 8-2b). Fertilizer was applied at the left and right boom. Pre-mixed liquid N fertilizer was stored in the chemical tank and delivered by a hydraulic centrifugal pump to the hydraulic control valves and finally to the spray boom nozzles. Two optical sensors located on the left and right sides of the tractor triggered spraying operation in the field. Tests were conducted using water and set at 5 discharge rates operating at 6.4 km/h. The spraying was triggered in two ways: by manually turning the sprayer on with the optical sensor off and by triggering the optical sensor. The spraying operation was video taped. Sprayer response time, from the switching on of the sprayer to the time all the nozzles were spraying liquid, was recorded by playing back the recorded spraying operation on a player capable of viewing video frame at 30 frames per second. Table 8-1 summarizes the results of the field tests where the sprayer response time ranged from 0.70 s to 1.20 s with the optical switch off while the response time was faster with the optical sensor on which ranged from 0.58 s to 0.79 s.

Qiu et al. (1998) reported there was still a 2.9 s overall delay despite a feed-forward command. Considering the ranges of response time results in Table 8-1, a delay time of 0 s and 2 s was selected in this study with 0 s representing the best sprayer response.

Navigation Error, DGPS Sampling Frequency, and Spray Pattern

In this study, two levels of the DGPS dynamic horizontal position resolution at 0 m and 2 m were selected. It was assumed that the real-time DGPS receiver used was capable of achieving this horizontal position resolution throughout the field operation. For example, some of the maximum cross-track errors for the Omnistar real-time DGPS dynamic horizontal error were at 1.88 m (Table 5-3).

Beside DGPS dynamic horizontal position resolution, the update rates of the DGPS receiver were selected at 0.5 Hz and 10 Hz. This selection reflects the common range of the sampling frequency for currently available commercial DGPS receivers where most operate at 1 Hz. The choice of 0.5 Hz in this study was assumed to be the lower range where the DGPS receiver update rate is set up to resolve its real-time positioning in a fringe area with poor real-time DGPS signal.

A total of 23 spray paths were needed to complete the fertilizer spraying covering an area defined by boundary A. A GPS tracking software, ArcView Tracking Analyst extension available from ArcView was used to model the DGPS positions along each spray path, considering both the machine forward travel speed at the two DGPS sampling frequencies. It was assumed that the spraying pattern was evenly distributed along a 9.14 m width spray boom and formed a rectangular spray pattern between two rows of tree. For all the odd number paths (Figure 8-3), the applicator transverse from the south to the north direction

at 7.98 km/h. While the applicator reverses its traveling direction along the north-south direction in all the even number paths. The spraying operation was assumed to start exactly at the beginning of the field boundary and stop exactly at the end of the field boundary. Different test runs using 0 m and 2 m DGPS dynamic horizontal error at 0.5 Hz and 10 Hz DGPS sampling frequencies were simulated. Figure 8-3 shows an example of the spray coverage overlaid with 0 m DGPS dynamic horizontal error with DGSP sampling frequency at 0.5 Hz. The simulated DGPS dynamic horizontal positions at 0 m error for all the 23 machine paths, at 0.5 Hz and 10 Hz, were further selected for modeling of the DGPS dynamic horizontal error at 2 m away from 0 m point. The approach of randomizing the angular distribution of the horizontal error, as described in Chapter 6, was used to model the DGPS dynamic horizontal error at 2 m. Figures 8-4a, 8-4b, 8-4c and 8-5 detail some examples of the modeled DGPS points along each of the 23 machine paths at 0 m, 2m DGPS dynamic horizontal error sampled at 0,5 Hz and 10 Hz.

Applied Map

Table 8-2 summarizes various combinations of variables selected for the development of applied maps. For each desired map developed at 0 m, 0.5 m, 1 m, 3 m and 5 m of G, corresponding applied maps were obtained using combinations of 0 m and 2 m of T, 0.5 Hz and 10 Hz of F and 0 s and 2 s of D representing simulated field spraying operation. All the desired map N

application rates that fall within the modeled DGPS points were assigned to each modeled DGPS position and their corresponding sprayed rectangular area based on their machine field location, using the ArcView computer program. In cases where D equal to 2 s, the applied rate of N was shifted, using a spreadsheet computer program, by a time scale of 2 s along the sprayed path. The legend of the shapefile for the sprayed rectangles was then edited reflecting the applied rate of N in kg/ha. All applied maps were then classified into six equal intervals of 75 kg/ha for visual comparison as the resulting applied maps.

Integrated Analysis

Similar map-based error analysis, described in Chapter 7, using a raster-based grid-cell geoprocessing system, *Grid*, available in the ArcVIew 3.1 and Spatial Analyst 1.1 was used to derive the absolute error maps between desired and applied map. The best desired map, defined by boundary B with the 506 original yield tub points (equivalent to 0 m GPS static horizontal error) and using kriging-Gaussian method was used as the base map for computing absolute error map.

Results and Discussions

Simulated Navigation Error and Spray Pattern

GPS positioning characteristic is dynamic and location specific. The present method in modeling DGPS dynamic horizontal error used a simplistic

approach considering the worst case scenario of 2 m DGPS dynamic horizontal error for all the DGPS positions. This may not be the case in reality. However, this approach allowed comparison of machine application error due to different levels of DGPS dynamic horizontal error. Applied maps can also be obtained by using the machine field evaluation approach where a desired map is downloaded to the applicator controller linked to a real-time DGPS which can record the actual field application rate of the machine at required field positions.

Alternatively, data points representing the machine field locations for different types of DGPS receivers with different level of navigation error can be obtained by mounting the DGPS receiver on an applicator and operating the machine along the 23 machine paths in the same orchard and record those machine location. The recorded files of machine locations can be used as input files in deriving applied maps.

The simulated rectangular spray pattern used for the present study may not represent the actual spray pattern of many commercial applicators. The present approach does not consider the variation in the spray pattern as an input in the model. Variation in spray pattern can be included in future studies when the behavior of a particular sprayer can be identified, either using a spray patternator or other spray pattern measuring devices, and modeled in the method described above.

Besides variation in DGPS dynamic error and spray pattern, further modifications to the present study also can include simulating the machine

capability of varying spray rate along the boom section depending on the horizontal position resolution of the DGPS receiver used.

Applied Map

Figures 8-6 to 8-15 show various applied maps obtained using desired maps at GPS static horizontal error of 0, 0.5, 1, 3 and 5 m in boundary B and kriging-Gaussian method. Two levels of DGPS dynamic horizontal error, two levels of DGPS sampling frequencies and two levels of machine delay time were used to simulate the sprayer field application. All the maps show a somewhat blocky pattern as it reflects the rectangular spray pattern covering a 9.14 m width between two rows of tree. It was observed that the spray pattern of 10 Hz DGPS sampling frequency is more refined than the 0.5 Hz DGPS sampling rate. This is due to the more frequent changes in the sprayer application rate detected by the 10 Hz DGPS sampling rate as the machine position in the field can be identified at a closer interval than the 0.5 Hz DGPS sampling rate.

Due to the effect of 2 s machine time delay, there are horizontal strips equivalent to a distance of 4.44 m in the applied map represent a 2 s interval where no fertilizer was applied. This happened for both the 0.5 Hz and 10 Hz DGPS sampling frequency. The spraying operation pattern along the south-north and north-south directions for all the 23 paths have resulted in the concentration of sprayed rectangles of 9.14 m x 4.44 m at the beginning of every sprayed path in the applied map.

Absolute Error Maps

Figure 8-16 to 8-25 show various absolute error maps computed between the best desired map described earlier (Chapter 7) and applied map using two levels each of T, F and D. Similar blocky patterns were observed due to the rectangular spray pattern. Generally, regions of high absolute error were observed in those absolute error maps computed with combination of 2 s machine delay time coupled with a higher DGPS navigation error. The absolute error of N maps were classified into 6 levels at 30 kg/ha each for the first five levels, which were the same as those absolute error maps in Chapter 7 with the last levels representing errors in regions of zero fertilizer application. Table 8-3 summarizes the results of 40 weighted mean absolute error of absolute error maps using a square cell size of 0.457 m. Each value represents the computed weighted mean absolute difference of 143,060 cells between the desired and applied map. The weighted mean absolute error of N rate ranges from 5.88 kg/ha to 42.29 kg/ha.

Comparing the results in Table 7-3 and Table 8-3, weighted mean absolute error for desired map in treatment BG#K increased by 24.87 kg/ha when G increases from 0 m to 5 m. However, the corresponding increases in weighted mean absolute errors due to: G, T, F and D (with a uniform spraying width of 9.14 m) ranges from 6.94 kg/ha to 18.80 kg/ha when the desired map at G=5 m (BG5K) was used in field application. This reduction in weighted mean

absolute error could be attributed to the rectangular spraying pattern in $N_{applied}$ map. The weighted mean absolute error of N rate in Table 7-3 was computed using DM_{BEST} and DM_{REJECT} maps (given by E_{DM}) where every square grid cells of 0.457 m in the two desired maps were based on its derived desired map at G = 0 m and G = 5 m. The number of N rate variations in the two desired maps were not 'modified' by the sprayed pattern rectangles as in $N_{applied}$ map. Therefore, we would expect a high variation in the weighted mean absolute error when computing E_{DM}. However, in computing the differences between DM_{BEST} and $N_{applied}$ the rectangular sprayed pattern is believed to have a 'homogenize' effect across every 9.14 m spraying width on $N_{applied}$ map. The blocky sprayed pattern of $N_{applied}$ maps could have reduced the levels of variation in N rate. Second, the integrated effects of G, T, F and D (especially F) also could have caused the applied N rate influenced by the input N rate read by the DGPS receiver sampling frequency, F. Table 8-3 shows that a higher F = 10 Hz resulted in a higher variation in the weighted mean absolute error than F = 0.5 Hz. The variation of weighted mean absolute error at F = 10 Hz ranges from 10.27 kg/ha to 18.80 kg/ha whereas at F = 0.5 Hz the range is from 6.94 kg/ha to 14.84 kg/ha. Again, this could be attributed to the more intensive reading of input N rate at 10 Hz than 0.5 Hz by the DGPS receiver resulting in a higher variation in the resultant sprayed areas.

Integrated Analysis

Figure 8-26 shows the effects of GPS static horizontal error, navigation error, DGPS sampling frequency and machine delay time on the weighted mean absolute error between desired and applied maps using desired map derived from boundary B and kriging-Gaussian method. Generally, the weighted mean absolute error increased as the GPS horizontal error increased. The rate of increase of weighted mean absolute error appeared to be similar to those of the desired map (Figure 7-10) and higher when the GPS horizontal error was greater than 1 m.

From statistical analysis using multiple regression method, the overall integrated model for T, F, D and G for the present set of data can be represented by (Figure 8-27):

$$M_I = 19.46 + 1.37T - 2.80\,F + 8.15\,D + 2.53\,G$$

with a correlation coefficient, $R^2 = 0.963$.

where,

T = -1 if the navigation error is 0 m, and 1 if 2 m

F = -1 if the sampling frequency is 0.5 Hz, and 1 if 10 Hz

D = -1 if the delay time is 0 s, and 1 if 2 s

G = 0, 0.5, 1, 3 and 5 m

It was assumed that the factor for T, F, D and G are additive since the lines are almost parallel. This general linear model described the relationship among all the forty weighted mean absolute error values listed in Table 8-3. All

estimated coefficients for T, F, D and G were significant at the 0.025 level using t-test. The constant term 19.46 cannot be interpreted independently as the value of T, F and D are coded variables and are not equal to zero. It can only be explained as part of the prediction equation.

There is a slight decrease in the weighted mean absolute error, ranging from 0.30 kg/ha to 0.67 kg/ha (1.13 % to 2.03 %), as G increases from 0 m to 0.5 m in the four combinations with a delay time of 2 s even though Table 7-1 shows an increase of 3.36 kg/ha in the weighted mean absolute error of N rate in the desired map as GPS horizontal error increases from 0 m to 0.5 m. It is believed that there is an interacting effects of T and F on the weighted mean absolute error which reduces the effect due to G.

It was observed that the weighted mean absolute error tend to converge as G increases from 0 m to 5 m. This phenomenon also was observed in the desired maps (Figure 7-10). One possible explanation of this behavior is that, as the GPS static horizontal error (G) increases to 5 m or larger the effects of T, F, D becomes relatively less. At a working speed of 2.22 m/s, the maximum spatial error: for T (2 m), F (4.44 m) and D (4.44 m) is smaller than the 5 m distance for G. Furthermore, the importance of accuracy in desired map has been highlighted earlier as it influence the weighted mean absolute error of applied map. In Chapter 7, the influence of coefficient G (3.94) in the integrated model derived from absolute error of desired maps is significant. The importance of G

is also reflected in the overall integrated model prediction equation where this coefficient is slightly reduced to 2.53.

The plots of Figure 8-26 showed a weighted mean absolute error of N rate increase by about 5 kg/ha or less as T increases from 0 m to 2 m. The smallest increase occurs in the combination with 10 Hz DGPS sampling rate with 2s machine delay. This smaller increase could be attributed to the effect of a higher F at 10 Hz which tends to reduce the weighted mean absolute error. Overall, the coefficient of T (1.37) is the second lowest among the four factors: T, F, D and G.

Generally, weighted mean absolute error decreased with F increased from 0.5 Hz to 10 Hz for all the combinations of T and D. This is due to the more intensive update of the desired machine input rate from the desired map between the 10 Hz to the 0.5 Hz sampling rate resulting in a more accurate spraying application. Overall, the influence of F ranked second (2.80) in the integrated model, at G = 1 m, and had a negative effect on the weighted mean absolute error as F increases.

Sprayer delay time, D, appeared to be the most important factor in the overall integrated linear model when G ranges from 0 m to 3 m. This factor contributed the highest weighted mean absolute error for all the combinations using T, F and G (0 m to 3 m). At G = 1 m, the coefficient of D at 8.15 is 5.9 times greater than T, 2.9 times greater than F and 3.2 times greater than G.

The overall integrated model for four spatial parameters: T, F, D and G using desired map derived from boundary B and using kriging-Gaussian method in Figure 8-27 showed that machine delay time was the most important factor affecting the accuracy of a MBSVR fertilizer application in a citrus orchard with G ranges from to 0 m to 3 m.

Conclusions

Applied maps for a MBSVR fertilizer applicator using three selected spatial parameters: T, F and D based on desired maps derived from boundary B, kriging-Gaussian method at 5 levels of G were developed. An integrated model, $M_I = 19.46 + 1.37T - 2.80 F + 8.15 D + 2.53 G$, for a MBSVRA system was developed based on the test conditions used in the present set of data. The values for T, F, D are coded dummy variables where, T = -1 (if the navigation error is 0 m), and 1 (if 2 m), F = -1 (if the sampling frequency is 0.5 Hz), and 1 (if 10 Hz), D = -1 (if the delay time is 0 s), and 1 (if 2 s) and G = 0, 0.5, 1, 3 and 5 m. The coefficient of D in the model is 5.9 times greater than T, 2.9 times greater than F and 3.2 times greater than G, at G=1 m.

Table 8-1. Summary of field tests on machine response time for a liquid fertilizer sprayer

Spray rate (L/ha)	Sprayer response time (s)			
	Optical sensor off		Optical sensor on	
	Time (s)	Standard deviation (s)	Time (s)	Standard deviation (s)
935.3	1.20	0.17	0.79	0.06
1122.3	0.96	0.12	0.70	0.04
1309.2	0.70	0.25	0.61	0.02
1403.1	0.81	0.22	0.60	0.03
1590.1	0.84	0.09	0.58	0.18

Table 8-2. Summary of variables used in the development of applied maps

Desired map with GPS horizontal error * (m)	Navigation horizontal error (m)	Real-time DGPS sampling frequency (Hz)	Machine delay time (s)
0	0	10	0
0.5	2	0.5	2
1			
3			
5			

* Using Boundary B and kriging-Gaussian interpolation method

Table 8-3. Summary of weighted mean absolute errors between desired map (using Boundary B, kriging-Gaussian method at 0 m GPS error) versus applied map using desired map at 5 levels of GPS horizontal error and 2 levels each for navigation error, DGPS sampling frequency and machine delay time.

Parameters	Weighted mean absolute error of N (kg/ha)				
	GPS horizontal error (m)				
	0	0.5	1	3	5
0 m navigation error					
10 Hz and 0 s delay	5.88	6.79	7.96	15.54	24.68
10 Hz and 2 s delay	25.62	25.26	25.86	29.44	35.58
0.5 Hz and 0 s delay	11.80	11.87	12.87	18.72	26.64
0.5 Hz and 2 s delay	32.97	32.30	32.89	35.33	39.91
2 m navigation error					
10 Hz and 0 s delay	10.56	10.98	11.88	18.58	27.17
10 Hz and 2 s delay	26.66	26.36	26.97	30.73	36.93
0.5 Hz and 0 s delay	15.89	15.96	16.76	22.15	29.63
0.5 Hz and 2 s delay	35.18	34.85	35.13	38.13	42.29

(a)

(b)

Figure 8-1. (a) Side view of a chemical liquid sprayer used in a citrus orchard and (b) the same sprayer applying chemical in between two rows of citrus trees.

(a)

(b)

Figure 8-2. (a) Variable rate controller located in the tractor console and (b) a section of the spray boom.

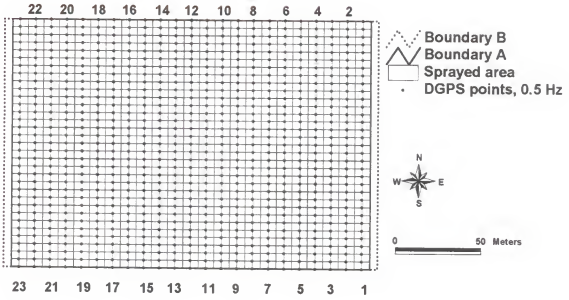

Figure 8-3 An example of 23 sprayed paths pattern with 0 m navigation error, DGPS sampling frequency of 0.5 Hz, travel at 7.98 km/h in boundary B where boundary A is the actual sprayed area.

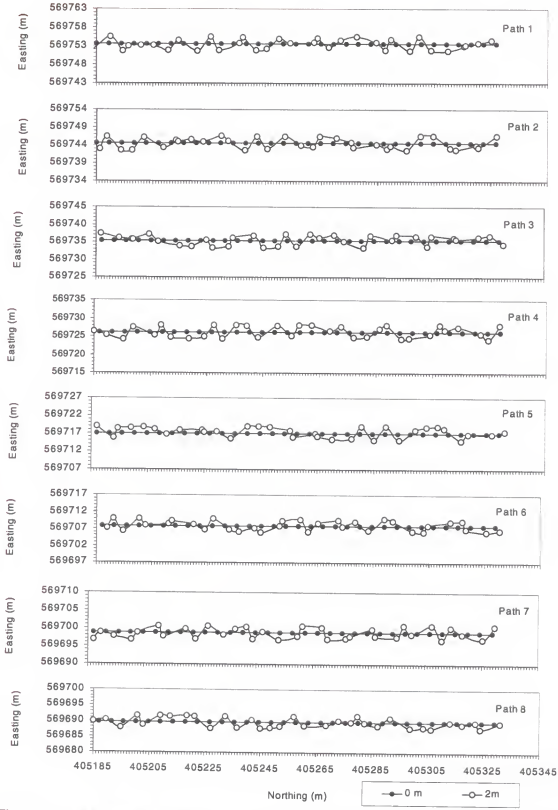

Figure 8-4a. Modeled machine paths 1 to 8 with 0 m and 2 m navigation error at 0.5 Hz DGPS sampling frequency traveling at 7.98 km/h.

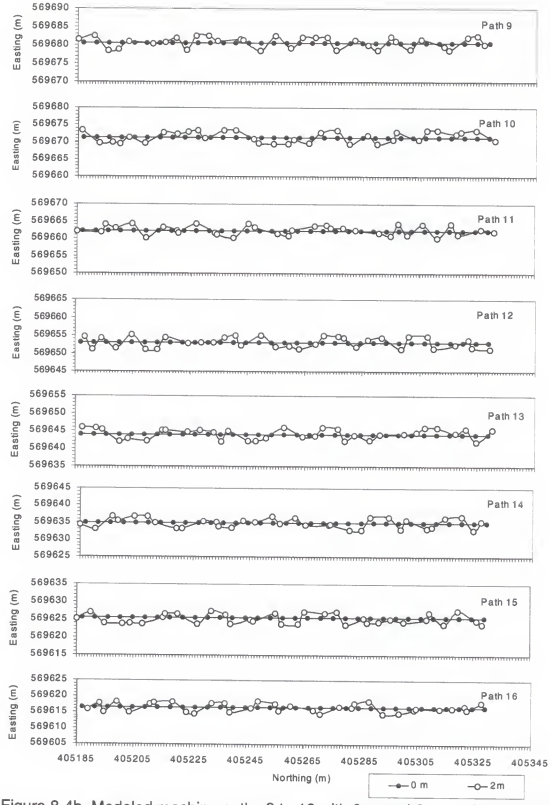

Figure 8-4b. Modeled machine paths 9 to 16 with 0 m and 2 m navigation error at 0.5 Hz DGPS sampling frequency travel at 7.98 km/h.

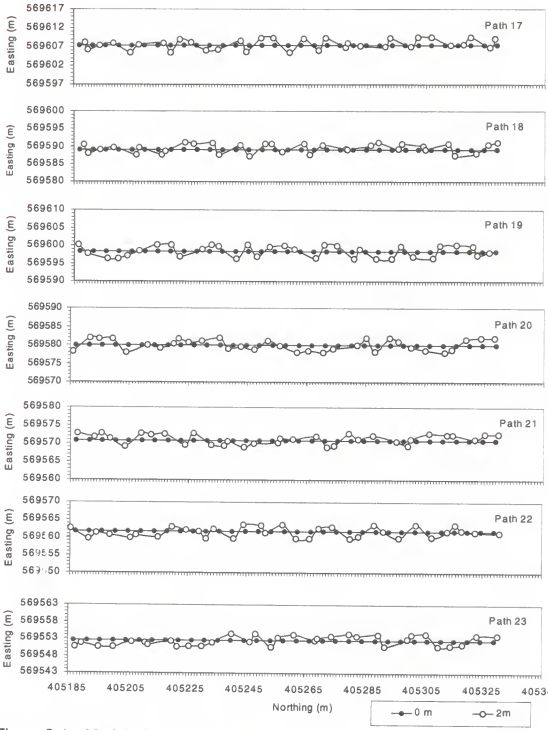

Figure 8-4c. Modeled machine paths 17 to 23 with 0 m and 2 m navigation error at 0.5 Hz DGPS sampling frequency travel at 7.98 km/h.

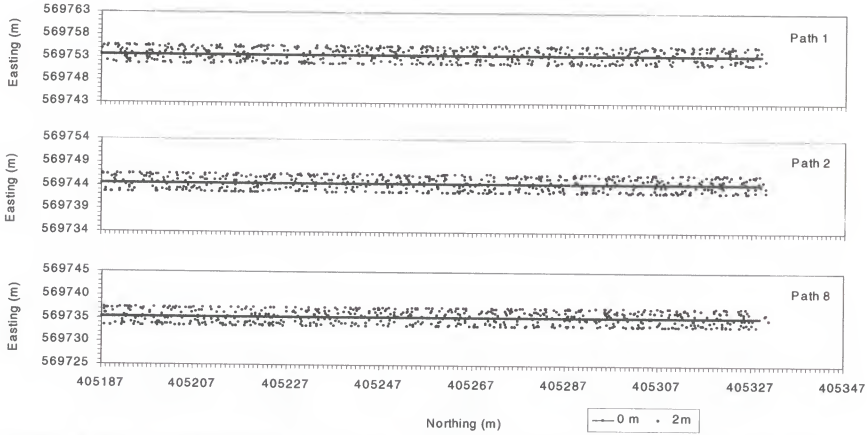

Figure 8-5. A sample of modeled machine paths 1 to 3 with 0 m and 2 m navigation error at 10 Hz DGPS sampling frequency travel at 7.98 km/h.

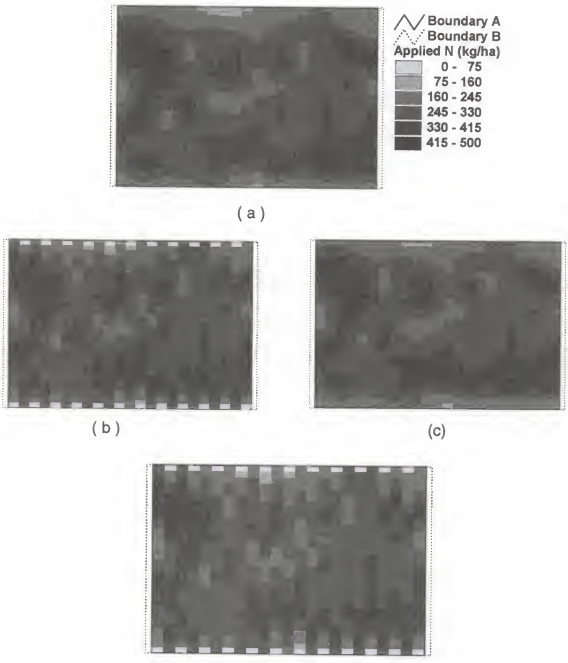

Figure 8-6. Applied N maps obtained using desired map, derived from boundary B, kriging-Gaussian method at GPS static horizontal error of 0 m, with sprayer operating at 7.98 km/h, having 0 m navigation error, at (a) F = 10 Hz, D = 0s, (b) F = 10 Hz, D = 2 s, (c) F = 0.5 Hz, D = 0 s and (d) F = 0.5 Hz, D = 2 s. (F=DGPS sampling frequency, D= spraying system delay time)

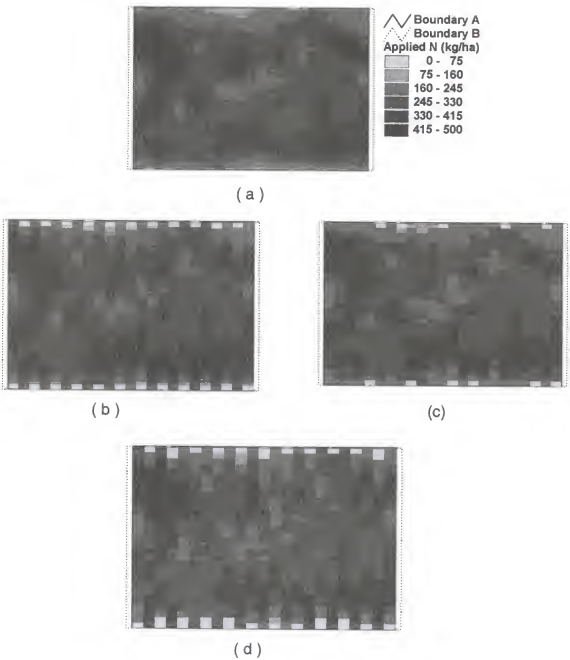

Figure 8-7. Applied N maps obtained using desired map, derived from boundary B, kriging-Gaussian method at GPS static horizontal error of 0 m, with sprayer operating at 7.98 km/h, having 2 m navigation error, at (a) F= 10 Hz, D = 0s, (b) F = 10 Hz, D = 2 s, (c) F = 0.5 Hz, D = 0 s and (d) F = 0.5 Hz, D = 2 s. (F=DGPS sampling frequency, D= spraying system delay time)

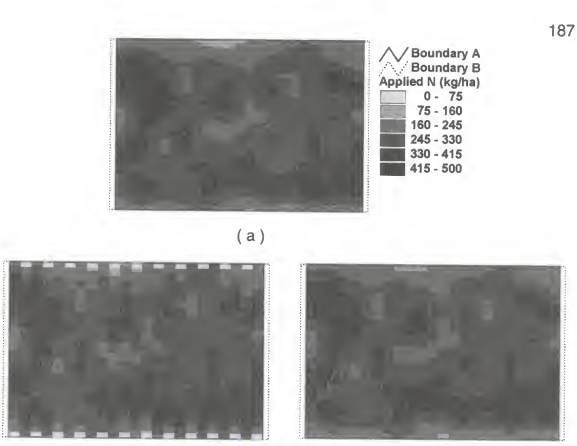

Figure 8-8. Applied N maps obtained using desired map, derived from boundary B, kriging-Gaussian method at GPS static horizontal error of 0.5 m, with sprayer operating at 7.98 km/h, having 0 m navigation error, at (a) F = 10 Hz, D = 0s, (b) F = 10 Hz, D = 2 s, (c) F = 0.5 Hz, D = 0 s and (d) F = 0.5 Hz, D = 2 s. (F=DGPS sampling frequency, D= spraying system delay time)

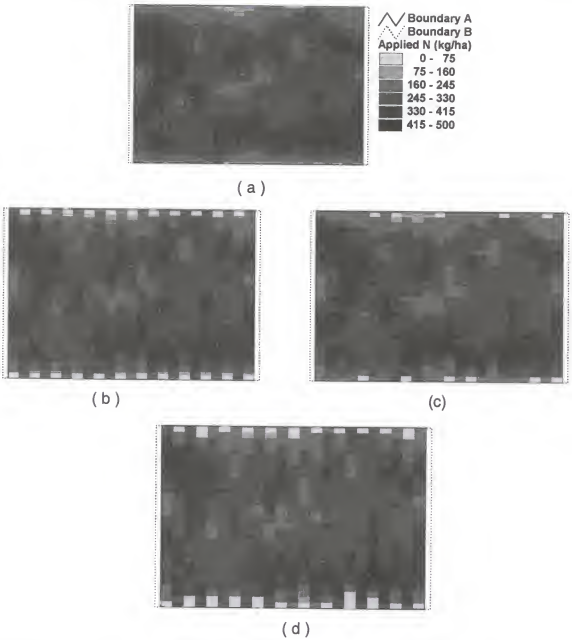

Figure 8-9. Applied N maps obtained using desired map, derived from boundary B, kriging-Gaussian method at GPS static horizontal error of 0.5 m, with sprayer operating at 7.98 km/h, having 2 m navigation error, at (a) F = 10 Hz, D = 0s, (b) F = 10 Hz, D = 2 s, (c) F = 0.5 Hz, D = 0 s and (d) F = 0.5 Hz, D = 2 s. (F=DGPS sampling frequency, D= spraying system delay time)

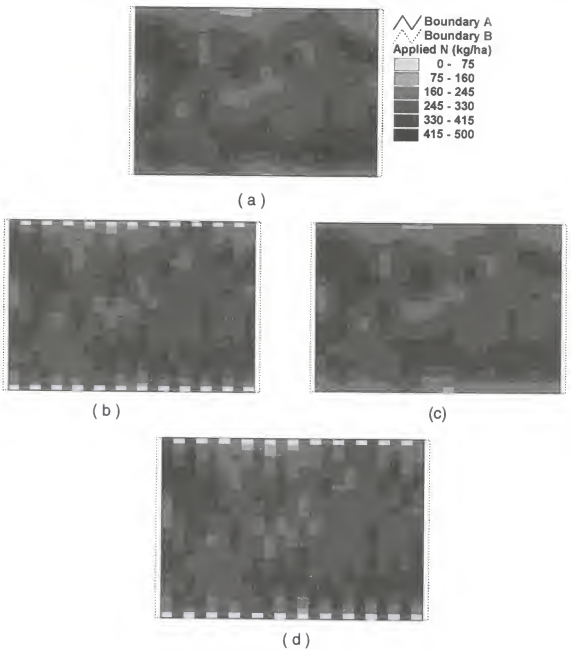

Figure 8-10. Applied N maps obtained using desired map, derived from boundary B, kriging-Gaussian method at GPS static horizontal error of 1 m, with sprayer operating at 7.98 km/h, having 0 m navigation error, at (a) F = 10 Hz, D = 0s, (b) F = 10 Hz, D = 2 s, (c) F = 0.5 Hz, D = 0 s and (d) F = 0.5 Hz, D = 2 s. (F=DGPS sampling frequency, D= spraying system delay time)

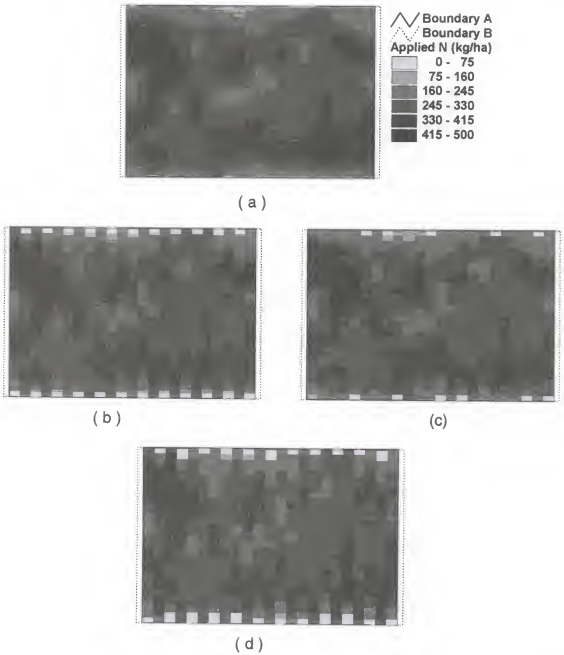

Figure 8-11. Applied N maps obtained using desired map, derived from boundary B, kriging-Gaussian method at GPS static horizontal error of 1 m, with sprayer operating at 7.98 km/h, having 2 m navigation error, at (a) F = 10 Hz, D = 0s, (b) F = 10 Hz, D = 2 s, (c) F = 0.5 Hz, D = 0 s and (d) F = 0.5 Hz, D = 2 s. (F=DGPS sampling frequency, D= spraying system delay time)

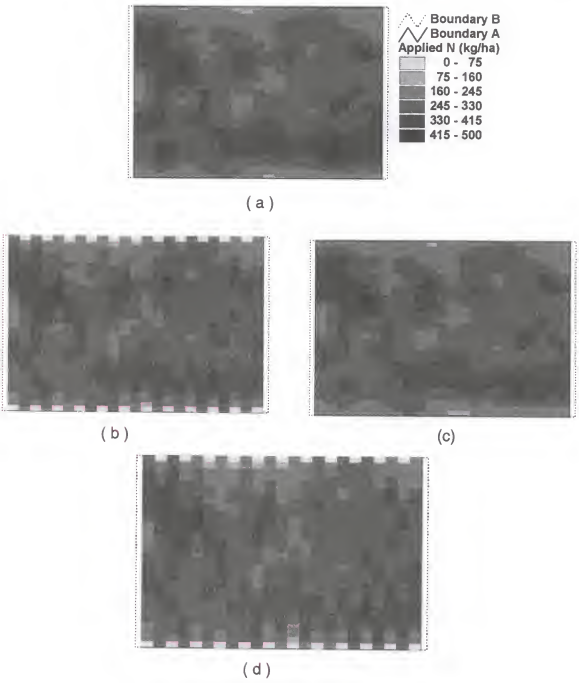

Figure 8-12. Applied N maps obtained using desired map, derived from boundary B, kriging-Gaussian method at GPS static horizontal error of 3 m, with sprayer operating at 7.98 km/h, having 0 m navigation error, at (a) F = 10 Hz, D = 0s, (b) F = 10 Hz, D = 2 s, (c) F = 0.5 Hz, D = 0 s and (d) F = 0.5 Hz, D = 2 s. (F=DGPS sampling frequency, D= spraying system delay time)

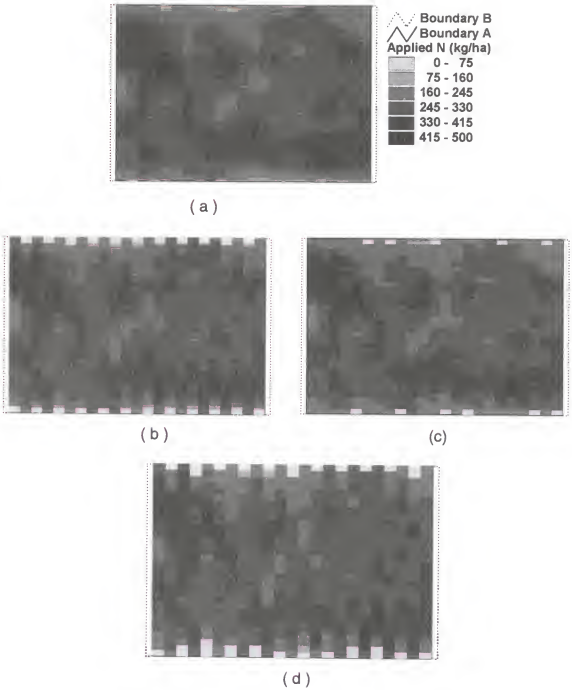

Figure 8-13. Applied N maps obtained using desired map, derived from boundary B, kriging-Gaussian method at GPS static horizontal error of 3 m, with sprayer operating at 7.98 km/h, having 2 m navigation error, at (a) F = 10 Hz, D = 0s, (b) F = 10 Hz, D = 2 s, (c) F = 0.5 Hz, D = 0 s and (d) F = 0.5 Hz, D = 2 s. (F=DGPS sampling frequency, D= spraying system delay time)

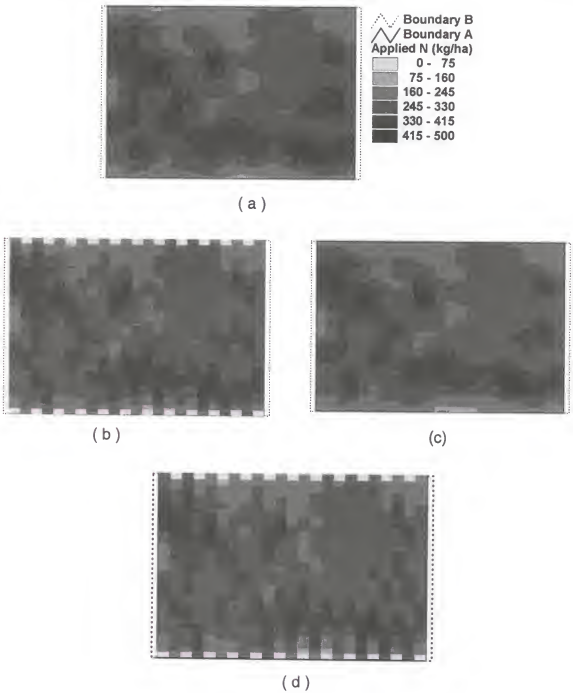

Figure 8-14. Applied N maps obtained using desired map, derived from boundary B, kriging-Gaussian method at GPS static horizontal error of 5 m, with sprayer operating at 7.98 km/h, having 0 m navigation error, at (a) F = 10 Hz, D = 0s, (b) F = 10 Hz, D = 2 s, (c) F = 0.5 Hz, D = 0 s and (d) F = 0.5 Hz, D = 2 s. (F=DGPS sampling frequency, D= spraying system delay time)

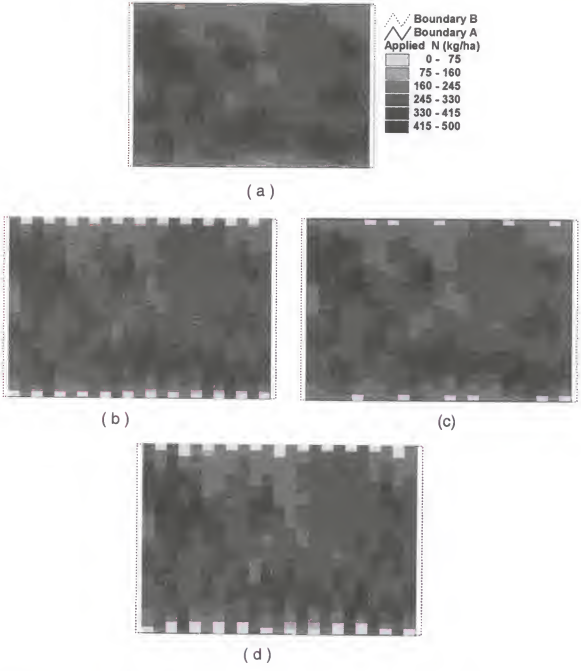

Figure 8-15. Applied N maps obtained using desired map, derived from boundary B, kriging-Gaussian method at GPS static horizontal error of 5 m, with sprayer operating at 7.98 km/h, having 2 m navigation error, at (a) F = 10 Hz, D = 0s, (b) F = 10 Hz, D = 2 s, (c) F = 0.5 Hz, D = 0 s and (d) F = 0.5 Hz, D = 2 s. (F=DGPS sampling frequency, D= spraying system delay time)

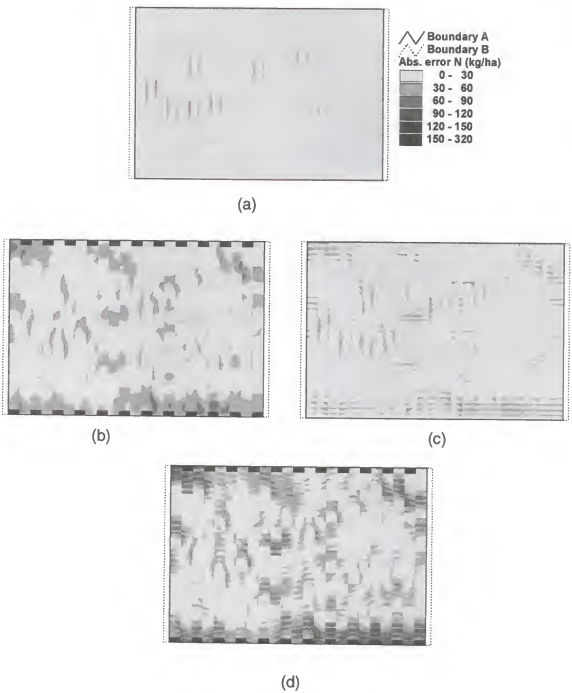

Figure 8-16. Absolute (Abs.) error maps derived from differences between desired map using boundary B, kriging-Gaussian method at GPS static horizontal error of 0 m (BG0K) versus applied map obtained with input from BG0K desired map and 0 m navigation error, at (a) F = 10 Hz, D = 0s, (b) F = 10 Hz, D = 2 s, (c) F = 0.5 Hz, D = 0 s and (d) F = 0.5 Hz, D = 2 s. (F=DGPS sampling frequency, D= spraying system delay time)

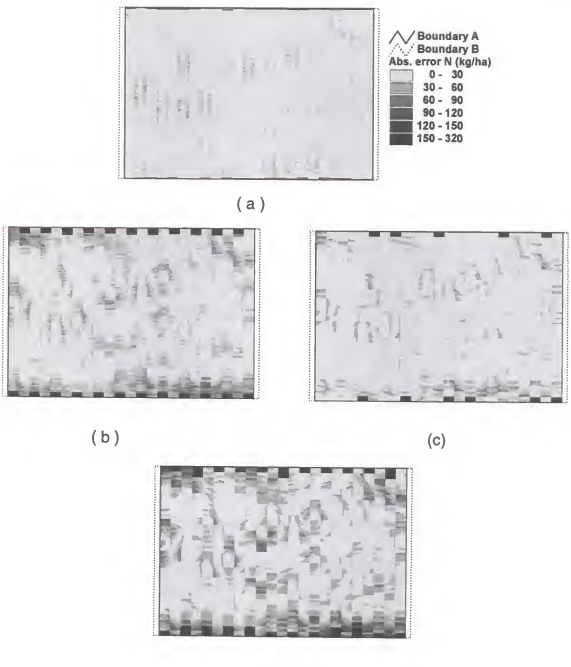

Figure 8-17. Absolute (Abs.) error maps derived from difference between desired map using boundary B, kriging-Gaussian method at GPS static horizontal error of 0 m (BG0K) versus applied map obtained with input from BG0K desired map and 2 m navigation error at (a) F = 10 Hz, D = 0s, (b) F = 10 Hz, D = 2 s, (c) F = 0.5 Hz, D = 0 s and (d) F = 0.5 Hz, D = 2 s. (F=DGPS sampling frequency, D= spraying system delay time)

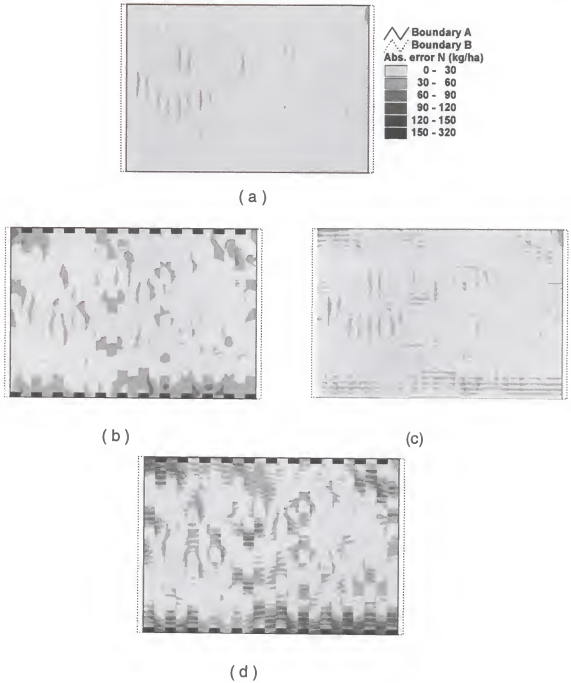

Figure 8-18. Absolute (Abs.) error maps derived from difference between desired map using boundary B (B), kriging-Gaussian method (K) at GPS static horizontal error (G) of 0 m (BG0K) versus applied map obtained with input from BG05K (G=0.5 m) desired map and 0 m navigation error at (a) F = 10 Hz, D = 0s, (b) F = 10 Hz, D = 2 s, (c) F = 0.5 Hz, D = 0 s and (d) F = 0.5 Hz, D = 2 s. (F=DGPS sampling frequency, D= spraying system delay time)

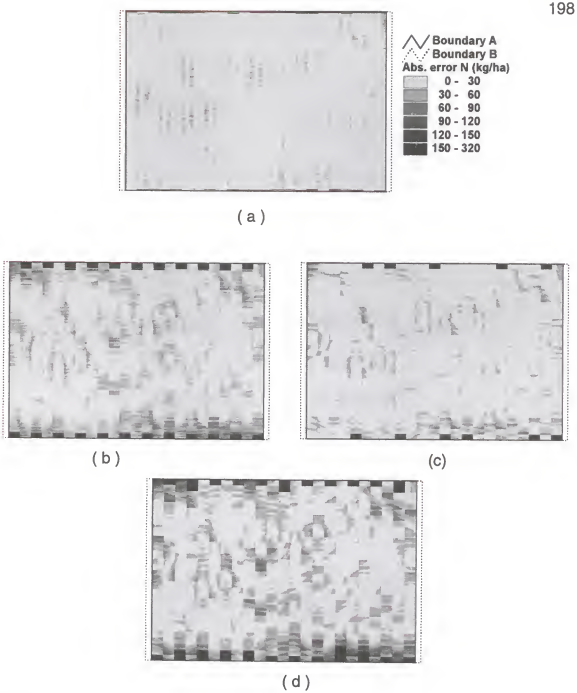

Figure 8-19. Absolute (Abs.) error maps derived from difference between desired map using boundary B (B), kriging-Gaussian method (K) at GPS static horizontal error (G) of 0 m (BG0K) versus applied map obtained with input from BG05K (G=0.5 m) desired map and 2 m navigation error at (a) F = 10 Hz, D = 0s, (b) F = 10 Hz, D = 2 s, (c) F = 0.5 Hz, D = 0 s and (d) F = 0.5 Hz, D = 2 s. (F=DGPS sampling frequency, D= spraying system delay time)

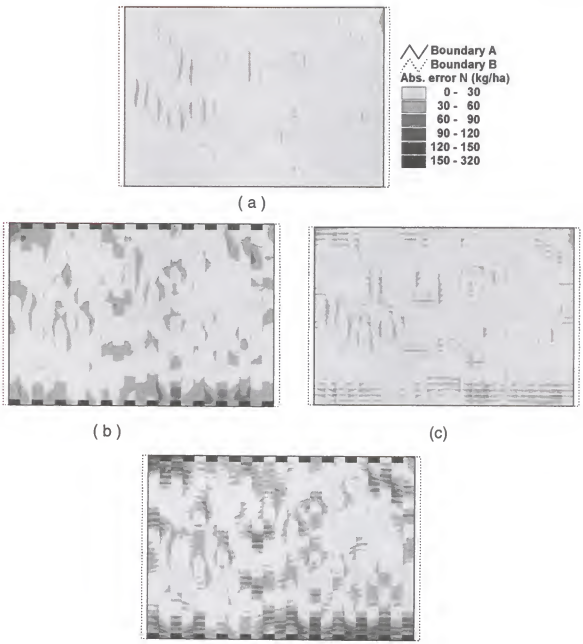

Figure 8-20. Absolute (Abs.) error maps derived from difference between desired map using boundary B (B), kriging-Gaussian method (K) at GPS static horizontal error (G) of 0 m (BG0K) versus applied map obtained with input from BG1K (G=1 m) desired map and 0 m navigation error at (a) F = 10 Hz, D = 0s, (b) F = 10 Hz, D = 2 s, (c) F = 0.5 Hz, D = 0 s and (d) F = 0.5 Hz, D = 2 s. (F=DGPS sampling frequency, D= spraying system delay time)

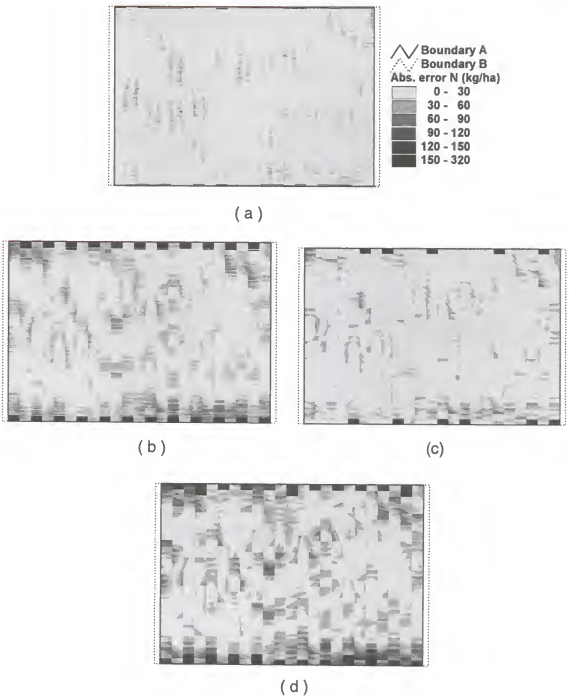

Figure 8-21. Absolute (Abs.) error maps derived from difference between desired map using boundary B, kriging-Gaussian method at GPS static horizontal error of 0 m (BG0K) versus applied map obtained with input from BG1K desired map and 2 m navigation error, at (a) F = 10 Hz, D = 0s, (b) F = 10 Hz, D = 2 s, (c) F = 0.5 Hz, D = 0 s and (d) F = 0.5 Hz, D = 2 s.

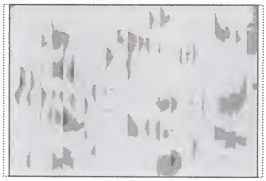

(a)

(b)

(c)

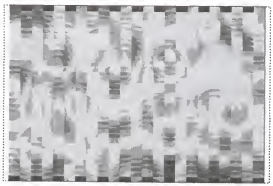

(d)

Figure 8-22. Absolute (Abs.) error maps derived from difference between desired map using boundary B, kriging-Gaussian method at GPS static horizontal error of 0 m (BG0K) versus applied map obtained with input from BG3K desired map and 0 m navigation error, at (a) F = 10 Hz, D = 0s, (b) F = 10 Hz, D = 2 s, (c) F = 0.5 Hz, D = 0 s and (d) F = 0.5 Hz, D = 2 s.

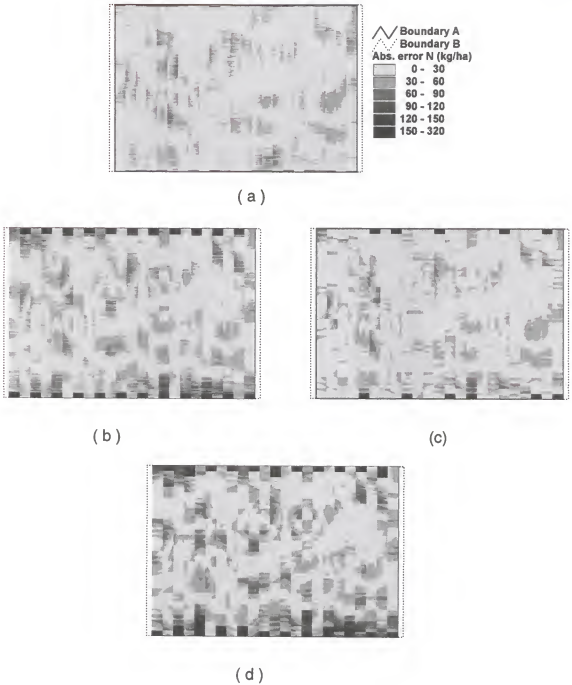

Figure 8-23. Absolute (Abs.) error maps derived from difference between desired map using boundary B, kriging-Gaussian method at GPS static horizontal error of 0 m (BG0K) versus applied map obtained with input from BG3K desired map and 2 m navigation error, at (a) F = 10 Hz, D = 0s, (b) F = 10 Hz, D = 2 s, (c) F = 0.5 Hz, D = 0 s and (d) F = 0.5 Hz, D = 2 s.

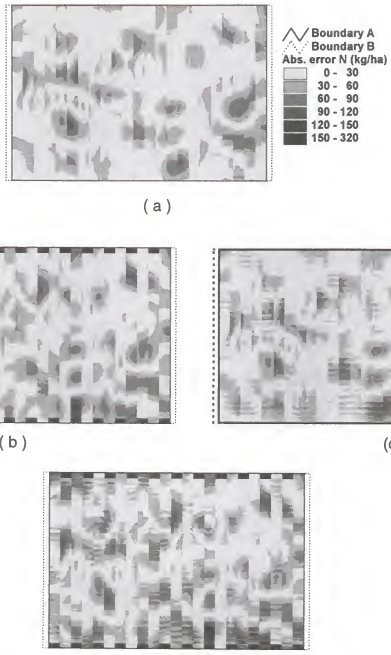

Figure 8-24. Absolute (Abs.) error maps derived from difference between desired map using boundary B, kriging-Gaussian method at GPS static horizontal error of 0 m (BG0K) versus applied map obtained with input from BG5K desired map and 0 m navigation error, at (a) F = 10 Hz, D = 0s, (b) F = 10 Hz, D = 2 s, (c) F = 0.5 Hz, D = 0 s and (d) F = 0.5 Hz, D = 2 s.

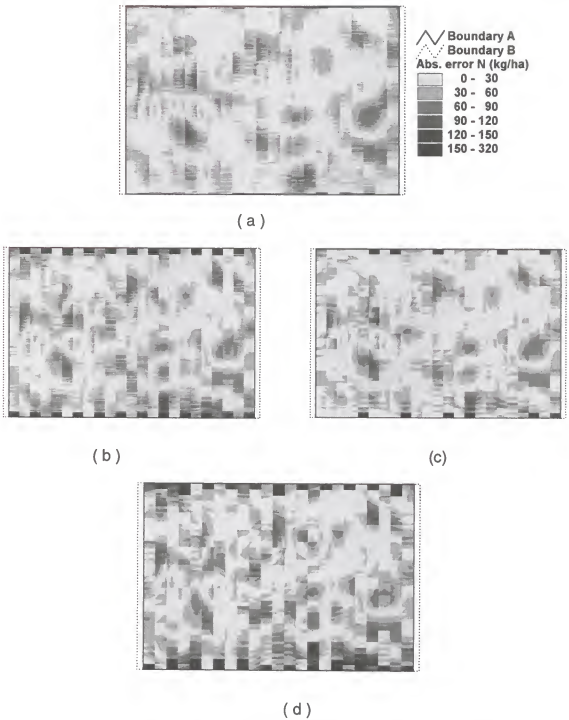

Figure 8-25. Absolute (Abs.) error maps derived from difference between desired map using boundary B, kriging-Gaussian method at GPS static horizontal error of 0 m (BG0K) versus applied map obtained with input from BG5K desired map and 2 m navigation error, at (a) F = 10 Hz, D = 0s, (b) F = 10 Hz, D = 2 s, (c) F = 0.5 Hz, D = 0 s and (d) F = 0.5 Hz, D = 2 s.

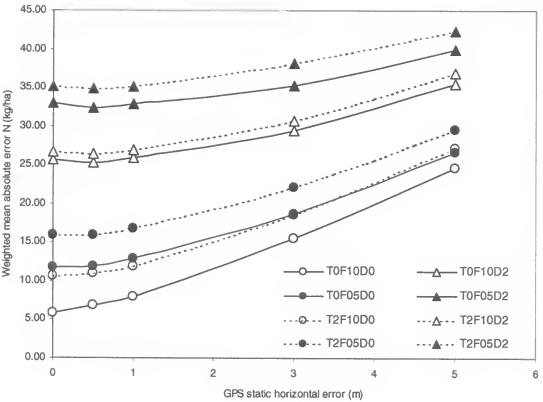

Figure 8-26. Integrated effects of navigation error (T), DGPS sampling frequency (F) and machine delay time (D) on the weighted mean absolute errors of absolute error maps computed using BG0K (best desired map) as the control. (B=boundary B, G=GPS static horizontal error, 0=0 m, K=kriging-Gaussian method).

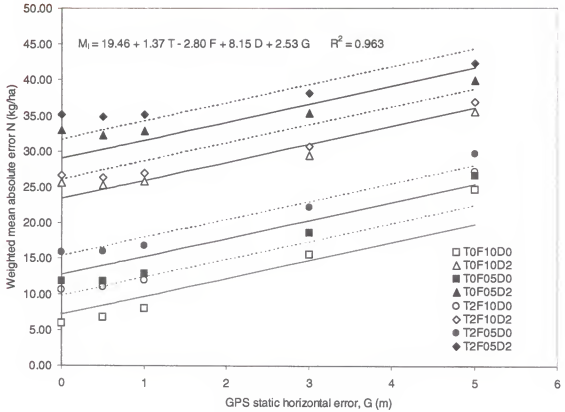

Figure 8-27. Integrated effects of navigation error (T), DGPS sampling frequency (F) and machine delay time (D) on the weighted mean absolute errors of absolute error maps computed using BG0K (best desired map) as the control. (B=boundary B, G=GPS static horizontal error, 0=0 m, K=kriging-Gaussian method). All estimated coefficients of T, F, D and G are significant at the 0.025 level using t-test. (T = –1 if 0 m, and –1 if 2m, F = -1 if 0.5 Hz, and 1 if 10 Hz, D = -1 if 0 s, and –1 if 2s).

CHAPTER 9
SPLIT N APPLICATIONS AND ERROR ANALYSIS

Introduction

An integrated error model for a MBSVR liquid fertilizer system was developed based on a single application of N fertilizer in this study. The model indicated the significance of G, T, F and D in a MBSVRA system. The influence of machine delay time was shown to be very important in a MBSVRA system. However, the example used was based on a single application of N fertilizer. Ferguson et al. (1995) reported that multiple N fertilizer applications in number of small doses may increase fertilizer efficacy. They also reported that split applications of fertilizer minimize leaching during summer rainy season and help maintain the supply of nutrients over the long growing season of Florida citrus.

Meanwhile, studies by Scholberg et al. (2000) also reported the advantages of split applications of nitrogen fertilizer. They mentioned that split applications of fertilizer and/or fertigation along with more frequent low volume irrigation can improve fertilizer use efficiency and hence reduce fertilizer cost. Applying nitrogen at high rates or using excessive irrigation can reduce nitrogen use efficiency and increase production cost.

Split N applications using a MBSVR applicator requires additional machine field applications based on the same desired map but at a reduced N rate depending on the number of split applications. It is therefore important to assess the implications of split N applications in a MBSVRA system with respect to the developed integrated model.

The objective of this study is to analyze the influence of 2 split N applications on a MBSVR fertilizer applicator using three selected parameters: at T = 2 m , F = 0.5 Hz and without overall machine delay time (D) with developed desired maps based on G = 0, 0.5, 1, 3 and 5 m in boundary B and kriging-Gaussian method.

Materials and Methods

Split N Desired Maps

From Chapter 7, five desired maps derived from analysis using boundary B, kriging-Gaussian method and at five levels of GPS static horizontal error were selected. The attribute tables of desired maps were edited reflecting 2 split N applications. Similar steps discussed in Chapter 8 were used to derive applied maps based on these new split N desired maps (Figure 9-1).

Split N Applied Maps

Two additional random simulations of navigation error (T) was conducted based on a horizontal error of 2 m. Methodology used for all other parameters,

G, F and D were the same as before. The rationale for this selection is that the influence of F and D were linear and along the field application path. Navigation error (T) is assumed to be subjected to a randomization horizontal positional error due to the behavior of GPS/DGPS discussed in Chapter 5. Similar assumption (Chapter 8) based on a circular horizontal positional error at 2 m away from the original point was used to model these machine field positions.

Table 9-1 summarizes various combinations of variables selected for the development of split N applied maps. For each split N desired map, developed at 0 m, 0.5 m, 1 m, 3 m and 5 m of GPS static horizontal error, combinations of 2 m of DGPS dynamic horizontal error, 0.5 Hz of DGPS sampling frequency and 0 s of machine delay time were used to simulate field spraying operation to obtain their corresponding applied map. Similar steps discussed in Chapter 8 were used.

Split N Integrated Analysis

Similar map-based error analysis, described in Chapter 7, using a raster-based grid-cell geoprocessing system, *Grid*, available in the ArcView 3.1 and Spatial Analyst 1.1 was used to derive the absolute error maps between split N desired and applied maps. The best desired map used for computing absolute error of each run of split N applications was based on the best desired map with ½ N rate. However, the best desired map in Chapter 7 (single application N rate)

was used to derived the absolute error map for the two combined two split N applications.

Results and Discussions

Split N Applied Maps

Figures 9-2 and 9-3 show two split N applications applied maps obtained using desired maps at GPS static horizontal error of 0 m, 0.5 m, 1 m, 3 m and 5 m in boundary B and kriging (Gaussian) method.

Split N Absolute Error Maps

Figures 9-4 to 9-5 show various split N applications absolute error maps computed between the best desired map described earlier. Similar blocky pattern were observed due to the rectangular spray pattern except that the magnitude of absolute error is reduced. Generally, the regions of high absolute error were observed in those absolute error maps computed with G equal to 5 m. The absolute error maps were classified into 6 levels at 30 kgN/ha each for the first five levels, which is the same as those absolute error maps in Chapter 8 and the last levels usually represent errors in those regions caused by zero fertilizer application. Figure 9-6 shows the two combined split N applications absolute error maps reflecting slightly higher variations in the absolute error at five levels of G.

Integrated Analysis

Table 9-2 summarizes the results of 15 absolute error maps using a cell size of 0.457 m. Each of these value represent the computed weighted mean absolute difference of 143,060 cells between the desired and applied map. The weighted mean absolute error of the two split N applications N ranges from 7.73 kg/ha to 15.33 kg/ha. The combined weighted mean absolute error for split N applications ranges from 15.80 to 29.74 kg/ha.

Figure 9-7 shows the effects of two split N applications with GPS static horizontal error (G), navigation error (T), 0.5 Hz DGPS sampling frequency (F) and 0 s machine delay time on the weighted mean absolute error between desired and applied maps using desired map derived from boundary B and kriging (Gaussian) method. Generally, the weighted mean absolute error increases as the GPS horizontal error increases. The rate of increase of weighted mean absolute error appears to be similar to those in Figure 8-26 and higher when the GPS horizontal error is greater than 1 m. There appears a slightly reduced weighted mean absolute in the combined split N applications. Linear regression line for both the single N and combined 2 split N applications were similar and were not significantly different at the 0.025 level using t-test. These results suggested an additive behavior of split N applications on the weighted mean absolute error.

It is expected that the weighted mean absolute error values for other split N applications combinations involving T (0 m), F (0.5 Hz and 10 Hz) and D (0 s

and 2 s) will be additive as F and D were linear and not subjected to randomization error in the simulation. The resultant lines for these linear combinations will be similar to those in Figure 8-26.

Conclusions

Split N applications at 2 field applications were simulated using T (2 m), F (0.5 Hz) and D (0 s) with split N desired maps derived at 5 levels of G for a MBSVR fertilizer applicator in a hypothetical citrus orchard. The resultant weighted mean absolute errors were additive.

Table 9-1. Summary of variables used in the development of ½ N applied maps

Desired map with GPS horizontal error * (m)	Navigation horizontal error (m)	Real-time DGPS sampling frequency (Hz)	Machine delay time (s)
0, 0.5, 1, 3, 5	2	0.5	0

* Using Boundary B and kriging (Gaussian) interpolation method

Table 9-2. Summary of weighted mean absolute errors between desired map (using Boundary B, kriging-Gaussian method at 0 m GPS error) versus applied map using desired map at 5 levels of GPS static horizontal error, 2 m navigation error, 0.5 Hz DGPS sampling frequency and 0 s machine delay time after ½-N applications.

Parameters	Weighted mean absolute error (KgN/ha)				
	GPS static horizontal error (m)				
	0	0.5	1	3	5
First ½ - N application	8.30	7.73	8.13	10.82	14.56
Second ½ - N application	8.30	8.40	8.75	11.41	15.33
Sum of first and second ½ - N applications (assuming additive)	16.60	16.13	16.88	22.23	29.89
Sum of first and second ½ - N applications (computed from absolute error maps)	15.80	15.96	16.69	22.08	29.74
Single rate application with 2 m navigation error, 0.5 Hz and 0 s delay	15.89	15.96	16.76	22.15	29.63

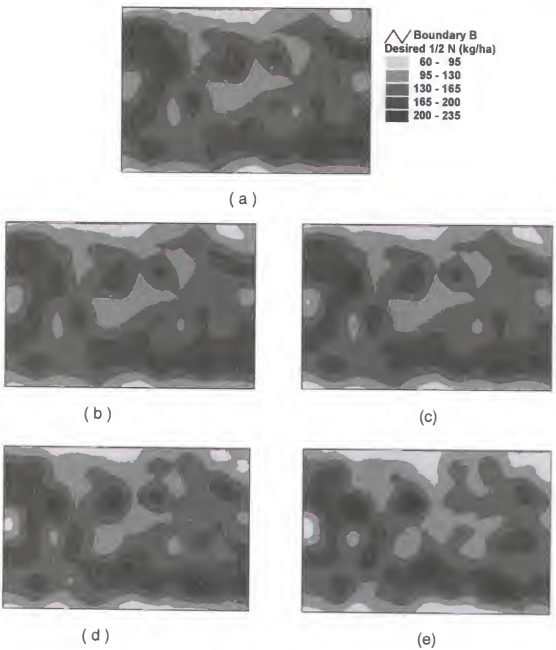

Figure 9-1. Desired ½ N application maps derived from yield maps using boundary B, kriging-Gaussian interpolation method at GPS static horizontal error of (a) 0 m, (b) 0.5 m, (c) 1 m, (d) 3 m and (e) 5 m and a rate of 4.45 kg N per t of oranges harvested.

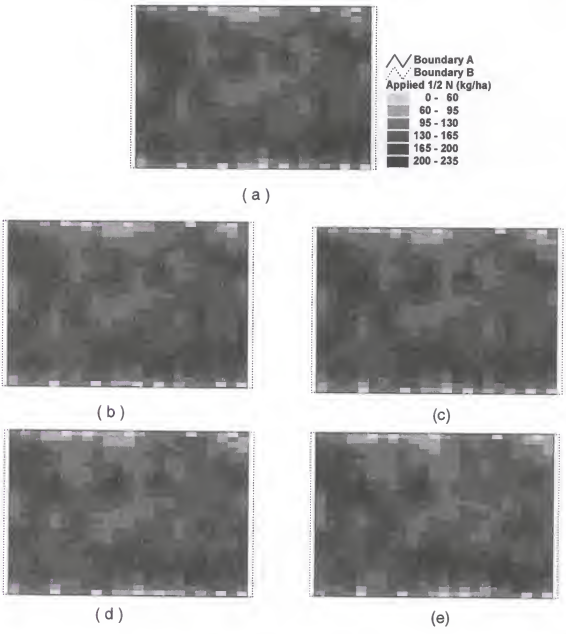

Figure 9-2. Applied ½ N maps obtained using desired maps, derived from boundary B, kriging-Gaussian method at GPS static horizontal error of (a) 0 m, (b) 0.5 m, (c) 1 m, (d) 3 m and (e) 5 m during the first application with a sprayer operating at 7.98 km/h, having 2 m navigation error at F = 0.5 Hz and D = 0s (F=DGPS sampling frequency, D= spraying system delay time).

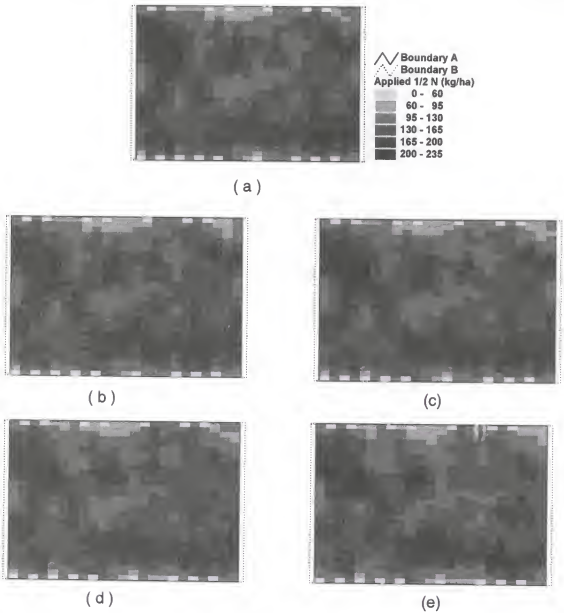

Figure 9-3. Applied ½ N maps obtained using desired maps, derived from boundary B, kriging-Gaussian method at GPS static horizontal error of (a) 0 m, (b) 0.5 m, (c) 1 m, (d) 3 m and (e) 5 m during the second application with a sprayer operating at 7.98 km/h, having 2 m navigation error at F = 0.5 Hz and D = 0s (F=DGPS sampling frequency, D= spraying system delay time).

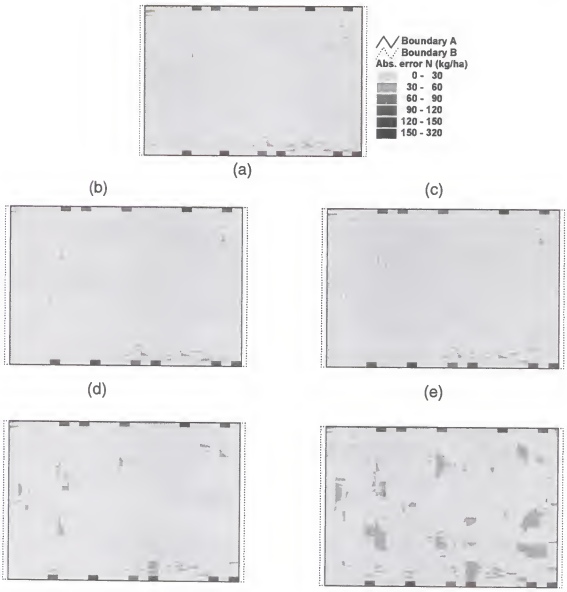

Figure 9-4. Absolute (Abs.) error maps derived from differences between desired map using boundary B, kriging-Gaussian method at GPS static horizontal error of 0 m versus first ½-N-application applied maps obtained with input from desired maps at GPS static horizontal error of (a) 0 m, (b) 0.5 m, (c) 1 m, (d) 3 m and (e) 5 m and 0.5 Hz DGPS sampling frequency, 0 s spraying system delay time.

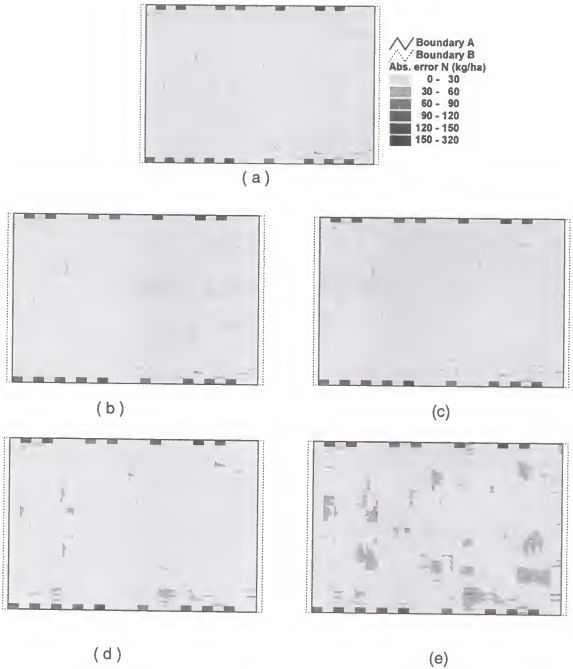

Figure 9-5. Absolute (Abs.) error maps derived from differences between desired map using boundary B, kriging-Gaussian method at GPS static horizontal error of 0 m versus second ½-N-application applied maps obtained with input from desired maps at GPS static horizontal error of (a) 0 m, (b) 0.5 m, (c) 1 m, (d) 3 m and (e) 5 m and 0.5 Hz DGPS sampling frequency, 0 s spraying system delay time.

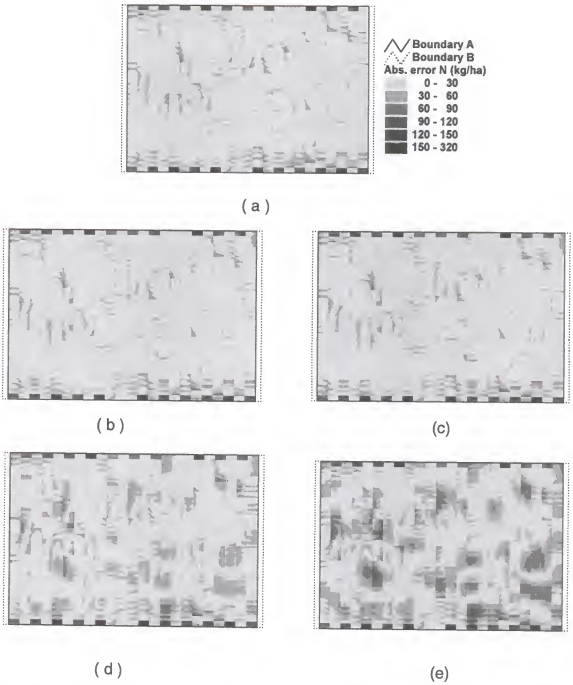

Figure 9-6. Absolute (Abs.) error maps derived from differences between desired map using boundary B, kriging-Gaussian method at GPS static horizontal error of 0 m versus sum of first and second ½-N-application applied maps obtained with input from desired maps at GPS static horizontal error of (a) 0 m, (b) 0.5 m, (c) 1 m, (d) 3 m and (e) 5 m and 0.5 Hz DGPS sampling frequency, 0 s spraying system delay time.

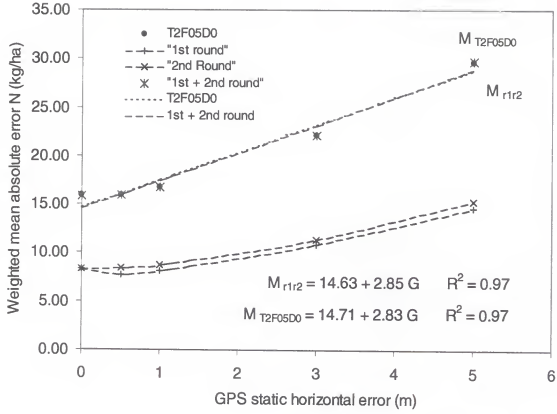

Figure 9-7. Effects of two split applications at ½ N on the weighted mean absolute errors of absolute error maps computed using BG0K (best desired map) as the control (B=boundary B, G=GPS static horizontal error, 0=0 m, K=kriging-Gaussian method) with T = 2m, F = 0.5 Hz and D = 0s.

CHAPTER 10
CONCLUSIONS AND IMPLICATIONS

Conclusions

Main Objective

An integrated model for a case study in MBSVR N fertilizer application system in a citrus orchard was developed based on the selection and analysis of the spatial accuracy/resolution requirement of three major components; GIS, GPS and machine dynamics. Six spatial parameters were selected and used in the development of the integrated model: boundary offset (Y), GPS static horizontal resolution (G), interpolation method (P), navigation error (T), DGPS sampling frequency (F) and machine delay time (D). This integrated development involved using a conceptual model that related the absolute error between the desired map and the applied map. Four spatial parameters: G, T, F and D were finally selected as variables for the integrated model, based on analysis of the desired map and the ease of data availability with the best base map and interpolation method for spatial parameter Y and P used in the desired maps. The desired maps used for the integrated model were based on the best field boundary B and kriging-Gaussian interpolation method. Besides the

integrated model, a sub-model relating the effects of Y, G and P used in the desired map was also developed.

With the test conditions used in the present set of data, the integrated model is given by, $M_I = 19.46 + 1.37T - 2.80F + 8.15D + 2.53G$ with a coefficient of determination (R^2) equal to 0.963. The values for T, F, D are coded dummy variables where, T = -1 (if the navigation error is 0 m), and 1 (if 2 m), F = -1 (if the sampling frequency is 0.5 Hz), and 1 (if 10 Hz), D = -1 (if the delay time is 0 s), and 1 (if 2 s) and G = 0, 0.5, 1, 3 and 5 m. This model shows that applied maps for a MBSVR fertilizer applicator using three selected parameters: T, F and D based on desired maps derived from boundary B, kriging-Gaussian method at 5 levels of GPS static horizontal error give a coefficient estimation for D = 8.15, which is 5.7 times greater than T, 2.9 times greater than F and 3.2 times greater than G (at G = 1 m). The developed integrated model will provide users of a MBSVRA system, especially in a tree-based crop similar to a citrus orchard, the accuracy requirements of the MBSVRA systems and its spatial components. Machine delay time, D, was a major application error component in the integrated model. This would provide justification for further development and improvement in the design of a MBSVR applicator towards the reduction in the machine delay time.

Map-based error analysis

A methodology applying the theoretical and simulation approached was developed using ArcView GIS computer program and its extension programs;

Spatial Analyst and Tracking Analyst. Besides deriving an integrated model, the spatial parameters for G, Y, P, T, F and D were either evaluated, modeled and/or analyzed. The present map-based analysis approach using geo-referenced grid cell requires intensive data processing. It is envisaged that this intensity of data processing and analysis will remain to be high considering the nature of data used in a MBSVRA involving GIS, GPS and machine dynamics.

GPS static horizontal accuracy

GPS is a major spatial factor in a MBSVRA system. It affects both the spatial accuracy of yield data collection and the machine field positioning during field application.

GPS static positioning is important in the yield data collection that was used to develop yield map using interpolation method. Real time DGPS signals were found to be important for static positioning. The higher 95-percentile static horizontal position resolution for both the Goat DGPS (4.0 m) and Omnistar DGPS receiver (2.5 m) than the Goat non-differential GPS static horizontal position resolution (60.5 m) clearly indicated this. Real-time differential correction signals also reduced the need for intensive data processing works in post processing of those non-differential GPS data.

Evaluation tests on Goat and Omnistar real-time DGPS receivers suggested a need for post processing of field position data, especially in poor areas where the real-time differential correction signal received by the DGPS receiver was weak. There were lower number of DGPS position data collected

for both the Goat and Omnistar DGPS receiver compared with the Goat non-differential receiver. Poor real time DGPS signal for the Goat unit could be attributed to the location of test site in the fringe area of receiving the US Coast Guard beacon signal. Further tests may be needed for the Omnistar, which used satellite-based differential correction signal, in identifying the reason for poor real time differential correction signals.

The Goat and Omnistar unit has a horizontal position resolution of 4.0 m and 2.5 m (95 percentile) respectively. The standard deviation of position resolution for the Omnistar unit (0.8 m) was lower than the Goat unit (2.3 m). Omnistar unit appeared to have a higher static horizontal position resolution than the Goat unit though it also costs more than the Goat unit.

DGPS dynamic horizontal accuracy in navigation

Both the Goat and Omnistar real time DGPS receiver were evaluated as used for machine field positioning in a tree-based MBSVRA field application. Navigation tests results of this study indicated that both the Goat DGPS and Omnistar DGPS receivers were not suitable to be used as a stand alone navigation device in field positioning. The presence of poor environmental factors such as high tension electrical lines may have degraded the DGPS signal. The possibility of integrating the real-time DGPS receiver with a dead-reckoning system, as reported in other studies, should be explored.

Influence of G, Y and P on desired map

Desired maps for N application rate using a recommended rate of 4.45 kg N per ha for each t/ha of harvested fruit were derived using yield maps derived from Y (boundaries B and L), G (at 0 m, 0.5 m, 1 m, 3 m and 5 m) with P (kriging-Gaussian and IWD) interpolation methods. The desired map is an important source of MBSVR fertilizer application error where the applicator controller obtains its machine input command. The sub-model for the desired map based on the present test conditions, $M_s = 9.56 + 3.94G + 4.43Y + 2.58D$ with a correlation coefficient of 0.967 indicated a good correlation among the three spatial parameters, G, Y and P. The parameters Y and P are coded dummy variables where Y = -1 (if boundary B is used), and 1 (if boundary L), P = -1 (if kriging-Gaussian method), and 1 (if IWD method) and, G = 0, 0.5, 1, 3 and 5 m. The coefficients estimate for G, Y and P are also significant at the 0.025 level using t-test.

Effects of GPS static horizontal position error, G. The influence of G ranked second at 3.94 (at G = 1 m) among the three factors; G, Y and P in the desired map. The coefficient of this factor G was slightly reduced in the overall integrated model to 2.56 indicating a higher influence of other factors such as machine delay time (D) and DGPS sampling frequency (F).

A simple randomized modeling of GPS static horizontal position was developed and used to simulate the effect of G, at 0, 0.5, 1, 3 and 5 m, in the desired map and the overall integrated model. and to study the effects of five

different GPS/DGPS static predictable horizontal errors in the development of a desired map for MBSVRA.

Effects of boundary offset, Y. Base map available from georeferenced aerial photos were used in defining field boundaries. Two boundaries, B and L were identified. A 4.6 m shift in field boundary, that is from boundary B to L, towards the south west direction caused an area change of about 0.12 ha (4 %) in boundary B and resulted in a regression coefficient of 4.43 in the sub-model weighted mean absolute error equation. This result suggested the importance in selecting the best base map. This can be achieved by using the best resolution geo-referenced aerial base map or by using a surveyed field map, if available, coupled with a good visual selection of a field boundary. The choice of a 1:30,000 scale 0.32 m resolution aerial photo was considered the best available base map used in this study.

Effects of yield map Interpolation method, P. Kriging interpolation method using the Gaussian model gives the closest estimated yield estimation with the lowest standard deviation to the ground truth yield using the sub-block yield comparison method. The best interpolation parameters for search radius and square cell size identified are 18.28 m and 0.457m respectively. The search radius and lag distance used for kriging-Gaussian interpolation method is 18.28 m and 9.14 m respectively.

Navigation error T and sampling frequency F

Three major spatial components: navigation error (T), DGSP sampling frequency (F) and machine delay time (D) were investigated for a MBSVRA spraying system. A rectangular sprayed pattern with a spraying width of 9.14 m was assumed.

Models of DGPS navigation error (T) for 23 machine spray paths were developed using a modified Tracking Analyst computer program at T equal to 0 m and 2 m based on two DGPS sampling frequencies of 0.5 Hz and 10 Hz.

Machine delay time D

Field tests of a commercial liquid fertilizer sprayer in a citrus orchard showed that the machine delay time ranges from 0.58 s to 1.20 s. Applied maps using D equal to 0 s and 2 s were investigated. The 2 s delay time was found to be a major sources of error in the overall integrated model.

Split N Applications

Split N applications at 2 field applications were simulated using T (2 m), F (0.5 Hz) and D (0 s) with split N desired maps derived at 5 levels of G for a MBSVR fertilizer applicator. The resultant weighted mean absolute errors were additive.

Implications

The integrated model may be used to assist users of a MBSVR fertilizer application in a tree-based crop in selecting appropriate accuracy level of GIS,

GPS and machine dynamic parameters. It may also be useful to other researchers working on improving GIS, GPS and machine dynamic spatial parameters.

GPS/Navigation

GPS in field data collection

Besides modeling of GPS static horizontal position, actual field tests in a citrus orchard, different GPS/DGPS receivers can be used to obtain yield data horizontal position for each receiver. These position data can be further analyzed using the same methodology developed in this study and the relative spatial resolution influence of different GPS/DGPS receivers in an integrated model can be identified.

The derivation of N desired map based on yield data alone might not be sufficient. Other data layers such as: soil, leaf analysis, water regime, which are collected using the same GPS/DGPS receiver soil should be similarly analyzed like the yield map. Compounded spatial errors due to additional data layers collected using GPS and later processed using interpolation method can be used as additional spatial parameters in the model analysis.

GPS/DGPS usage

The choice of a GPS/DGPS receiver in the overall application of a MBSVRA is a subjective question that depends on the overall objective of its usage. However, GPS constituted three of the four spatial parameters used in

this study. Static horizontal accuracy (G) ranked third in the spatial accuracy requirement in the integrated model. If the same DGPS receiver is used for machine navigation, due to maximization of DGPS receiver usage, then the combined effect of G, T and F will contribute a significant sources of error to the overall model besides machine delay time.

Modeling of navigation error

More levels of navigation error T at different sampling frequency should be modeled and used as input to the overall model. A good choice of navigation errors would be to first investigate the most probable types of GPS/DGPS available before it is being modeled. Alternatively, the intended GPS/DGPS machine navigation system should be operated in an actual orchard and its position data files and frequency recorded into a file used as input in the development of an integrated model.

GIS/mapping

It may be required to investigate the effects of using base map of different scale in the development of a desired map for situation where the choice of aerial photograph or boundary selection involved additional cost. The problem in choice of base map is not expected to be critical as some commercial MBSVRA systems are using GPS/DGPS to mark the field boundary. In this case, the static horizontal resolution of the GPS/DGPS receiver should be included in the analysis of the integrated model.

Attribute of data point

Current yield map data was represented by tonnes of harvested fruit per hectare. An instrumented Goat truck has been developed capable of collecting citrus yield base on weight (Miller and Whitney, 1999). The effect of yield map based on actual weight of harvested fruit per individual tree basis should be investigated. Furthermore, yield data per individual tree basis should be obtained so a comparison of the best interpolation method and its best choice of interpolation parameters can be accurately identified.

Interpolation method

The present study selected kriging-Gaussian as the best interpolation method due to its closest correlation to the ground truth yield coupled with its advantage in interpolating clustered citrus yield data points. It may be necessary to investigate the effect of different interpolation method when the individual tree yield data are available as the coefficients of correlation for both IWD and kriging-Gaussian were quite similar (Table 6-5). The effect of using IWD interpolation method as the best yield map may be used as it provided the best point estimation to the density map though it underestimate the overall ground truth yield and had problems with clustered citrus yield data points.

Machine Dynamics

Machine delay time of 2 s highly influence the weighted mean absolute error in a MBSVR fertilizer application integrated model. Feed-forward command

in spatially variable control can reduce the effect of machine delay time (D) when the two assumptions in feed-forward command were met. The first was that the machine path of the applicator was known. The second was that the working speed of the applicator remained constant. Violation of these assumptions would degrade the performance of the feed-forward command. Furthermore, machine failure during field application will cause the error to add up.

Spraying pattern

Different spray patterns can be incorporated in future study to investigate the behavior of different types of SVR spray nozzles, spacings and heights in the spatial accuracy of a MBSVRA. Furthermore, a refined spray pattern considering lateral resolution along the spray boom using estimated spatial position of spray nozzle which can vary its application rate along the spray boom.

Finally, different field application speeds require investigation for the development of an integrated model.

GLOSSARY

2dRMS	Twice the distance RMS
AE	Absolute error
C/A	Coarse acquisition
CEP	Circular error probable
D	Machine delay time, s
DGPS	Differential global positioning system
DoD	Department of Defense
DOQ	Digital orthophoto quadrangles
DOP	Dilution of precision
DM_{BEST}	Best desired map (expressed in rate of application)
DM_{REJECT}	Any other desired map other than the best desired map (expressed in rate of application)
E_{DM}	Desired map errors (expressed in rate of application)
E	Applied map error (expressed in rate of application)
F	DGPS sampling frequency, Hz
G	GPS/DGPS static horizontal positional error, m
GIS	Geographical information system
GPS	Global positioning system

HDOP	Horizontal dilution of precision for horizontal measurements (latitude and longitude) refers to a measure of the accuracy of a GPS position based on the relative positions of the satellites.
M	Weighted mean absolute error
M_I	Integrated weighted mean absolute error
M_S	Sub-model weighted mean absolute error
MBSVR	Map-based spatially variable rate
MBSVRA	Map-based spatially variable rate application
N	Nitrogen
$N_{applied}$	Applied map (expressed in rate of application)
P	Interpolation method
PDOP	Position dilution of precision for the horizontal and vertical measurements (latitude, longitude and altitude) refers to a measure of the accuracy of a GPS position based on the relative positions of the satellites.
RMS	Root means square
R95	Horizontal 95-percentile error
RTK	Real time kinematic
SPS	Standard positioning service
SSF	Site specific farming
SVR	Spatially variable rate
T	Navigation error or DGPS dynamic horizontal error, m
UTC	Universal time coordinated
Y	Boundary offset

APPENDIX A
SUMMARY OF GOAT UNIT MODEL 1002-103 SPECIFICATIONS

Parameters		Specifications
Size	–	8.75" W x 5.75" x 2.25"D
Power	–	2.5W. 9-30 V
Data storage	–	The Goat can store in excess of 2,000 data points
GPS	–	Uses Lassen-SK8 GPS board
	–	power + 5 volts DC
	–	L1 frequency, C/A code (SPS), continuous tracking receiver, 32 correlators
	–	update rate Trimble TSIP data format @ 1 Hz; NMEA @ 1 Hz.
	–	8 channel real time differential correction ready
	–	25 m horizontal accuracy circular error probable without selective availability
	–	velocity accuracy, 0.05 m/s
	–	time, ± 500 nano-seconds (nominal)
	–	Battery back-up RAM to enable Hot and Warm Starts
	–	Post processing ready
DGPS	–	Uses CSI Model SBX-2 board, cold start less than 60 s, warm start less than 2 s, 5 V DC
	–	less than 1 W nominal power consumption
	–	correction output protocol RTCM SC-104
	–	Input/Status protocol NMEA 0183 V2.0
Data acquisition	–	15 s, hot start (with ephemeris data stored)
	–	45 s, warm start (with last position, time and almanac data stored)
	–	120 s, cold start (with no initialization)
Data transfer	–	via a computer serial port through a detachable 9 or 25 pin cable
	–	With analog to digital option
Antennas	–	GPS antenna, 40.6 mm x 48.3 mm x 13.9 mm
	–	MBA-3 beacon whip DGPS antenna, 39 mm diameter x 371 mm length, with frequency range of 283.5 to 325 kHz

APPENDIX B
SUMMARY OF OMNISTAR OS7000 SPECIFICATIONS

Parameters		Specifications
Frequency	–	Spread spectrum
	–	C-band (3750/4250 Mhz)
	–	L1 band, C/A code, 8 channel, continuous tracking
Data acquisition	–	cold start, less than 90 s
	–	warm start, less than 90 s
Data output	–	NMEA 0183 Version 2.1sentences providing position, GPS DOP and active satellites, and recommended minimum specific GPS data @ 1 Hz plus number of satellite in view data @ 0.2 Hz @ 4800 baud rate
Power		
	–	12 V DC, $\pm$ 4 V
	–	power consumption 10 W
Dimensions		
	–	Cylindrical, 7.5 in diameter, 4.5 in height
Accuracy		
	–	less than 3 m horizontal at 1 sigma,
	–	1.5 m, 1 sigma nominal dependent on GPS satellite geometry and local conditions

APPENDIX C
PARAMETERS USED IN ARCVIEW TO CREATE YIELD MAPS

A. Density Calculation

1. Highlight the tub location Shapefile containing latitude, longitude, tons of fruit per tub.
2. Select Analysis/Calculate Density.
3. Output grid extent - select the line Shapefile that defines the harvest area - cell size = 0.457 m (1/20 the between tree rows spacing).
4. Population field - choose tons.
5. Search radius 18.28 m
6. Kernel density.
7. Area units -hectares.

B. Map Calculation

1. Highlight the Density Surface created in the preceding steps and select Analysis/Map Calculator.
2. Double click on the Density Surface to move it into the calculation box to evaluate (Density Surface x 1) Integer.

C. Shapefile

1. Highlight the Map Calculator theme.
2. Select Theme/Convert to Shapefile.

D. Merging Point and Polygon Shapefiles

1. Open the attribute table for the Map Calculator theme.
2. Highlight the Shape field of that table.
3. Open the attribute table for the original tub location point file.
4. Highlight the Shape field of that table, and join the two tables.

E. Surface Interpolation

1. Highlight the Point Shapefile created in D4.
2. Select Surface/Interpolation grid.
3. Output grid extent - use the same line Shapefile used in A3.
4. Cell size - 0.457 m.
5. Type of interpolation - IDW or kriging (Boeringa, 1998)
6. Z-value - gridcode from joined table.
7. Search radius as in A5, with a power of 2, Barrier - select no barrier.
8. In kriging, select create variogram, select model to fit variogram, choose selected model to create yield surface.

(From Whitney et al. 1999a and Chan et al. 1999a with some modifications on the parameters used in sections A and E).

APPENDIX D
SUMMARY OF MAP-BASED ERROR ANALYSIS METHOD

A. To obtain absolute error map

1. Convert the selected desired map into integer grid, choose analysis cell size=0.457 m.
2. Convert the selected applied map into integer grid, choose analysis cell size equal to 0.457 m.
3. Select Analysis/Map Calculator.
4. Select desired map gird,
5. Select minus (-) operator
6. Select applied map grid
7. Choose absolute value for output
8. Click evaluate and add new gird to be displayed
9. Convert the new absolute error grid map into integer grid

B. To obtain weighted mean absolute error

1. From A 7 obtain the attribute table of integer absolute error map
2. Export the integer absolute error map table to a text file or a database file.
3. Use a spreadsheet program to compute the weighted mean absolute error for the absolute error map.

REFERENCES

Al-Gaadi, K.A., & P.D. Ayers. 1999. Integrating GIS and GPS into a spatially variable rate herbicide application system. *Applied Engineering in Agriculture* 15(4): 255-262.

Alcalã-Jiménez, A.R., & S. Alamo-Romero. 1998. Using GPS for yield mapping in olive orchards. In *Proceedings of the First International Conference on Geospatial Information In Agriculture And Forestry* 2. Ann Arbor, MI: ERIM, 633-637.

Anderson, E.W. 1997. The treatment of navigation errors. *Navigation* 3: 362-371.

Anderson, G. L., & C. Yang. 1996. Multispectral videography and geographic information systems for site specific farm management. In *Proceedings of the Third International Conference on Precision Agriculture*, edited by P.C. Robert, R.H. Rust, & W.E. Larson. Madison, WI: ASA/CSSA/SSSA, 681-692.

Anderson, N.W., & D.S. Humburg. 1997. Application equipment for site specific management. In*The State of Site-Specific Management for Agriculture*, edited by F.J. Pierce, & E.J. Sadler, Madison, WI: ASA/CSSA/SSSA, 245-281.

Anonymous 1995. Global positioning system standard positioning service signal specification. US Coast Guard Navigation Center Technical Reports.

Anonymous 1997. *The precision farming guide for agriculturists*. Moline, IL: John Deere, 20 p.

Anonymous 2000. Florida farm commodities - Citrus. Http://www.fl-ag.com/agfacts/citrus.htm. (15 February 2000).

Balsari, P., M. Tamagnone, & A. Bertola. 1997. Directional control of agricultural vehicles. In *Proceedings of First European Conference on Precision Agriculture,* edited by J.V. Stafford. Oxford, UK: BIOS Scientific, 551-558.

Barnes, J.B., & P.A. Cross. 1998. Processing models for very high accuracy GPS positioning. *Navigation* 51(2):180-185.

Birrell, S.J., S.C. Borgelt, & K.A. Sudduth. 1995. Crop yield mapping: Comparison of yield monitors and mapping techniques. In *Proceedings of the Second International Conference on Site-Specific Management for Agricultural Systems*, edited by P.C. Robert, R.H. Rust, & W.E. Larson. Madison, WI: ASA/CSSA/SSSA, 15-32.

Blackmore, S. 1994. Precision farming: An introduction. *Outlook on Agriculture.* 23(4): 275-280.

Blackmore, B.S., & C.J. Marshall. 1996. Yield Mapping; Errors and Algorithms. In *Proceedings of the Third International Conference on Precision Agriculture*, edited by P.C. Robert, R.H. Rust, & W.E. Larson. Madison, WI: ASA/CSSA/SSSA, 403-415.

Blackmore, B.S., P.N. Wheeler, R.M. Morris, & R.J.A. Jones. 1995. The Role of Precision Farming in Sustainable Agriculture; A European Perspective. In *Proceedings of the Second International Conference on Site-Specific Management for Agricultural Systems*, edited by P.C. Robert, R.H. Rust, & W.E. Larson. Madison, WI: ASA/CSSA/SSSA, 777-793.

Boeringa, M. 1998. Kriging 1.1 for ArcView spatial analyst. Http://andes.esri.com/arcscripts/ (15 October 1998).

Borgelt, S.C., J.D. Harrison, K.A. Sudduth, & S.J. Birrell. 1996. Evaluation of GPS for applications in precision agriculture. *Applied Engineering in Agriculture* 12: 633-638.

Buick, R. 1998. How precise are parallel swathing systems ? *Modern Agriculture* 1(6): 32-34.

Cahn, M.D., & J.W. Hummel. 1995. A variable rate applicator for side dressing liquid N fertilizer. In *Proceedings of the Second International Conference on Site-Specific Management for Agricultural Systems*, edited by P.C. Robert, R.H. Rust, & W.E. Larson. Madison, WI: ASA/CSSA/SSSA, 683-689.

Chan, C.W., J.K. Schueller, W.M. Miller, J.D. Whitney, & T.A. Wheaton. 1999a. Interpolation errors in citrus yield mapping. ASAE Paper No. 99-FL101. St. Joseph, MI:ASAE.

Chan, C.W., J.K. Schueller, W.M. Miller, J.D. Whitney, & T.A. Wheaton. 1999b. Accuracy in spatially-variable crop production and an illustration in citrus yield mapping. In *Proceedings of the Second European Conference on Precision Agriculture*, edited by J.V. Stafford. Sheffield, UK: Sheffield Academic Press, 805-813.

Clark, R. L. 1996. A comparison of rapid GPS techniques for topographic mapping. In *Proceedings of the Third International Conference on Precision Agriculture*, edited by P.C. Robert, R.H. Rust, & W.E. Larson. Madison, WI: ASA/CSSA/SSSA, 651-662.

Clark, R.L., & W.W. Worley. 1994. Accuracy of DGPS position information from land based moving vehicles with a C/A code GPS receiver. ASAE Paper No. 94-3545. St. Joseph, MI:ASAE.

Cox, G. 1997. Yield mapping sugar cane. Http://neptune.eng.usq.au/~coxg/ymapping.htm (7 September 1998).

Dampney, P.M.R., & M. Moore. 1999. Precision agriculture in England: Current practice and research-based advice to farmers. In *Proceedings of the Fourth International Conference on Precision Agriculture*, edited by P.C. Robert, R.H. Rust, & W.E. Larson. Madison, WI: ASA/CSSA/SSSA, 661-674.

Diggelen F.V. 1998. GPS accuracies: Lies, Damn lies, and statistics. *GPS World* 1-4.

Dobermann, A., & M. Bell. 1997. Precision farming for intensive rice systems in Asia. China-IRRI Dialogue Nov. 1997. Manila, Philippines:IRRI. Unpublished paper, 31 p.

Foote, K.E., & D.J. Huebner. 1995. Error, accuracy, and precision. Http://www.utexas.edu/depts/grg/gcraft/notes/error/error_ftoc.html (17 July 1998).

Ferguson, J.J., F.S. Davies, D.P.H. Tucker, A.K. Alva, & T.A. Wheaton. 1995. Fertilizer guidelines. In *Nutrition of Florida Citrus Trees*, edited by D.P.H. Tucker, A.K. Alva, L.K. Jackson, & T.A. Wheaton. Gainesville, FL:IFAS, University of Florida, 21-25.

Fergusson, R.B., C.A. Gotway, G.W. Hergert, & T.A. Peterson. 1996. Soil sampling for site specific nitrogen management. In *Proceedings of the Third International Conference on Precision Agriculture*, edited by P.C.

Robert, R.H. Rust, & W.E. Larson. Madison, WI: ASA/CSSA/SSSA, 13-22.

Glancey, J.L., & W.E. Kee. 1998. Yield and soil property variations in processed vegetable production on the Delmarva Peninsula. ASAE Paper No. 98-1099. St. Joseph, MI:ASAE.

Glazer, F., B. Pinette, & C. Blazquez. 1998. In *Proceedings of the First International Conference on Geospatial Information in Agriculture and Forestry* 1. Ann Arbor, MI: ERIM, 621-628.

Goense, D. 1997. The Accuracy of farm machinery for precision agriculture: a case for fertilizer application. *Netherlands Journal of Agricultural Science* 45: 201-217.

Han, S., J.W. Hummel, C.E. Goering, & M.D. Cahn. 1994. Cell size selection for site-specific crop management. *Transaction of the ASAE* 37(1):19-26.

Hellebrand, H.J., & H. Beuche. 1997. Multi-component positioning for site-specific farming. In *Proceedings of the First European Conference on Precision Agriculture*, edited by J.V. Stafford. Oxford, UK: BIOS Scientific, 575-583.

Huff, M. 1997. Omnistar - A versatile DGPS positioning tool. Omnistar Inc., Unpublished paper, 10 p.

Ingram, P. 1998. An introduction to geostatistics. Http://137.111.98.10/users/pingram/geostat.html (14 August 1998).

Isaaks, E.H., & R.M. Srivastava. 1989. *An introduction to applied geostatistics.* Oxford, England:Oxford University Press, 561 p.

Jackson, L.K., A.K. Alva, D.P.H. Tucker, & D.V. Calvert. 1995. Factors to consider in developing a nutrition program. In *Nutrition of Florida Citrus Trees*, edited by D.P.H. Tucker, A.K. Alva, L.K. Jackson, & T.A. Wheaton. Gainesville, FL: IFAS, University of Florida, 3-11.

Lachapelle, G., & J. Henriksen. 1995. GPS under cover: The effect of foliage on vehicular navigation. *GPS World* 6(3): 26-35.

Lang, L. 1997. Use of GIS, GPS and remote sensing spread to California's winegrowers. *Modern Agriculture* 1(2): 12-16

Lange, A.F. 1996. Centimeter accuracy differential GPS for precision agriculture application. In *Proceedings of the Third International Conference on Precision Agriculture*, edited by P.C. Robert, R.H. Rust, & W.E. Larson. Madison, WI: ASA/CSSA/SSSA, 675-680.

Larscheid, G., & B.S. Blackmore. 1996. Interactions Between Farm Managers and Information Systems with Respect to Yield Mapping. In *Proceedings of the Third International Conference on Precision Agriculture*, edited by P.C. Robert, R.H. Rust, & W.E. Larson. Madison, WI: ASA/CSSA/SSSA, 1153-1163.

Larsen, W.E., D.A. Tyler, & G.A. Nielsen. 1988. Field navigation using the global positioning system. ASAE Paper No. 88-1604. St. Joseph, MI:ASAE.

Le Bars, J.M., & D. Boffety. 1997. Location improvement by combining a DGPS system with on-field vehicle sensors. In *Proceedings of the First European Conference on Precision Agriculture*, edited by J.V. Stafford. Oxford, UK: BIOS Scientific, 585-591.

Mack, G. 1997. Precise positioning for agriculture. In *Proceedings of the First European Conference on Precision Agriculture*, edited by J.V. Stafford. Oxford, UK: BIOS Scientific, 593-602.

McCauley, J.D., & B.A. Engel. 1997. Approximation of noisy bivariate traverse data for precision mapping. *Transactions of the ASAE* 40(1): 237-245.

Mertikas, S., D. Wells, & P. Leenhouts. 1985. Treatment of navigational accuracies: proposal for the future. *Navigation* 32(1): 68-84.

Miller, W.M., & J.D. Whitney. 1999. Evaluation of weighing systems for citrus yield monitoring. *Applied Engineering in Agriculture* 15(6): 609-614.

Molin, J.P., & E.R.S. Ruiz. 1999. Accuracy of DGPS for ground application in parallel swaths. ASAE Paper No. 99-1043. St. Joseph, MI:ASAE.

Monson, R.J. 1997. A methodology for quantifying the capabilities of a GPS navigation system. ASAE Paper No. 97-3060. St. Joseph, MI:ASAE.

Moore, M. 1997. An investigation into the accuracy of yield maps and their subsequent use in crop management, Unpublished Ph.D. Dissertation Silsoe College, UK.

Morgan, M.T. 1995. Precision Farming: Sensors vs. Map-Based. Http://dynamo.ecn.purdue.edu/~biehl/SiteFarming/sensors.html (11 July 1998).

Murphy, P., E. Schnug, & S. Haneklaus. 1994. Yield mapping - A guide to improved techniques and strategies. In *Proceedings of the Second International Conference on Site-Specific Management for Agricultural Systems*, edited by P.C. Robert, R.H. Rust, & W.E. Larson. Madison, WI: ASA/CSSA/SSSA, 33 - 48.

Nowark, P. 1998. Part 2: Thinking about precision agriculture. May 1988, *@gInnovator* 5(8): 1 p.

Olieslagers, R., H. Ramon, H. Delcourt, & L. Bashford. 1995. The accuracy of site-specific fertilizer application by means of a spinning-disc fertilizer spreader. In *Proceedings of the Second International Conference on Site-Specific Management for Agricultural Systems*, edited by P.C. Robert, R.H. Rust, & W.E. Larson. Madison, WI: ASA/CSSA/SSSA, 709-719.

O'Connor, M., T. Bell, G. Elkaim, & B. Parkinson. 1996. Automatic steering of farm vehicles using GPS. In *Proceedings of the Third International Conference on Precision Agriculture*, edited by P.C. Robert, R.H. Rust, & W.E. Larson. Madison, WI: ASA/CSSA/SSSA, 767-777.

Paice, M.E.R., P.C.H. Miller, & W. Day. 1996. Control requirements for spatially selective herbicide sprayers. *Computers and Electronic in Agriculture* 14. 163-177.

Perry, C.D., D.L. Thomas, G. Vellidis, & J.S. Durrence. 1997. Integration and coordination of multiple sensor and GPS data acquisition for precision farming systems. ASAE Paper No. 97-3143. St. Joseph, MI:ASAE.

Pierce, F.J., N.W. Anderson, T.S. Colvin, J.K. Schueller, D.S. Humburg, & N.B. McLaughlin. 1997. Yield mapping. In *The State of Site-Specific Management for Agriculture*, edited by F.J. Pierce, & E.J. Sadler. Madison, WI:ASA/CSSA/SSSA, 211-243.

Qiu, W., G.A. Watkins, C.J. Sobolik, & S.A. Shearer. 1998. A feasibility study of direct injection for variable-rate herbicide application. *Transactions of the ASAE* 41(2): 291-299.

Righetti T.L. 1997. Precision horticulture - applying information technologies to orchards. *GPS World; Supplement on Precision Farming* 8(4): 19-26.

Rockwell, A.D., & P.D. Ayers. 1996. A variable rate, direct nozzle injection field sprayer. *Applied Engineering in Agriculture*. 12(5): 531-538.

Rupert, C., & R.L. Clark. 1994. Accuracy of DGPS position information point data with a C/A code receiver. ASAE Paper No. 94-3546. St. Joseph, MI:ASAE.

Sampson, S.R. 1985. A survey of commercially available positioning systems. *Navigation* 32(2): 139-148.

Saunders, S. P., G. Larscheid, B.S. Blackmore, & J.V. Stafford. 1996. A Method for Direct Comparison of Differential Global Positioning Systems Suitable for Precision Farming. In *Proceedings of the Third International Conference on Precision Agriculture*, edited by P.C. Robert, R.H. Rust, & W.E. Larson. Madison, WI: ASA/CSSA/SSSA, 663-674.

Schmitz, T.G., & C.B. Moss. 1998. Investing in precision agriculture. Manuscript submitted to the *Quarterly Journal of Economics*. 34 p.

Schneider, S.M., S. Han, R.H. Cambell, R.G. Evan, & S.L. Rawlins. 1996. Precision agriculture for potatoes in the Pacific Northwest. In *Proceedings of the Third International Conference on Precision Agriculture*, edited by P.C. Robert, R.H. Rust, & W.E. Larson. Madison, WI: ASA/CSSA/SSSA, 443-452.

Schnug, E., D. Murphy, E. Evans, S. Haneklaus, & J. Lamp. 1993. Yield mapping and application of yield maps to computer-aided local resource management. In *Proceedings. First Workshop on Soil Specific Crop Management*, edited by P.C. Robert, R.H. Rust, & W.E. Larson. Madison, WI:ASA/CSSA/SSSA, 87-93.

Scholberg, J.M.S., L.R. Parsons, & T.A. Wheaton. 2000. Citrus nitrogen nutrition: Some production considerations for more efficient nitrogen use. In *Citrus Industry*. 18-19.

Schueller, J. K. 1988. Machinery and systems for spatially-variable crop production. ASAE Paper No. 88-1608. St. Joseph, MI:ASAE.

Schueller, J. K. 1992. A review and integrating analysis of spatially-variable control of crop production. *Fertilizer Research* 33. Dordrecht, The Netherlands:Kluwer, 1-34.

Schueller, J.K. 1996. Short Communication - Impediments to spatially-variable field operations. *Computers and Electronics in Agriculture* 14: 249-253.

Schueller, J.K., & M.W. Wang. 1994. Spatially-variable fertilizer and pesticide application with GPS and DGPS. *Computers and Electronics in Agriculture* 11: 69-83.

Schueller, J.K., J.D. Whitney, W.M. Miller, T.A. Wheaton, & A.E.Turner. 1999. Low-cost automatic yield mapping in hand-harvested citrus. *Computers and Electronics in Agriculture* 23: 145-153.

Searcy S.W., J.K. Schueller, H.Y. Bae, S.C. Borgelt, & B.A. Stout. 1989. Mapping of spatially-variable yield during grain combining. *Transactions. ASAE* 32 (3): 826-829.

Spruce, M.D., S.E. Taylor, & J.H. Wilhoit. 1993. Using GPS to track forest machines. ASAE Paper No. 93-7504. St. Joseph, MI:ASAE.

Stafford, J. V. 1996a. Introduction - Spatially variable field operation. *Computers and Electronics in Agriculture* 14: 99-100.

Stafford, J. V. 1996b. Essential technology for precision agriculture. In *Proceedings of the Third International Conference on Precision Agriculture*, edited by P.C. Robert, R.H. Rust, & W.E. Larson. Madison, WI: ASA/CSSA/SSSA, 595-604.

Stafford, J.V. 1999. GPS in agriculture - a growing market. *Navigation* 52 (1): 60-69.

Stafford, J.V., & B. Ambler. 1994. In-field location using GPS for spatially variable field operations. *Computers and Electronics in Agriculture* 11: 23-26.

Stoll, A., & H.D. Kutzbach. 1999. Concept of a guidance system for agricultural vehicles. In *Proceedings of the Second European Conference on Precision Agriculture*. edited by J.V. Stafford. Sheffield, UK: Sheffield Academic Press, 825 - 835.

Sudduth, K.A., S.C. Borgelt, & J. Hou. 1995. Performance of a chemical injection spraying system. *Applied Engineering in Agriculture* 11(3): 343-348.

Tyler, D.A., D.W. Roberts, & G.A. Nielsen. 1997. Location and guidance for site-specific management. In *The State of Site-Specific Management for*

Agriculture, edited by F.J. Pierce, & E.J. Sadler. Madison, WI: ASA/CSSA/SSSA, 161-182.

Vetter, A.A. 1995. Quantitative evaluation of DGPS guidance for ground-based agricultural applications. *Applied Engineering In Agriculture* 11(3): 459 - 464.

Walter, J. D., V.L. Hofman, & L.F. Backer. 1996. Site-specific sugarbeet yield monitoring. In *Proceedings of the Third International Conference on Precision Agriculture*, edited by P.C. Robert, R.H. Rust, & W.E. Larson. Madison, WI: ASA/CSSA/SSSA, 835-844.

Wang, M.W. 1994. Multivariate dynamic control of a GIS-based spatially-variable applicator. Unpublished PhD. Dissertation. University of Florida, Gainesville.

Whitney, J.D., W.M. Miller, T.A. Wheaton, & M. Salyani. 1998. Precision farming applications in Florida citrus. ASAE Paper No. 98-1097. St. Joseph, MI:ASAE.

Whitney, J.D., W.M. Miller, T.A. Wheaton, M. Salyani, & J.K. Schueller. 1999a. Precision farming applications in Florida citrus. *Applied Engineering in Agriculture* 15(5): 399-403.

Whitney, J.D., Q. Ling, W.M. Miller, & T.A. Wheaton. 1999b. A DGPS yield monitoring system for Florida citrus. ASAE Paper No. 99-1056. St. Joseph, MI:ASAE.

Xu, L.J. 1991. Dynamic and static analysis of a servovalve controlled hydraulic motor driven centrifugal pump. Unpublished M.S. Thesis. University of Florida, Gainesville.

Yang, C., G.L. Anderson, J.H. Everitt, & J.M. Bradford. 1998. Nitrogen and phosphorous management using a variable rate liquid fertilizer applicator. ASAE Paper No. 98-1050. St. Joseph, MI:ASAE.

Yang, X., & M. Schlemmer. 1998. The soil nutrient modeling and sampling for precision agriculture. In *Proceedings. Of the First International Conference on Geospatial Information in Agriculture and Forestry 2.*Ann Arbor, MI: ERIM, 123-130.

Zhao, Y. 1997. *Vehicle Location And Navigation Systems.* Norwood, MA: ARTECH HOUSE, 329 p.

Zhu, H., R.D. Fox, H.E. Ozkan, R.D. Brazee, & R.C. Derksen. 1998. Time delay for injection sprayers. *Transactions. Of the ASAE* 41(3): 525-530.

BIOGRAPHICAL SKETCH

Chee-Wan Chan was born in Malaysia on June 27, 1956. He earned a Bachelor of Engineering degree in agricultural engineering from the Agricultural University of Malaysia in Serdang, Selangor, Malaysia in 1981. After graduating from college, he worked as a technical executive in Multico (Malaysia) Limited Co. dealing with machinery sale and services. He also worked as a service executive for Kubota Agricultural Machinery (M) Sdn. Bhd. for two years. He later joined the Malaysian Agricultural Research and Development Institute (MARDI) as a research officer in 1984. At MARDI, he was involved in agricultural mechanization research specializing in power and machinery automation. In 1990, he was offered a scholarship by MARDI to pursue his Master of Science study in Agricultural Engineering at the Ohio State University, Columbus, OH. He received his Master of Science degree in September 1992 and will receive his Ph.D. from the University of Florida in August 2000.

I certify that I have read this study and that in my opinion it conforms to acceptable standards of scholarly presentation and is fully adequate, in scope and quality, as a dissertation for the degree of Doctor of Philosophy.

William M. Miller, Chair
Professor of Agricultural and
Biological Engineering

I certify that I have read this study and that in my opinion it conforms to acceptable standards of scholarly presentation and is fully adequate, in scope and quality, as a dissertation for the degree of Doctor of Philosophy.

John K. Schueller, Co-Chair
Associate Professor of
Mechanical Engineering

I certify that I have read this study and that in my opinion it conforms to acceptable standards of scholarly presentation and is fully adequate, in scope and quality, as a dissertation for the degree of Doctor of Philosophy.

Jodie D. Whitney
Professor of Agricultural and
Biological Engineering

I certify that I have read this study and that in my opinion it conforms to acceptable standards of scholarly presentation and is fully adequate, in scope and quality, as a dissertation for the degree of Doctor of Philosophy.

J. David Mattsoff
Professor of Horticultural Sciences

I certify that I have read this study and that in my opinion it conforms to acceptable standards of scholarly presentation and is fully adequate, in scope and quality, as a dissertation for the degree of Doctor of Philosophy.

J. Wayne Mishoe
Professor of Agricultural and
Biological Engineering

This dissertation was submitted to the Graduate Faculty of the College of Engineering and to the Graduate School and was accepted as partial fulfillment of the requirements for the degree of Doctor of Philosophy.

August 2000

M.J. Ohanian
Dean, College of Engineering

Winfred M. Phillips
Dean, Graduate School